catalysts

MDPI

Review

Activation, Deactivation and Reversibility Phenomena in Homogeneous Catalysis: A Showcase Based on the Chemistry of Rhodium/Phosphine Catalysts †

Elisabetta Alberico [1], Saskia Möller [2], Moritz Horstmann [2], Hans-Joachim Drexler [2] and Detlef Heller [2,*]

1 Istituto di Chimica Biomolecolare—CNR, Tr. La Crucca 3, 07100 Sassari, Italy
2 Leibniz-Institut für Katalyse e.V., Albert-Einstein-Strasse 29a, 18059 Rostock, Germany
* Correspondence: detlef.heller@catalysis.de
† Dedicated to Piet W. N. M. van Leeuwen.

Received: 5 June 2019; Accepted: 29 June 2019; Published: 30 June 2019

Abstract: In the present work, the rich chemistry of rhodium/phosphine complexes, which are applied as homogeneous catalysts to promote a wide range of chemical transformations, has been used to showcase how the in situ generation of precatalysts, the conversion of precatalysts into the actually active species, as well as the reaction of the catalyst itself with other components in the reaction medium (substrates, solvents, additives) can lead to a number of deactivation phenomena and thus impact the efficiency of a catalytic process. Such phenomena may go unnoticed or may be overlooked, thus preventing the full understanding of the catalytic process which is a prerequisite for its optimization. Based on recent findings both from others and the authors' laboratory concerning the chemistry of rhodium/diphosphine complexes, some guidelines are provided for the optimal generation of the catalytic active species from a suitable rhodium precursor and the diphosphine of interest; for the choice of the best solvent to prevent aggregation of coordinatively unsaturated metal fragments and sequestration of the active metal through too strong metal–solvent interactions; for preventing catalyst poisoning due to irreversible reaction with the product of the catalytic process or impurities present in the substrate.

Keywords: Rh; homogeneous catalysis; catalyst deactivation

1. Introduction

The term "catalysis" was first introduced by the Swedish chemist Jöns Jacob Berzelius in a report published in 1835 by the Swedish Academy of Sciences [1]. The report was a reflection on earlier findings by European scientists on chemical changes both in homogeneous and heterogeneous systems. Although far from being understood, the recorded phenomena were unified, according to Berzelius, by the fact that "*several simple or compound bodies, soluble and insoluble, have the property of exercising on other bodies an action very different from chemical affinity. By means of this action they produce, in these bodies, decompositions of their elements and different recombinations of these same elements to which they remain indifferent*." [2] Berzelius designated this unifying property as "catalytic force" and coined the term "catalysis" to describe the decomposition of bodies by this force. Catalysis is the macroscopic manifestation of the reduction of the activation energy of an exergonic reaction. It is as such a purely kinetic phenomenon; Berzelius however did not know the concept of reaction rate yet and therefore he could only describe known findings phenomenologically.

It was not until 1894 that Wilhelm Ostwald succeeded in giving an exact description of catalysis [3]. Later, in his Nobel Lecture of 1909, he said about catalysis that " ... the essence of which is not to be sought in the promotion of a reaction, but in its acceleration, ... " [4] Further introduction into the history of catalysis can be found in references [5–8].

An updated definition to be found in the IUPAC Compendium of Chemical Terminology, though, suggests a clear distinction between a catalyst, that is a substance that *increases* the rate of a reaction, and an inhibitor, which instead *reduces* it [9].

Catalysis is widely applied both in industry [10–13] and academia [14,15]: the switch from a stoichiometric process to a catalytic one represents a way to greatly improve efficiency, as less energy input and less feedstock are usually required, less waste is generated, and a greater product selectivity is in general achieved.

Although heterogeneous catalysts were the first to be applied at the industrial level, where they dominated the scene for several decades, homogenous catalysts started to raise increasing attention in the early 1960s when they were considered for the large scale production of bulk chemicals. One major contribution came in those years from Slaugh and coworkers at Shell Research (USA) [16] later on supported by further developments in Wilkinson's laboratory [17], of Co- and Rh-phosphine catalysts which were applied in the rapid, selective liquid-phase hydroformylation and hydrogenation of alkenes under mild conditions. The possibility to tailor the catalyst properties by proper selection of additional ligands triggered further research which led in the following decades to the development of important industrial processes based on the use of homogeneous catalysts such as the SHOP process

for the oligomerization of ethylene or the production of enantioenriched herbicide Metholachlor and the aroma ingredient citronellal [11].

The discovery of a novel catalyst for a certain process may be serendipitous or the result of extensive screening. Yet improvement of the catalyst productivity and efficiency, both in terms of activity and selectivity in the desired product, requires knowledge of the chemical transformations the catalyst undergoes during the course of the reaction. The nature and distribution of the resulting species may vary over time due to the interaction with the substrate, the product, the solvent, and additives. Some of these species may be catalytically inactive and hence negatively affect the outcome of the catalytic process. Although the exact nature of these species depends on the specific catalytic process and the experimental conditions under which it is carried out, inactivation of an homogeneous catalyst can be in general ascribed to the following: metal deposition due to reducing reaction conditions or ligand loss; ligand decomposition; reaction of the metal–ligand bond, such as metal–carbon or metal–hydride bond, with polar species such as water, acids, and alcohols; blocking of the catalyst active site by polar impurities, by metal fragments aggregation, and by ligand metalation. However, if studies are carried out that allow identification of the conditions which favor catalyst inactivation, then countermeasures can be adopted. As it was recently written " ... *Since such studies are currently underrepresented in the catalysis literature, our science will advance, and our community will benefit from increased emphasis on the productivity* (activity and selectivity) *metric*" [18].

The topic of catalyst activation, deactivation, and stability for several metals, for homogeneous and heterogeneous catalysts, has been dealt with in excellent review publications [19–22]. Here we would like to report on recent findings in the chemistry of rhodium/diphosphine complexes, both from others and our laboratory [23], which have allowed understanding of the activity profile of these complexes when used as precatalysts. In several cases the acquired knowledge has allowed improvement of the catalyst performance considerably.

2. In Situ Generation of Precatalysts

Neutral dinuclear rhodium complexes of the type [Rh(diphosphine)(μ_2-X)]$_2$ (X = Cl^-, OMe^-, OH^- ...) are very often applied as catalyst precursors in homogeneous catalysis [24–37]. These coordination compounds are usually not commercially available and must therefore be synthesized. This is mostly done in situ by addition of a diphosphine to a suitable precursor complex; previous work from our group has shown that, contrary to common belief, this procedure is far from being fast and selective in the formation of the desired neutral dinuclear rhodium species [Rh(diphosphine)(μ_2-Cl)]$_2$ [23,38–40]. In many cases, depending on the rhodium precursor, the diphosphine ligand, the solvent, the reaction temperature, and reaction time, other unexpected coordination species are formed, either cationic and/or trinuclear, either exclusively or in admixture with other complexes [38–40] (Scheme 1) which can negatively affect the catalytic activity. The range of species displayed in Scheme 1 might be extended as a result of further investigations.

In light of these findings, mechanistic investigations have been carried out on the rhodium-catalyzed propargylic CH activation which relied on the in situ generation of the catalytically active species. This reaction proceeds with good yields (up to 89%) and excellent selectivities (up to 95% ee) and offers great potential as a novel method for the construction of C–C and C–X bonds [41–47]. A broad range of substrates can be employed and, more interestingly, the reaction shows ligand-specific chemoselectivity (Scheme 2).

In the case of the P,N ligand DPPMP (a complete list of abbreviations, including ligand names, used in this article can be found in Table A2) it could be shown that its reaction with the COD precursor [Rh(COD)(μ_2-Cl)]$_2$ does not produce the desired dinuclear neutral complex [Rh(DPPMP)(μ_2-Cl)]$_2$, but an ionic species [Rh(DPPMP)$_2$][Rh(COD)Cl$_2$] in which both the anion and the cation are rhodium coordination compounds (Figure 1, left) [48].

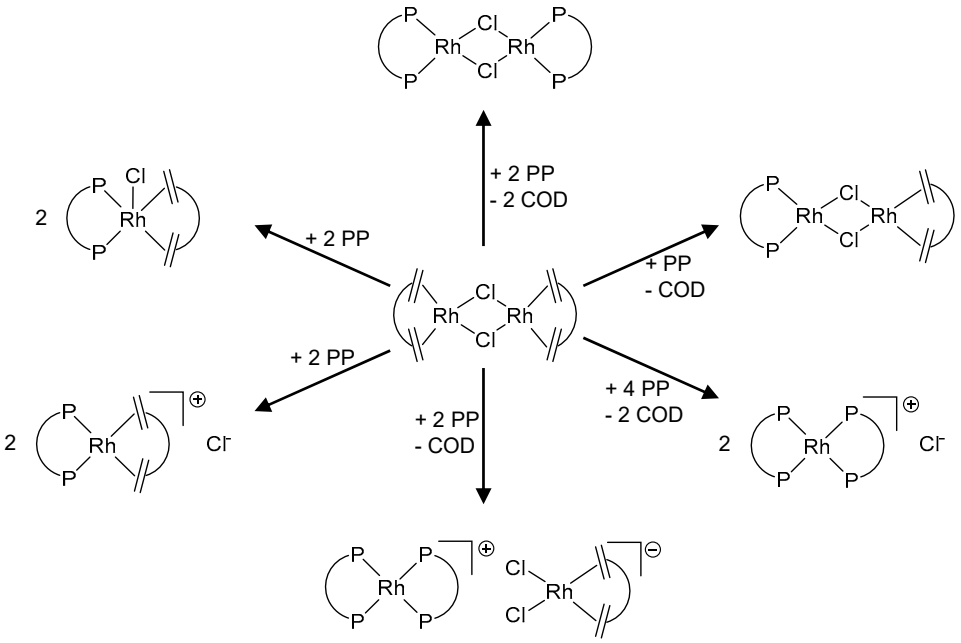

Scheme 1. In situ generation of rhodium/diphosphine complexes—known range of species which can be formed during the in situ reaction of rhodium diolefin precursors with diphosphine ligands.

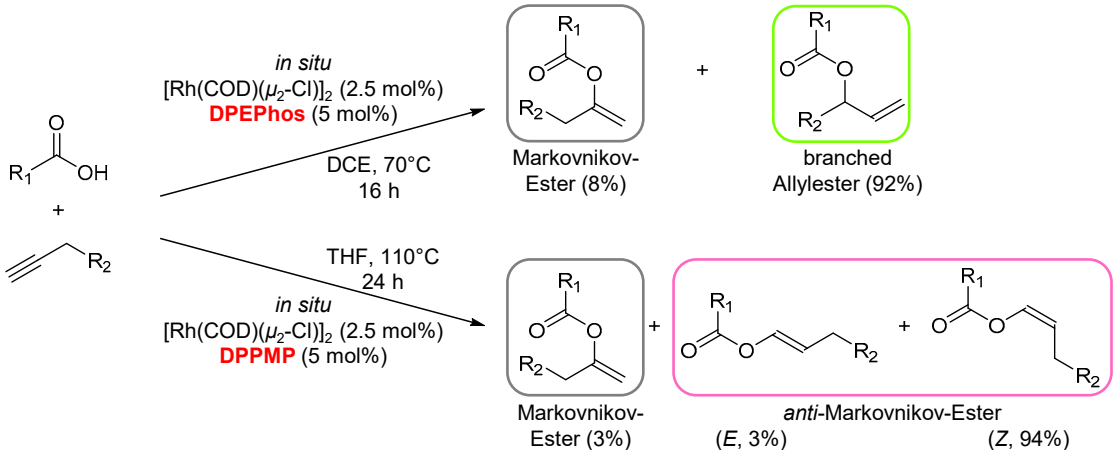

Scheme 2. Schematic representation of the rhodium-catalyzed propargylic CH activation with the ligands DPEPhos, above, and DPPMP, below [41–43].

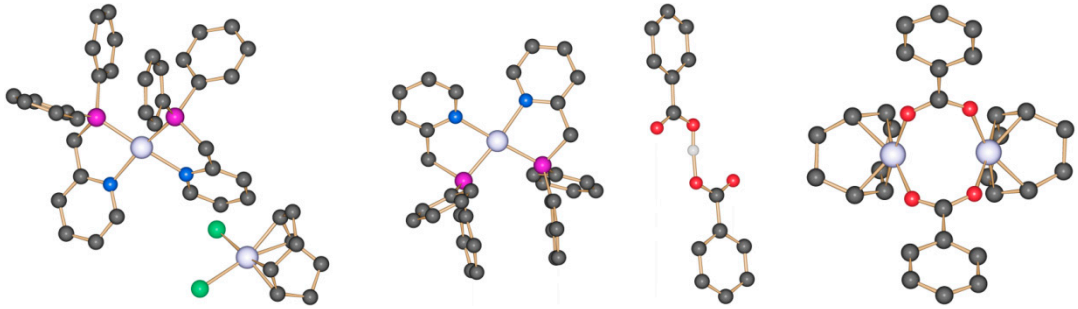

Figure 1. Molecular structure of $[Rh(DPPMP)_2][Rh(COD)Cl_2]$, left, molecular structure of $[Rh(DPPMP)_2][H(benzoate)_2]$ and $[Rh(COD)(\mu_2\text{-benzoate})]_2$, right. Hydrogen atoms (except $H(benzoate)_2$) are omitted for clarity [49].

In addition, it was demonstrated that the chloride ligands in the COD precursor [Rh(COD)(μ_2-Cl)]$_2$ have a deactivating effect on the catalytic reaction, which is why the chloride-free rhodium precursor [Rh(COD)(acac)] has been used instead. The reaction of [Rh(COD)(acac)] with DPPMP in the presence of the substrate benzoic acid leads to a mixture of two complexes [Rh(DPPMP)$_2$][H(benzoate)$_2$] and [Rh(COD)(μ_2-benzoate)]$_2$, which synergistically behave as the active "catalyst" (Figure 1, right) [48].

This example clearly shows that the classical in situ synthesis of rhodium(I) precatalysts can deliver unexpected compounds with poor or no catalytic activity. Only through an in depth investigation of the in situ process can the experimental factors which favor the formation of such species be clarified. Based on this knowledge, conditions can be rationally controlled to achieve better efficiency, activity, and selectivity (Scheme 3). In the following section, the factors which affect the in situ synthesis of rhodium(I) precatalysts will be introduced and their influence will be discussed.

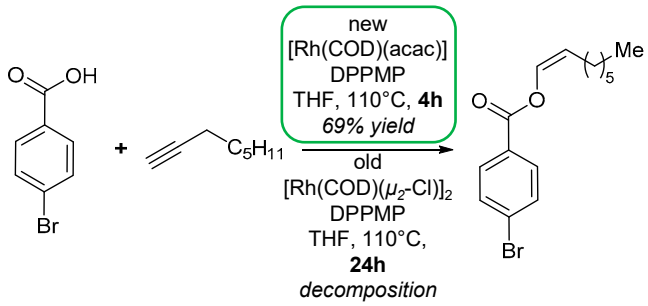

Scheme 3. Optimized reaction conditions for the rhodium catalyzed reaction of 4-bromo-benzoic acid and 1-octyne [48].

2.1. Influence of Reaction Conditions on Outcome of In Situ Synthesis

Rhodium(I) precatalysts of the type [Rh(diphosphine)(μ_2-Cl)]$_2$ are usually formed in situ at room temperature by the reaction of a diphosphine ligand with a stable olefin or diolefin-containing rhodium precursor. At first sight it is plausible to assume that a twofold ligand exchange takes place which affords a precatalyst the general structure of which [Rh(diphosphine)(μ_2-Cl)]$_2$ is the same, regardless of the ligand used (Scheme 4). From such a precatalyst the catalytically active species should eventually be formed.

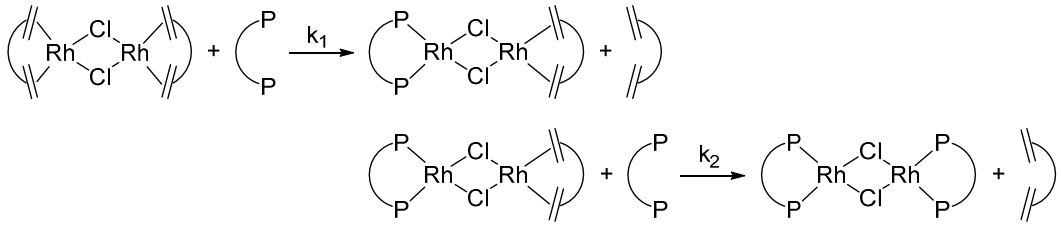

Scheme 4. Sequence of the competing consecutive reactions leading to [Rh(disphosphine)(μ_2-Cl)]$_2$ from [Rh(diolefin)(μ_2-Cl)]$_2$.

Systematic investigations have instead shown that the outcome of the in situ procedure is by no means as straightforward as shown in Scheme 4 and some illustrative cases are discussed below.

When [Rh(NBD)(μ_2-Cl)]$_2$ is reacted with either SEGPhos, DIPAMP, or DPEPhos the product of ligand exchange depends on the diphosphine used. With SEGPhos, when the reaction is carried out in THF at room temperature using a 1:2 metal to ligand ratio, then the desired neutral, dinuclear complex [Rh(SEGPhos)(μ_2-Cl)]$_2$ is obtained at 80% yield. However a small amount of the μ_2-chloro-bridged intermediate [(NBD)Rh(μ_2-Cl)$_2$Rh(SEGPhos)], (Figure 2a) is also formed [38]. When [Rh(NBD)$_2$(μ_2-Cl)]$_2$ is reacted with DIPAMP under the same conditions, a cationic complex results almost quantitatively, in which the rhodium center is coordinated by two DIPAMP molecules and the chloride acts as a counterion (Figure 2b) [38]. With DPEPhos a species is formed in which the

diphosphine, the diolefin, and a chloride ligand bind to rhodium to give a penta-coordinated complex (Figure 2c) [50]. Similar coordination compounds of the form [Rh(disphosphine)(diolefin)Cl] have been reported as well and discussed in detail [38,39].

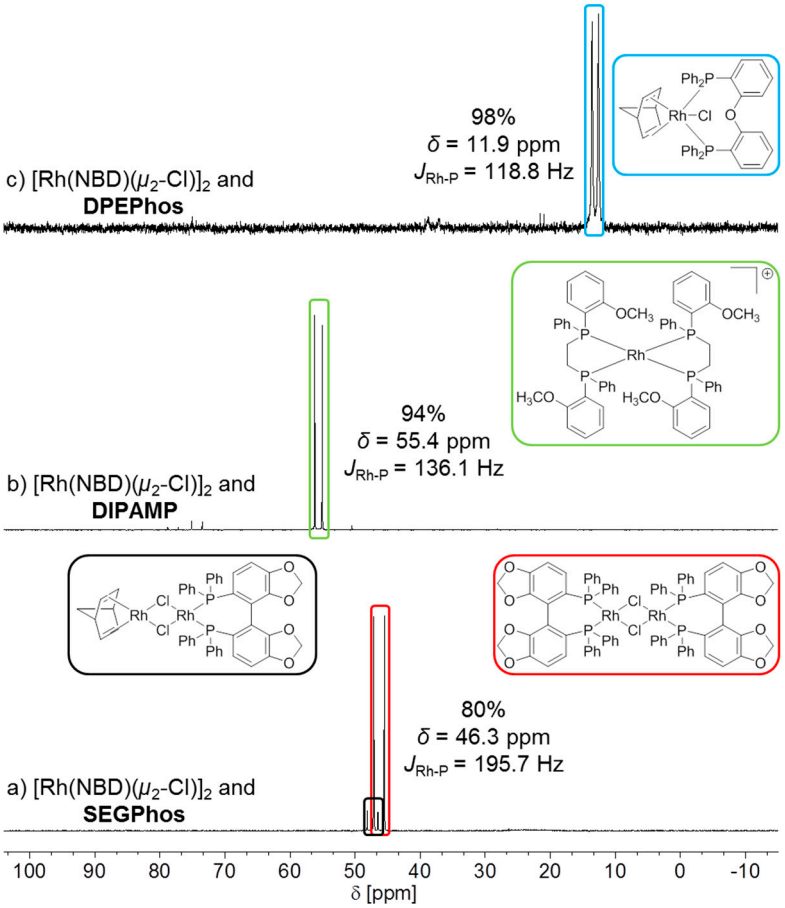

Figure 2. ^{31}P NMR spectra of the reaction solution for the in situ ligand exchange at room temperature in THF-d_8 between [Rh(NBD)(μ_2-Cl)]$_2$ and (**a**) SEGPhos, (**b**) DIPAMP, (**c**) DPEPhos.

The solvent also plays a key role in the outcome of the in situ procedure. Although the course of a catalytic reaction is often solvent-specific, rarely has this correlation been attributed to the formation of different catalytic species [51–53]. For example, when [Rh(COD)(μ_2-Cl)]$_2$ reacts with SEGPhos in a 1:2 ratio at room temperature in THF the desired species, [Rh(SEGPhos)(μ_2-Cl)]$_2$ is produced quantitatively, Figure 3a [38,54]. In DCM an additional monomeric cationic species is formed, in which the rhodium center is coordinated by two SEGPhos molecules and the chloride as possible counterion, Figure 3b [38]. In MeOH the prevailing species is a monomeric cationic complex in which the rhodium center is coordinated by a SEGPhos molecule and COD, Figure 3c [38].

In the literature the used rhodium species is often not discussed and is generalized with the abbreviation "[Rh]" [55–57]. But, as the following example will clearly show, the choice of the rhodium precursor is also decisive for the outcome of the in situ synthesis. When the diphosphine ligand DPPB is reacted with [Rh(COE)(μ_2-Cl)]$_2$ at room temperature in THF, the desired dinuclear rhodium complex [Rh(DPPB)(μ_2-Cl)]$_2$ is formed quantitatively (Figure 4a) [38]. If [Rh(NBD)(μ_2-Cl)]$_2$ is used instead, the reaction affords exclusively a pentacoordinated rhodium species containing chloride and the chelating ligands DPPB and NBD (Figure 4b) [38,39]. With [Rh(COD)(μ_2-Cl)]$_2$ the reaction is unselective and affords several species, as evident from the large number of signals in the corresponding ^{31}P NMR spectrum (Figure 4c) [38].

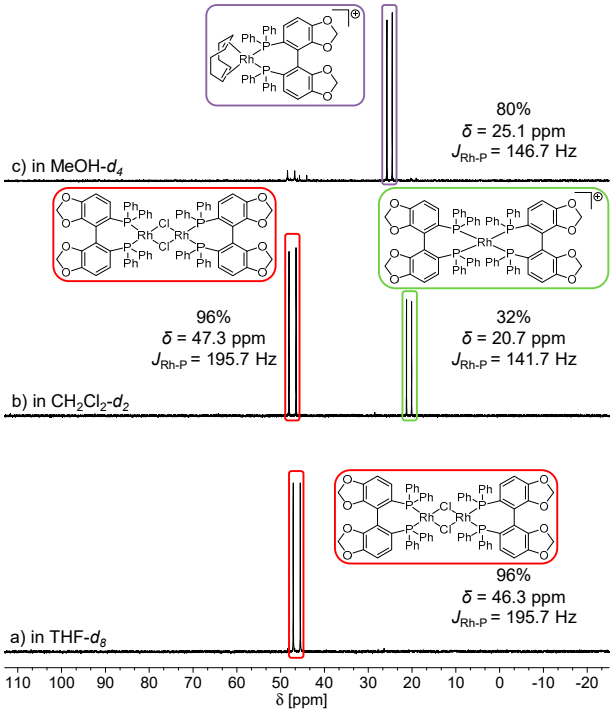

Figure 3. ^{31}P NMR spectrum of the solution resulting from the in situ reaction of [Rh(COD)(μ_2-Cl)]$_2$ and SEGPhos in the ratio 1:2 at room temperature: (**a**) in THF-d_8, (**b**) DCM-d_2, (**c**) MeOH-d_4.

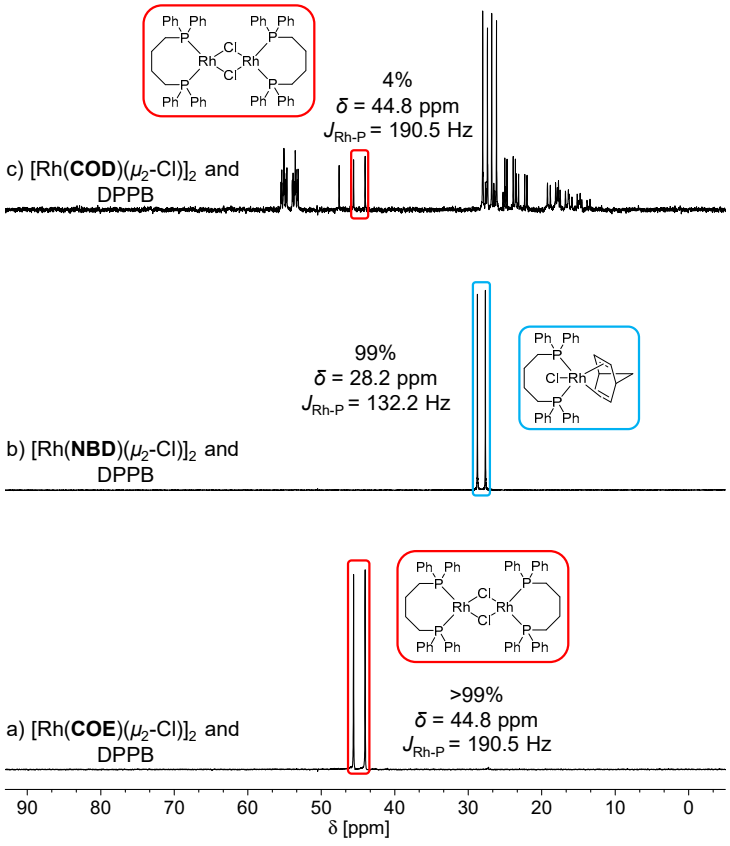

Figure 4. ^{31}P NMR spectrum of the solution resulting from the in situ reaction of DPPB in THF-d_8 with (**a**) [Rh(COE)(μ_2-Cl)]$_2$, (**b**) [Rh(NBD)(μ_2-Cl)]$_2$, (**c**) [Rh(COD)(μ_2-Cl)]$_2$.

The reaction temperature at which the ligand exchange between diolefin and diphosphine takes place may also affect the selectivity of the in situ procedure. Experiments with the chiral ligand DIOP have shown that a mixture of different complexes is formed when the reaction is carried out at 25 °C (Figure 5a). However, if the ligand exchange occurs at −10 °C, then the desired dinuclear precatalyst [Rh(DIOP)(μ_2-Cl)]$_2$ is obtained quantitatively (Figure 5b) [38]. With DPPE the in situ procedure does not work at room temperature, instead at 125 °C in toluene it affords the target compound [Rh(DPPE)(μ_2-Cl)]$_2$ quantitatively [58].

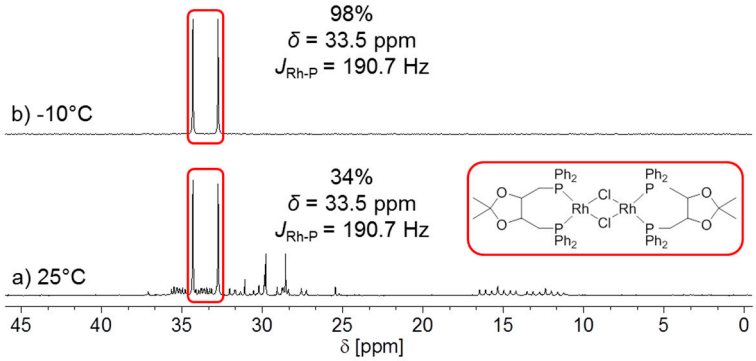

Figure 5. ^{31}P NMR spectrum of the solution resulting from the in situ reaction of [Rh(COD)(μ_2-Cl)]$_2$ and DIOP in THF-d_8 at (**a**) 25 °C and (**b**) −10 °C.

2.2. Mechanistic Investigations into the in situ Generation of Precatalysts

The examples reported above serve to illustrate how experimental conditions affect the outcome/selectivity of the in situ synthesis of rhodium/diphosphine precatalysts. However, with the ligands BINAP, SEGPhos, DM-SEGPhos, and Difluorphos, the target complex [Rh(disphosphine)(μ_2-Cl)]$_2$ is formed quasi quantitatively in THF. Less is known about the rate of formation of such species and the kinetics of the underlying two-stage ligand exchange process (Scheme 4). Quantitative studies of classical ligand exchange reactions can be accomplished using UV-Vis spectroscopy (diode array in combination with a stopped-flow unit) because during the reaction a color change takes place [54,59].

From a kinetic point of view, each stage of the ligand exchange process is a second order reaction, and the two reactions compete with each other. The solid state structure of the intermediate [(COD)Rh(μ_2-Cl)$_2$Rh(diphosphine)] has been determined for various disphosphines [38,60,61]. Only recently has it been shown that indeed an equilibrium exists between the starting and the product complexes on the one hand and the intermediate on the other (Scheme 5) which of course complicates kinetic investigations [54].

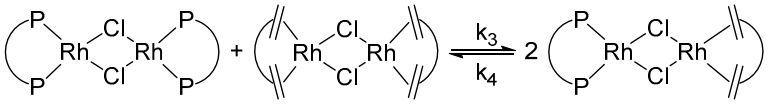

Scheme 5. Equilibrium between the starting [Rh(diolefin)(μ_2-Cl)]$_2$ and target complex [Rh(diphosphine)(μ_2-Cl)]$_2$ and the intermediate [(diolefin)Rh(μ_2-Cl)$_2$Rh(diphosphine)].

Figure 6 shows the ^{31}P NMR spectrum recorded shortly after crystals of [(COD)Rh(μ_2-Cl)$_2$Rh(DPEPhos)] have been dissolved in benzene-d_6; beside the signals of [(COD)Rh(μ_2-Cl)$_2$Rh(DPEPhos)], black, broad signals due to [Rh(DPEPhos)(μ_2-Cl)]$_2$, red, can be observed.

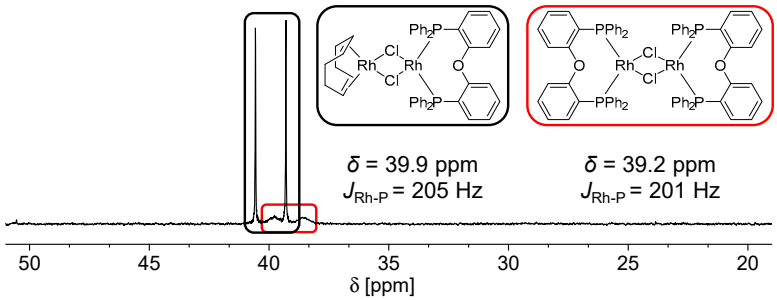

Figure 6. ^{31}P NMR spectrum of the solution obtained by dissolving crystals of [(COD)Rh(μ_2-Cl)$_2$Rh(DPEPhos)], black, in benzene-d_6; following the establishment of an equilibrium, [Rh(DPEPhos)(μ_2-Cl)]$_2$ is formed, red.

The rate constants of the reaction steps described in Schemes 4 and 5 for the ligands BINAP, SEGPhos, DM-SEGPhos, and Difluorphos are collected in Table 1.

Table 1. Rate constants of the ligand exchange reactions described in Schemes 4 and 5 for BINAP, SEGPhos, DM-SEGPhos, and Difluorphos [54].

Ligand	k_1 (L·mol^{-1}·s^{-1})	k_2 (L·mol^{-1}·s^{-1})	k_3 (L·mol^{-1}·s^{-1})	k_4 (L·mol^{-1}·s^{-1})	$t_{98\%\ conv.}$ (min)
BINAP	1790	18	39.3	1.10	22
SEGPhos	10,617	121	16.7	1.43	3
DM-SEGPhos	13,466	14	0.3	0.60	28
Difluorphos	8080	220	-	-	2

These data show that, for all the ligands investigated, the exchange of the first COD ligand to give the intermediate [(COD)Rh(μ_2-Cl)$_2$Rh(diphosphine)] is much faster than the exchange of the second one (k_1 >> k_2). The latter is therefore the rate-determining step of the overall reaction. The rapid color change, occasionally described in the literature, is due to the formation of the intermediate and thus cannot be used, in the in situ generation of the precatalyst, as an indication of the formation of the target complex. The experimentally determined rate constants, Table 1, allow then the calculation of the time required for the complete formation of the desired dinuclear precatalysts under normal conditions [62]: 22 min are necessary with BINAP, up to 28 with DM-SEGPhos [54], far more than usually expected.

With the ligands DPEPhos and DIOP the mechanism leading to the formation of the corresponding precatalysts [Rh(disphosphine)(μ_2-Cl)]$_2$, which have been applied in propargylic CH activation, is more complex [41,42,63–66]. Indeed, beside the intermediate [(COD)Rh(μ_2-Cl)$_2$Rh(diphosphine)], a previously unknown diphosphine-bridged species [Rh$_2$(μ_2-diphosphine)(COD)$_2$(Cl)$_2$] could be isolated and characterized [61]. When the reaction of [Rh(COD)(μ_2-Cl)]$_2$ and DPEPhos in benzene is monitored by ^{31}P NMR, 10 min after mixing of the reagents the signals relative to such species (Figure 7, yellow) could be observed, beside those of [Rh(DPEPhos)(μ_2-Cl)]$_2$ (Figure 7, red) and [(COD)Rh(μ_2-Cl)$_2$Rh(DPEPhos)] (Figure 7, black).

Therefore the known twofold ligand exchange sequence described in Scheme 4 must be corrected as shown in Scheme 6, at least for these diphosphines [38,61], to accommodate the newly observed intermediate [Rh$_2$(μ_2-diphosphine)(COD)$_2$(Cl)$_2$].

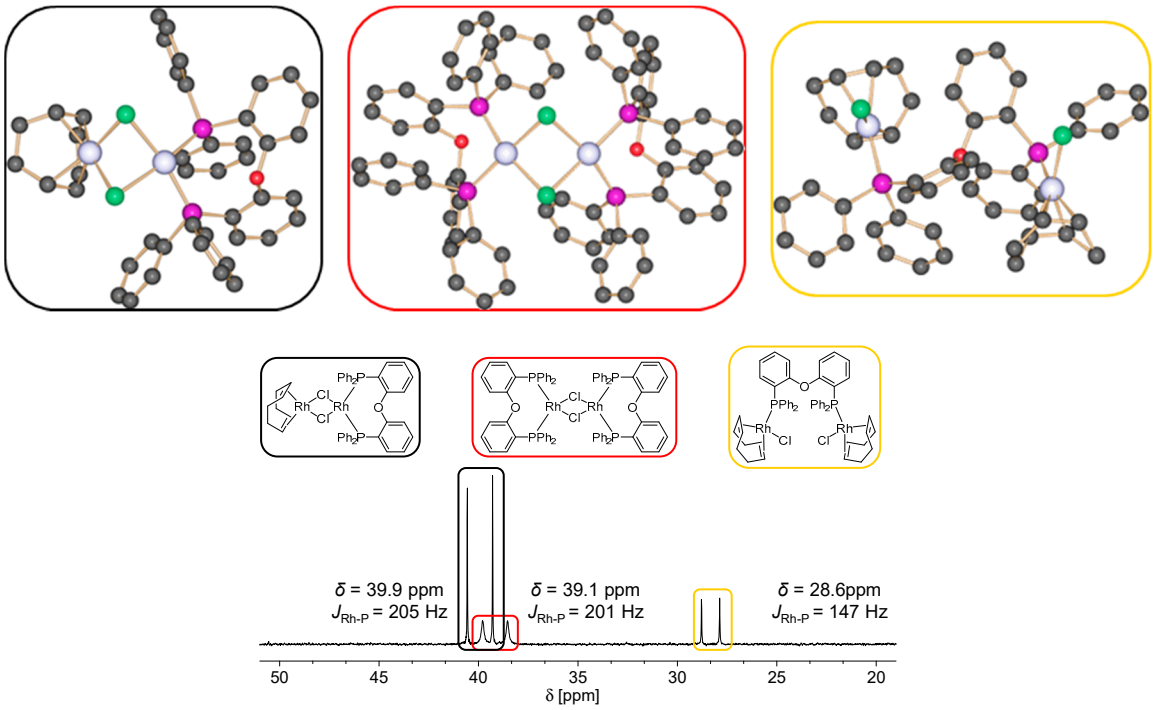

Figure 7. ^{31}P NMR spectrum of the solution obtained from reaction of [Rh(COD)(μ_2-Cl)]$_2$ and DPEPhos, in a 1:2 mixture, 10 min after mixing of the reagents: X-ray structures of the species detected in solution [(COD)Rh(μ_2-Cl)$_2$Rh(DPEPhos)], black, [Rh(DPEPhos)(μ_2-Cl)]$_2$, red, and [Rh$_2$(μ_2-DPEPhos)(COD)$_2$(Cl)$_2$], yellow.

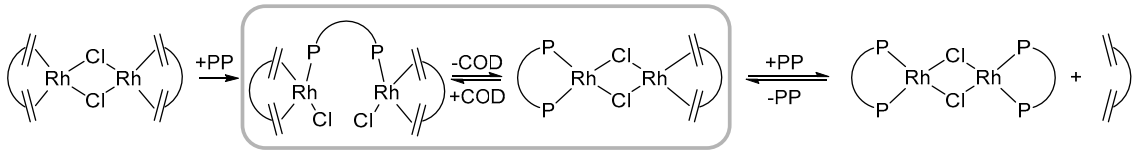

Scheme 6. Schematic representation of the modified ligand exchange mechanism for the formation of the rhodium precatalyst [Rh(diphosphine)(μ_2-Cl)]$_2$.

In the first step, the precursor [Rh(COD)(μ_2-Cl)]$_2$ is cleaved and the first reacting diphosphine acts as a bridging ligand between the two homoleptic rhodium fragments to afford [Rh$_2$(μ_2-diphosphine)(COD)$_2$(Cl)$_2$]. Then, following the loss of one COD ligand and diphosphine rearrangement to become bidentate at one of the two rhodium centers, an equilibrium is established between [Rh$_2$(μ_2-diphosphine)(COD)$_2$(Cl)$_2$] and the newly formed [(COD)Rh(μ_2-Cl)$_2$Rh(diphosphine)]. Such equilibrium can be shifted by altering reaction conditions (COD concentration, solvent, temperature). Exchange of COD for a second molecule of the diphosphine in [(COD)Rh(μ_2-Cl)$_2$Rh(diphosphine)] eventually affords the desired precatalyst [Rh(disphosphine)(μ_2-Cl)]$_2$. While in the case of DPEPhos quantitative formation of the precatalyst requires 30 min, for DIOP the equilibria lie far to the side of the intermediates. This is equivalent to a partial catalyst deactivation.

The examples discussed above clearly show that the in situ synthesis of rhodium precatalysts may not be selective thus affording a complex mixture of species. Even more complex, as shown in Scheme 7, is the network of equilibria which have been documented for the ligand DPPP [39,60,61,67–69]. To the best of our knowledge, the species [Rh(DPPP)(diolefin)]Cl, which is also possible in principle, is not known. It has been described for other diphosphine ligands [70–76]. The nature of the species that are actually present under stationary conditions cannot be predicted a priori and which one, among these, is responsible for the catalytic activity may be difficult to establish. It should also be noted that even the starting diolefin precursor can be catalytically active [77–85]. Because selectivity is mostly

determined by the type of ligand coordinated to the metal, if the diolefin precursor is not completely converted, selectivity will be negatively affected.

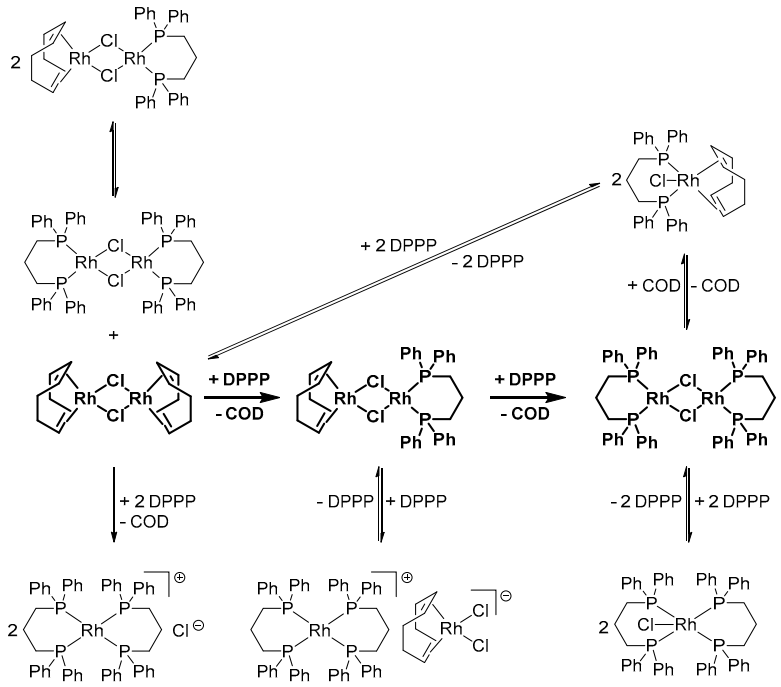

Scheme 7. In situ synthesis of the rhodium catalyst precursor [Rh(disphosphine)(μ_2-Cl)]$_2$ with the ligand DPPP and known by-products arising from side-reactions.

3. Catalyst Activation—Induction Periods

Catalytic processes, either homogeneous or heterogeneous, are often characterized by an initial slow stage after which the reaction accelerates. During the so-called induction period [86], the species which has been added to the reaction medium to function as the catalyst undergoes a series of chemical transformations before it can actually enter the catalytic cycle and promote the catalytic reaction.

For homogeneous catalysts, ligand (reactant) addition and ligand substitution and/or exchange at the catalyst precursor and/or oxidation–reduction of the metal with reactants/co-substrates, ligands, solvents, and other components of the system gradually convert the catalyst precursor into the catalytically active species. The concentration of the latter increases with time in the initial phase of the reaction, hence the induction period [87]. Catalytically active species are characterized by high reactivity/sensitivity, which makes them short-lived and difficult to characterize, hence the need to generate them from suitable catalyst precursors which are more stable, possess a longer shelf life, and are therefore easier to handle.

A classic example is provided by the Wilkinson catalyst [RhCl(PPh_3)$_3$] which, in the solid state, is indefinitely stable in air. It is a suitable precursor both for hydroformylation and hydrogenation of olefins. In solution it dissociates to release one PPh_3 and generate a coordinatively unsaturated species [RhCl(PPh_3)$_2$] [17,88,89]. Under hydroformylation conditions, several equilibria are established which are sensitive functions of experimental conditions: [RhCl(PPh_3)$_2$] reacts with CO to form *trans*-[RhCl(CO)(PPh_3)$_2$]. This species in turn oxidatively adds molecular hydrogen to afford [RhH(CO)(PPh_3)$_2$], and HCl. Hence an induction period is observed, unless an organic base such as triethylamine is used to favor the latter reaction. The dicarbonyl species [RhH(CO)$_2$(PPh_3)$_2$] has also been postulated to be present and active during hydroformylation. Under hydrogenation conditions, [RhCl(PPh_3)$_2$] can oxidatively add H_2 to generate [RhClH_2(PPh_3)$_2$], an extremely efficient catalyst for the hydrogenation of non-conjugated olefins and acetylenes at ambient temperature and hydrogen pressures of 1 atm or below. In both cases a rhodium hydride species makes the catalytic cycle turn.

An example from the most recent literature is provided by the following: A rhodium complex [Rh(κ^2-PP-DPEphos){$\eta^2\eta^2$-$H_2B(NMe_3)(CH_2)_2t$-Bu}]$BAr^F{}_4$ is a competent precatalyst for the dehydropolymerization of $H_3B{\cdot}NMeH_2$ to form N-methylpolyaminoborane $(H_2BNMeH)_n$ [90]. Before faster turnover is established, an induction period is observed which becomes longer with increasing total initial catalyst loading. An in-depth kinetic and mechanistic investigation has shown that the induction period is due to the formation, inter alia, of a dimeric rhodium species from which the monomeric catalytically active species is slowly generated. This process can be accelerated by the addition of NMe_2H which breaks down the dimer to form a rhodium amine complex [Rh(κ^2-PP-DPEphos)$H_2(NMeH_2)_2$]$BAr^F{}_4$. The latter is a far better precatalyst than [Rh(κ^2-PP-DPEphos){$\eta^2\eta^2$-$H_2B(NMe_3)(CH_2)_2t$-Bu}]$BAr^F{}_4$. Its isolation, while possible, is tedious but its in situ generation from [Rh(κ^2-PP-DPEphos){$\eta^2\eta^2$-$H_2B(NMe_3)(CH_2)_2t$-Bu}]$BAr^F{}_4$ in the presence of added NMe_2H is equally effective in suppressing the induction period. The structure of the active species though remains unknown.

3.1. Quantification of Induction Periods

The asymmetric hydrogenation of prochiral olefins is promoted by rhodium complexes of suitable chiral diphosphines. Such complexes are often commercialized as stable cationic diolefin precatalysts having the general formula [Rh(diphosphine)(diolefin)]$^+$ (dioelfin = COD, NBD); alternatively they can be generated in situ from the corresponding cationic diolefin rhodium complex and the chiral diphosphine. In either case, generation of the active species from the precatalyst requires hydrogenation of the diolefin. In this way, a free coordination site is made available at the metal for the binding of the substrate.

Figure 8, left, shows the difference in hydrogen uptake as a function of time between the asymmetric hydrogenation of mac in MeOH as promoted by the active catalyst [Rh((*R*,*R*)-Et-ButiPhane)$(MeOH)_2$]BF_4, green curve, and the same reaction as promoted by the commercially available precatalyst [Rh((*R*,*R*)-Et-ButiPhane)(COD)]BF_4, blue curve [91]. An induction period is present for the latter, i.e., the hydrogenation accelerates—the moles of hydrogen consumed per unit time as a function of time increase in the initial stages of the reaction (Figure 8, right, blue) as more of the catalytically active species [Rh((*R*,*R*)-Et-ButiPhane)$(MeOH)_2$]BF_4 is generated in the "activation" phase through hydrogenation of COD.

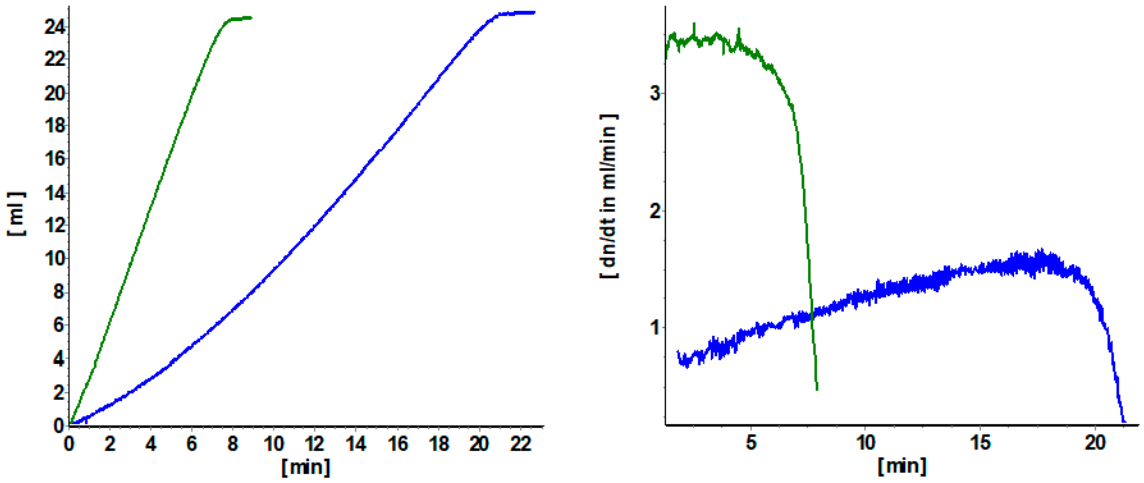

Figure 8. Left: Hydrogen uptake (ml) as a function of time (min) in the hydrogenation of mac with [Rh((*R*,*R*)-Et-ButiPhane)(COD)]BF_4 (99.0% ee, blue) and with [Rh((*R*,*R*)-Et-ButiPhane)$(MeOH)_2$]BF_4 (99.0% ee, green) under standard conditions [92]. Right: moles of hydrogen consumed per unit time (dn/dt) as a function of time (min) in the hydrogenation of mac with [Rh((*R*,*R*)-Et-ButiPhane)(COD)]BF_4 (blue) and [Rh((*R*,*R*)-Et-ButiPhane)$(MeOH)_2$]BF_4 (green).

Induction periods, which have been recognized, at least qualitatively, for a long time [93,94] cause a maximum in the rate profile (Figure 8, right). It should be noted that enantioselectivity is not affected by the different methods used for catalyst preparation (Figure 8, left) [91].

Several factors affect the induction period: the diolefin (stability of the corresponding diolefin rhodium complex), the prochiral olefin (its concentration and the stability of the corresponding rhodium substrate complex), the ligand, the solvent, and the temperature.

An in-depth discussion of the issues concerning diolefin hydrogenation (COD vs. NBD) can be found in references [22,95]. In Table A1 a list of related (pseudo) rate constants for ca. 80 rhodium/diphosphine complexes of the type [Rh(diphosphine)(diolefin)]$^+$ can be found. Rate constants for rhodium complexes of monophosphines, [Rh(MonoPhos)$_2$(NBD)]BF$_4$ [96], [Rh(MonoPhos)$_2$(COD)]BF$_4$ [97], and [Rh(PPh$_3$)$_2$(COD)]BF$_4$ [98], have also been measured.

Several methods have been reported in the literature which allow, under isobaric conditions, to measure the pseudo 1st order rate constant ($k'_{2diolefin}$) for the diolefin hydrogenation en route to the solvent complexes, according to the following Scheme 8.

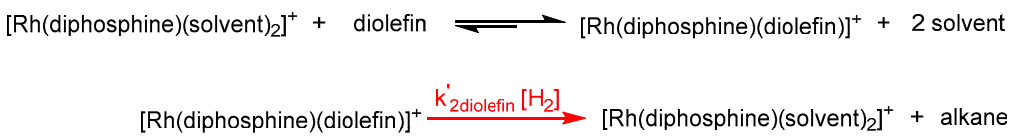

Scheme 8. Generation of the catalytically active species [Rh(diphosphine)(solvent)$_2$]$^+$ through hydrogenation of the diolefin in [Rh(diphosphine)(diolefin)]$^+$ and related equilibrium.

For most diphosphine ligands, the equilibrium (Michaelis–Menten kinetics) between the solvent complex and the free diolefin lies to the side of the diolefin complex due to the high stability of the latter. Under isobaric conditions, the hydrogen concentration is constant and therefore the stoichiometric reaction is pseudo 1st order in the diolefin concentration. In the presence of a large excess of the diolefin ("catalytic conditions"), the hydrogenation reaction becomes zero order (Michaelis–Menten kinetics in the saturation range).

In principle, it is possible to track either the stoichiometric hydrogenation (by measuring the hydrogen uptake [99] using ^{31}P NMR [100] or UV-Vis spectroscopy [101]) or the catalytic hydrogenation with an automatic recording device [102,103] in the presence of an excess of the diolefin [104] under several pressure regimes [105]. It is likewise possible by means of ^{1}H NMR spectroscopy to assess the H_2 concentration in solution during diolefin hydrogenation under isochoric conditions [106,107]. Through on-line recording of hydrogen consumption and subsequent parameter optimization using a suitable kinetic model, the pseudo rate constant for the diolefin hydrogenation can also be determined [108].

3.2. *Influence of the Diolefin*

Experimental evidence shows that, regardless of the diphosphine ligand, the hydrogenation of COD is always slower than that of NBD, meaning a longer induction period. The reason for such difference is not clear. A perusal of the solid state structures of several rhodium complexes of the general formula [Rh(diphosphine)(diolefin)]$^+$ with diphosphines forming 5-membered chelated rings shows deviations from the expected square-planar structure, that is the centroids of the double bonds, the phosphorus atoms of the diphosphine, and the rhodium central atom are not in the same plane [109]. The rotation of the diolefin away from the ideal square planar coordination serves to partly accommodate the steric demands of the diphosphine ligand while keeping a profitable overlap of the orbitals involved in the binding of the diene to the rhodium atom. Because NBD is smaller than COD, the tetrahedral distortion it brings about is inferior. Therefore it has been suggested that the greater tetrahedral distortion induced by COD might hamper the oxidative addition of dihydrogen from the axial position as the required orbital overlap is not easily achieved.

The very small pseudo rate constants observed for the hydrogenation of COD in [Rh(diphosphine)(COD)]$^+$ in MeOH with DPPE and DIPAMP as diphosphine (Table A1) imply that at room temperature and normal pressure 24 and 30 h are necessary, respectively, for the complete removal of the COD in the two catalyst precursors. This confirms previous findings concerning the challenging quantitative hydrogenation of COD [110,111]: failure to recognize these rather long induction periods may lead to underestimation of the real efficiency of the corresponding rhodium/diphosphine catalyst in the hydrogenation of specific substrates, especially in relation to the application of high throughput methods in catalyst testing [112]. The pseudo rate constants are not affected by the counteranion in the catalyst precursor as shown for the ligand BINAP [113].

Despite their low reactivity, COD containing catalyst precursors are readily available and therefore often preferred in industrial applications. It has been shown for the Rh–DuPhos family that this can still be a sensible choice because the difference between the use of COD and NBD precatalysts becomes increasingly insignificant as the substrate to catalyst ratios increase up to values generally implemented in industry (≥10,000) [114].

An elegant experiment which is very sensitive and allows appreciation of the difference in precatalyst activation rates, that is the difference in COD versus NBD hydrogenation, has been devised. The method requires that equimolar amounts of COD and NBD rhodium precursors [Rh(diphosphine)(COD)]$^+$ and [Rh(diphosphine)(NBD)]$^+$, having the same diphosphine ligand but of opposite chirality, are used in the same hydrogenation reaction [114]. Since the precatalysts generate "enantiomeric" catalytic active species, then the closer the overall productivity given by the NBD and COD precatalysts, the closer the product will be to racemic. For example, in the hydrogenation of dimethyl itaconate with Rh/Me–DuPhos under these circumstances (10,000:1 as substrate/catalyst ratio, 5 bar hydrogen pressure), an almost racemic product was obtained indicating that the active catalyst is formed at almost the same rate from both the COD and NBD precatalysts. However, it must be said that, although very low, the recorded enantiomeric excess (ee < 3%) is not negligible when referred to the absolute product amount (911 mg over 30 g in the example reported above).

During exploratory experiments the substrate/catalyst ratio employed is usually 100. Under these conditions, when using the catalyst precursors [Rh((*S*,*S*)-Me-DuPhos)(COD)]BF_4 and [Rh((*R*,*R*)-Me-DuPhos)(NBD)]BF_4 in a 1:1 ratio (0.005 mmol each) in 15 mL MeOH and 1 bar total pressure, the recorded ee is 95.1%. Such value is only slightly lower than the one, 97.4–98% ee, obtained for hydrogenation with only the NBD complex [114]. This can be explained by the fact that the NBD complex is hydrogenated about 320 times faster than the one with COD (Table A1) therefore, when using the equimolar mixture of the two catalyst precursors of opposite chirality, hydrogenation and thus selectivity are determined almost exclusively by the NBD complex.

3.3. Generation of Solvent Complexes

In order to avoid undesirable induction periods and benefit from the full activity expected for the amount of "catalyst" added to the reaction vessel, it is advisable to use solvent complexes having the general formula [Rh(diphosphine)(solvent)$_2$]$^+$. They are prepared through hydrogenation of the corresponding diolefin complexes in the absence of the prochiral olefin. Solvent complexes are also better suited for kinetic investigations. By measuring the rate constant of the precatalyst activation/hydrogenation, it is possible to define the required experimental conditions under which formation of the active species is quantitative before the substrate is added.

While several solvent complexes with different diphosphine ligands have been characterized by ^{31}P NMR spectroscopy, the first X-ray structures of such reactive species have been published only recently [115–117]. In Figure 9 the molecular structures of complex anions [Rh(DPEPhos)(acetone)$_2$]$^+$ and [Rh(BINAP)(THF)$_2$]$^+$ are presented.

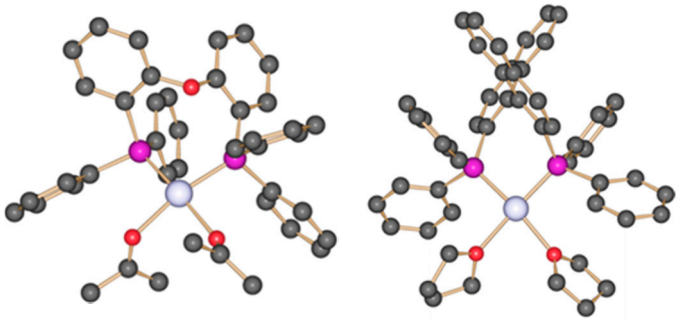

Figure 9. Molecular structure of the cations of the solvent complexes $[Rh(DPEPhos)(acetone)_2]^+$ and $[Rh(BINAP)(THF)_2]^+$. Hydrogen atoms are omitted for clarity.

Besides prochiral olefin hydrogenation, another case in which the use of solvent complexes proved beneficial is the rhodium-promoted asymmetric ring-opening of benzo-7-oxabicyclo-[2.2.1]-heptadiene with nucleophiles. This is an important process for the formation of C–C and C–X bonds which gives access to pharmaceutically relevant hydronaphatelenes. The efficiency and enantioselectivity of the process as originally developed [118] could be improved by using the preformed solvent complex $[Rh((R,S)\text{-PPF-P}(t\text{-Bu})_2)(THF)_2]^+$ instead of the in situ generated dimeric species $[Rh(((R,S)\text{-PPF-P}(t\text{-Bu})_2)(\mu_2\text{-Cl})]_2$ [119].

Data presented in Table A1 allow to calculate for how long the precatalyst $[Rh(diphosphine)(diolefin)]^+$ has to be hydrogenated in order to quantitatively generate the corresponding solvent complex $[Rh(diphosphine)(solvent)_2]^+$ ($t_{1/2} = \ln 2/k'$, seven half lives correspond to 99.2% (practically complete) conversion of the diolefin in $[Rh(diphosphine)(diolefin)]^+$).

If hydrogenation lasts longer, then formation of dinuclear or trinuclear hydride complexes may occur (Figure 10) [120–122].

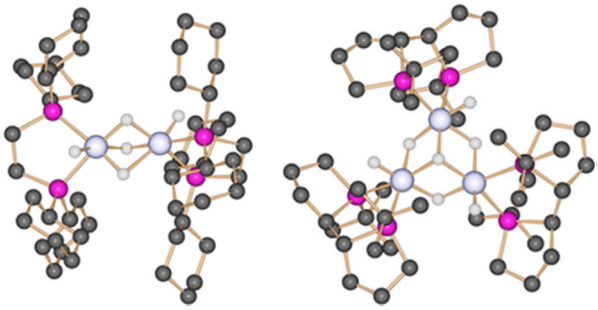

Figure 10. Molecular structure of the hydride complexes $\{[Rh(DCPE)H]_2(\mu_2\text{-H})_3\}^+$, left, and $\{[Rh(Tangphos)H]_3(\mu_2\text{-H})_3\ (\mu_3\text{-H})\}^{2+}$, right. Hydrogen atoms are omitted for clarity.

In some cases the formation of such species starts even before $[Rh(diphosphine)(diolefin)]^+$ is fully hydrogenated. This is the case for the Me–BPE/COD–MeOH system and ^{31}P NMR spectroscopy allows detection of the various species which coexist in solution (Figure 11) [123]. This means that the procedure for the synthesis of the solvent complex is not selective under these conditions. The problem can be solved using the precatalyst $[Rh(Me\text{-BPE})(NBD)]^+$ as hydrogenation of NBD is faster than COD and faster than the formation of polynuclear rhodium hydride.

An alternative entry to the solvent complexes, which circumvents the prehydrogenation step required for diolefin-containing precatalysts and the possible related problems, is represented by ammonia complexes of the general formula $[Rh(diphosphine)(NH_3)_2]^+$ which are very stable species and therefore easy to handle [95]. The solvent complex can be generated in situ by the addition of stoichiometric amounts of acid such as HBF_4 which displace NH_3 as the corresponding ammonium salt (using HBF_4, BF_4^- remains the sole counteranion for any cationic rhodium species in solution). The ammonia precatalyst is in turn easily prepared from $[Rh(diphosphine)(diolefin)_2]^+$ by reaction with a

saturated solution of ammonia. Figure 12 shows the solid state structure of the rhodium ammonia catalyst precursor [Rh((*Sc*,*Rp*)-Duanphos)$(NH_3)_2]^+$.

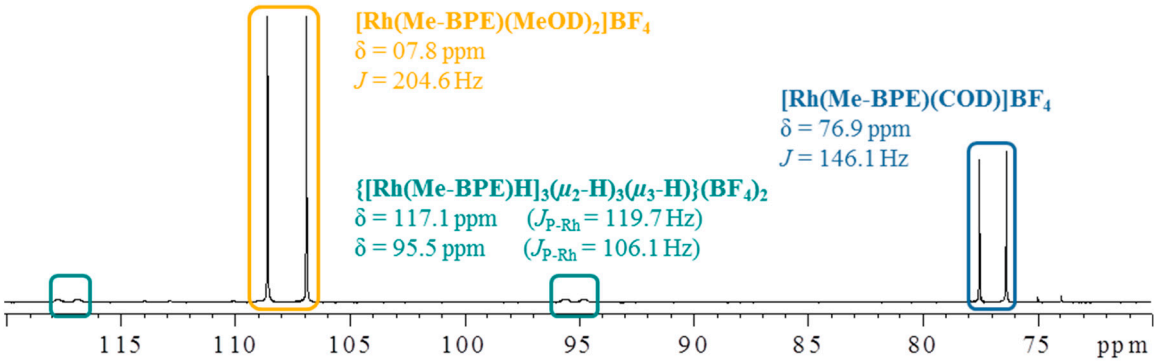

Figure 11. ^{31}P NMR spectrum of the solution obtained following hydrogenation of [Rh(Me-BPE)(COD)]$^+$ in MeOH-d_4 at 25 °C under 1 bar total pressure [123].

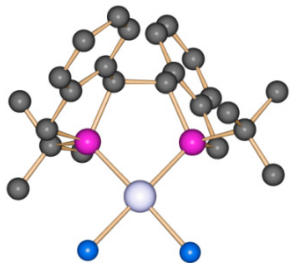

Figure 12. Molecular structure of the rhodium ammonia catalyst precursor [Rh((*Sc*,*Rp*)-Duanphos)$(NH_3)_2]^+$. Hydrogen atoms are omitted for clarity.

This and [Rh((*S*,*S*)-Et-Ferrotane)$(NH_3)_2]^+$ proved to be competent catalysts for the [2+2+2] cycloaddition of selected triynes, providing equal and, in some cases, better selectivity than the corresponding independently generated solvent complexes (Scheme 9) [95].

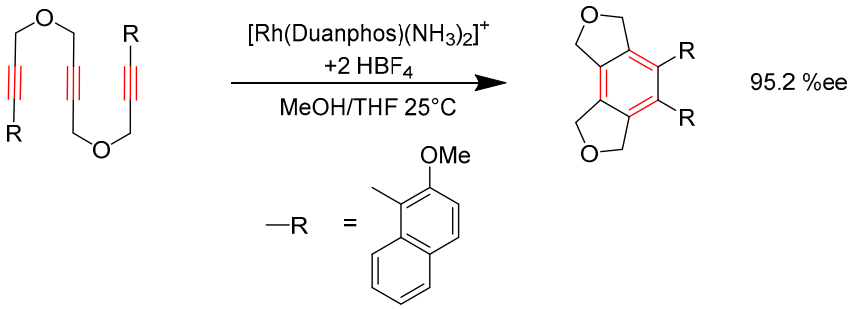

Scheme 9. [2+2+2] Cycloaddition of a triyne catalyzed by the rhodium ammonia catalyst precursor [Rh((*Sc*,*Rp*)-Duanphos)$(NH_3)_2]^+$.

As shown above, hydrogenation of [Rh(diphosphine)(diolefin)]$^+$ in a coordinating solvent such as MeOH or THF generates [Rh(diphosphine)$(solvent)_2]^+$. When the diphosphine is electron-rich, that is the substituents at phosphorus are alkyl rather than aryl groups, it contributes to stabilizing the solvent dihydride species [Rh(diphosphine)$(H)_2(solvent)_2]^+$, now a Rh(III) instead of a Rh(I) species, the product of hydrogen oxidative addition to rhodium. [Rh(diphosphine)$(H)_2(solvent)_2]^+$ can therefore be detected, although in the majority of cases only at sufficiently low temperatures. [Rh(diphosphine)$(H)_2(solvent)_2]^+$ is in equilibrium with the parent solvent complex. Examples of such diphosphines are Tangphos, Me–BPE, and *t*-Bu-BisP* [122–124].

As already mentioned, if the solvent complex is left under a hydrogen atmosphere long enough and its diphosphine ligand lacks aryl substituents which would otherwise trigger the formation of stable arene-bridged dimeric species (vide infra), it evolves into a trinuclear polyhydride species $\{[Rh(diphosphine)H]_3(\mu_2\text{-}H)_3(\mu_3\text{-}H)\}^{2+}$ which instead is stable at room temperature [120–122]. The formation of $\{[Rh(diphosphine)H]_3(\mu_2\text{-}H)_3(\mu_3\text{-}H)\}^{2+}$ from the solvent complex is reversible and must proceed through the rhodium dihydride $[Rh(diphosphine)(H)_2(solvent)_2]^+$ mentioned above [125]. In the context of asymmetric olefin hydrogenation, it has been shown that $\{[Rh(diphosphine)H]_3(\mu_2\text{-}H)_3(\mu_3\text{-}H)\}^{2+}$ transfers its hydrogen to the substrate mac quite slowly, over days, as it very likely must first be converted into a species of lower nuclearity to become catalytically active. The formation of these species then withdraws part of the total initial rhodium concentration, negatively affecting activity [126].

4. Catalysis in the Presence of Strongly Coordinating Ligands

Characteristic of each catalytic reaction, either homogeneous, heterogeneous, or enzymatic, is the formation of a catalyst–substrate complex. Through the key steps of the catalytic cycle and the reaction with further reagents, the catalyst–substrate complex evolves into the catalyst–product complex which eventually releases the desired free product molecule. If other species are present in solution which can also coordinate to the catalyst, then such species—inhibitors—compete with the substrate and reduce the amount of catalyst available for the catalytic process of interest. At a macroscopic level, a reduction of activity is therefore observed.

Also in nature, i.e., in the cells of living organisms, biochemical reactions are accelerated by catalysts, the enzymes. Here, too, catalyst deactivation (inhibition) plays an important role, e.g., in the regulation of the enzyme activity. As shown in Scheme 10, different types of inhibition are possible, depending on whether the free enzyme (k_i/k_{-i}) or the enzyme–substrate complex ($k_{i'}/k_{-i'}$) form an adduct with the inhibiting molecule [127].

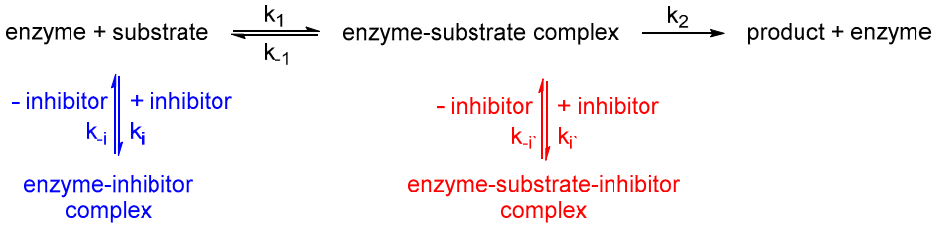

Scheme 10. Competitive, blue, uncompetitive, red, and mixed, blue and red, inhibition in enzyme catalysis.

4.1. Formation of Non-Reactive, Monomeric Species

Well-known inhibitors for cationic Rh-complexes are carbon monoxide CO and diolefins such as COD and NBD, because the corresponding complexes possess very high stability constants. For example, it has been shown that when the hydrogenation of olefins is carried out in primary alcohols with a catalyst prepared in situ from $[Rh(NBD)Cl]_2$ and monophosphines such as PPh_2Et catalyst deactivation takes place due to the formation of $[Rh(CO)(PPh_2Et)_2Cl]$. Under the reaction conditions, 50 °C and 1 bar H_2, the catalyst is also able to promote the reduction of the olefin by transfer of hydrogen from the solvent alcohol. The resulting aldehyde can be decarbonylated by the catalyst with the ensuing formation of $[Rh(CO)(PPh_2Et)_2Cl]$. This species is catalytically inactive. Catalyst deactivation is enhanced at higher temperature and does not take place in the absence of the olefin which acts as hydrogen acceptor, thus promoting the otherwise unfavorable alcohol dehydrogenation [128].

Less known is the fact that molecules which contain aromatic moieties can also act as inhibitors as they form stable η^6-arene rhodium complexes. These are coordinatively saturated 18-electron species which cannot coordinate incoming substrates or undergo oxidative addition and are consequently catalytically inactive. The formation of such species is however reversible; the extent of inactivation is

determined by the concentration of the competing complexing agents present in solution which might displace the coordinated arene and the ratio of the stability constants of the corresponding rhodium complexes. Two representative structures of η^6-arene rhodium complexes are shown in Figure 13. Aromatic amines provide an interesting case: coordination of aniline derivatives to rhodium, for example, takes place through the arene, not through the nitrogen lone pair (Figure 13, right).

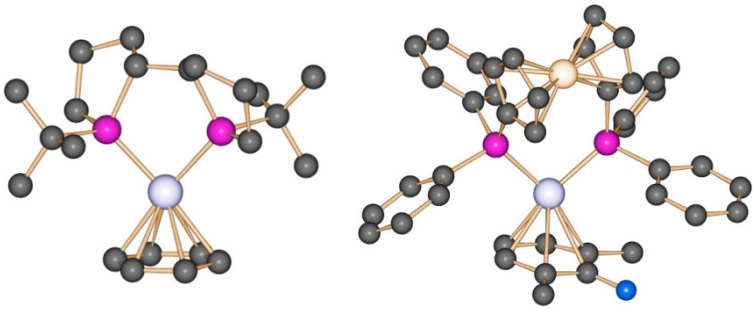

Figure 13. Molecular structure of the cation [Rh(*S*,*S*,*R*,*R*)-Tangphos)(η^6-benzene)]$^+$, left, and of the cation [Rh(DPPF)(2,6-dimethyl-η^6-aniline)]$^+$, right. Hydrogen atoms are omitted for clarity.

The sensitivity of the ^{103}Rh chemical shift to the local organic substituents makes ^{103}Rh NMR spectroscopy a valuable probe to unambiguously assign η^6-arene rhodium complexes [129,130]. Compared to those of the corresponding solvent complexes, the signals of η^6-arene rhodium complexes are shifted to higher fields. ^{103}Rh chemical shifts are also influenced by the size of the chelate ring formed by the coordinated diphosphine [131,132]. The ^{1}H and ^{13}C NMR chemical shifts of the arene provide further evidence of its η^6-coordination to the metal.

The stability of the η^6-arene rhodium complexes as expressed by their stability constants (Scheme 11) can be easily assessed, for example by UV-Vis spectroscopy.

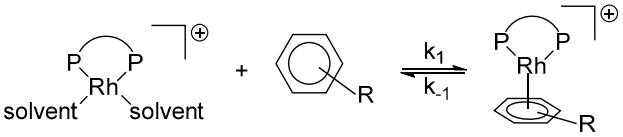

Scheme 11. Equilibrium between solvent complex, free arene, and η^6-arene rhodium complex.

The classical method entails the titration of the solvent complex with the aromatics of interest [133–136]. Alternatively it is possible to monitor and quantify the established equilibrium between the solvent complex and the arene-containing molecule as a function of time; this is done using stopped flow techniques under anaerobic conditions which rely on the use of a diode array [59]. It makes no difference from which side the establishment of the equilibrium is examined: both the solvent complex and the isolated η^6-arene rhodium species can be used as starting material. In either case, the method provides the rate constant for the forward and back reaction, the ratio of which corresponds to the stability constant. The data evaluation is carried out either by graphical [137–140] or numerical methods [141–146]. For the η^6-arene complexes shown in Figure 11, the following values were determined: [Rh(*S*,*S*,*R*,*R*)-Tangphos)$(MeOH)_2$]BF_4/[Rh(*S*,*S*,*R*,*R*)-Tangphos)(η^6-benzene)]BF_4: 70 L/mol; and [Rh(DPPF)$(MeOH)_2$]BF_4/[Rh(DPPF)(2,6-dimethyl-η^6-aniline)]BF_4: 1500 L/mol [136]. Further values, also for the temperature dependence, can be found in reference [136].

The source of aromatics which can act as inhibitors can be diverse and detailed examples can be found in reference [23]. Aromatic solvents like benzene and toluene are often used in catalytic reactions such as hydrogenations. Many benchmark substrates contain phenyl rings that can lead to coordinatively saturated 18 electron η^6-arene complexes. This is the case, for example, of α-acetamidocinnamic acid: for this substrate, the chelate coordination through the double bond and the oxygen of the amido group is by far preferred over coordination of the phenyl ring. However, once

the double bond is reduced, the hydrogenated product coordinates to rhodium through its phenyl substituent and can therefore negatively affect the catalytic activity, especially towards the end of the reaction when its concentration is higher (Figure 14).

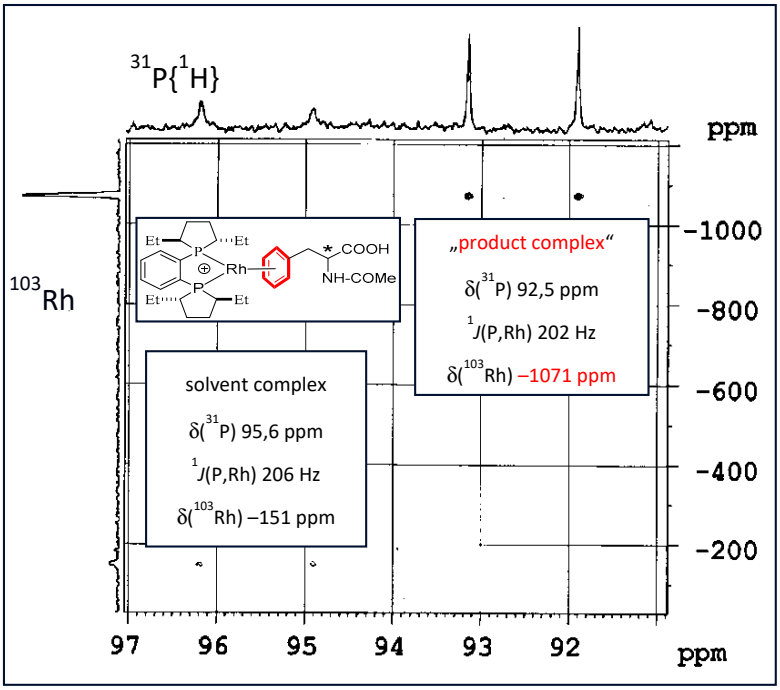

Figure 14. $^{31}P\{^{1}H\}$-^{103}Rh HMQC spectrum of the rhodium-α-acetamidocinnamic acid $(H)_2$ adduct [Rh(Et-DuPhos)(η^6-α-acetamidocinnamic acid $(H)_2$)]$^+$, in MeOH-d_4, its signals are clearly distinguishable from those of the solvent complex [Rh(Et-DuPhos)(solvent)$_2$]$^+$.

A similar catalyst–product complex has been observed also in the course of the asymmetric hydrogenation of mac in methanol with the rhodium catalyst precursor [Rh(*t*-Bu-BisP*)(NBD)]BF_4 containing the purely aliphatic ligand *t*-Bu-BisP* (Scheme 12) [147,148].

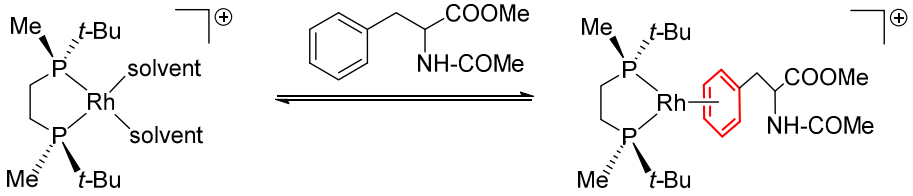

Scheme 12. Equilibrium showing the formation of the rhodium–product complex [Rh(*t*-Bu-BisP*)(η^6-mac$(H)_2$)]BF_4 following the hydrogenation of mac with [Rh(*t*-Bu-BisP*)(NBD)]BF_4.

The concentration of rhodium in the form of the arene complex $[Rh]_{(arene)}$ as compared to the total or initial rhodium concentration $[Rh]_{(0)}$ can be calculated according to Equation (1) [136].

$$[Rh]_{(arene)} = \frac{[Rh]_0}{\left(\frac{K_{substrate}[substrate]}{K_{arene}[arene]}\right) + 1} \quad (1)$$

Examples of calculated values are reported in reference [23]. The equation clearly shows that deactivation is not only a function of the stability constants of both the substrate- and the η^6-arene complex but also depends on the ratio of substrate- to arene-containing species concentrations. Therefore the extent of deactivation is in principle a dynamic variable which can be controlled. In fact the substrate is consumed during catalysis, which of course alters the ratio of concentrations

of substrate- to arene-containing species depending on the degree of conversion. In addition, the effective kinetics, usually of Michaelis–Menten type, influences the macroscopic manifestation of the deactivation process as the following two examples show.

When the stability constant of the catalyst–substrate complex is very low, the reaction rate is 1st order in the substrate concentration. An example is provided by the hydrogenation of dimethyl itaconate with [Rh(Ph-*β*-glup-OH)$(MeOH)_2$]BF_4 in methanol at room temperature and normal pressure. If a "poisoning" arene is present, then only the latter, but not the substrate, can effectively compete with the solvent, that is largely in excess, for the metal (Scheme 10, blue). The methyl ester of aminocrotonic acid, on the other hand, forms a very stable adduct with the catalyst precursor [Rh(DIPAMP)$(MeOH)_2$]BF_4 which implies that the reaction is zero order in the substrate concentration. When its hydrogenation is carried out in methanol at room temperature and normal pressure, then the substrate can effectively compete with the inhibiting arene for the metal (Scheme 10, red) [149]. In the first case, despite the presence of inhibitors, the reaction, while slower, remains 1st order in the substrate concentration and no apparent change takes place. In the second case, inhibition manifests itself with a continuous decrease in reaction rate instead, because the concentration of the inhibitor remains constant during the reaction while that of the prochiral olefin diminishes with increasing conversion. Therefore an important (tacit) assumption of the formal kinetic treatment of catalysis, that the active catalyst concentration remains constant over the course of the reaction, no longer applies.

Aromatic moieties are also present in polystyrene, commonly used to provide an insoluble support to homogeneous Rh catalysts in order to facilitate their separation from the reaction medium and subsequent reuse. In the case of cationic rhodium complexes, the weakly coordinating counteranion can be replaced by a "polymerizable" one. In this way, the unmodified homogeneous catalyst is attached to the polymer by ionic interactions [150,151]. Alternatively, the diphosphine ligand can be properly derivatized to be covalently attached to a polystyrene support [152–158].

Using soluble, low molecular weight polystyrenic resins, the formation of aromatic complexes with the phenyl rings of the "carrier" could be demonstrated by means of ^{103}Rh NMR spectroscopy. It was also possible to determine the corresponding stability constants which, although not very high, are "compensated" for by the high "concentration" of the phenyl rings. For the complex [Rh(*Et*-DuPhos)(η^6-PS30000)]BF_4 the measured equilibrium constant in acetone is 17 L/mol—PS30000 is a polystyrene soluble in THF which contains 288 monomer units. Such a stability constant is comparable with that of the related complex [Rh(DPPE)(η^6-benzene]BF_4, 18 L/mol [58,133]. If part of the Rh is bound to the resin as the η^6-coordinated aromatic complex, this is at least the case if Rh is bound to the support by ionic interaction, then the latter is in equilibrium with the solvent complex (Scheme 13) and can be washed out from the resin if the resin is rinsed with the solvent after catalyst loading and recycling [159]. Quantitative estimations of metal leaching can be found in reference [159].

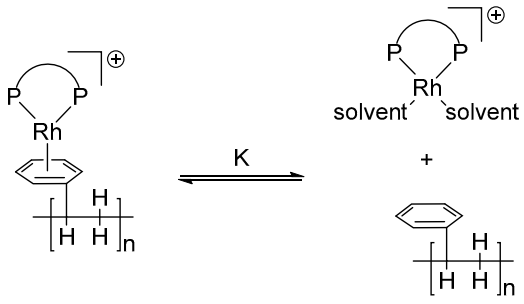

Scheme 13. Equilibrium between the η^6-arene coordinated Rh complex and the solvent complex and the polystyrene polymer matrix.

This gives rise to the well-known problem of "Rh leaching". Each time the resin is rinsed with fresh solvent, a new equilibrium is established that can lead to a further loss of the metal bound to the polystyrene support. This effect is essentially unavoidable.

The hydrogenation of prochiral organic substrates like itaconic acid and dimethyl itaconate can be carried out in aqueous solution in the presence of surfactants like sodium dodecyl sulfate, SDS or, 4-(*1,1,3,3*-Tetramethylbutyl)*phenyl*-polyethylene glycol, Triton X-100. The resulting micelles can be recycled by membrane ultrafiltration [160]. For the rhodium-BPPM/dimethyl itaconate system, the TOF decreases as the Triton X-100 concentration is increased. Selectivity, 60% ee in MeOH, is unaffected. A singlet in the ^{103}Rh NMR spectrum at −1006 ppm suggests the formation of a new η^6-arene complex. Furthermore, in the ^{1}H NMR spectrum the signals for the aromatic hydrogens are shifted to higher fields than expected for the free arene: 7.17, 6.98, 6.37, and 6.05 ppm [160]. The observed catalyst deactivation could then be confidently ascribed to the formation of η^6-arene complexes between rhodium and the phenyl substituents in the additive Triton X-100.

4.2. Formation of Non-Reactive, Multinuclear Species

Dinuclear Species

In 1977 the dimerization of the solvent complex $[Rh(DPPE)(MeOH)_2]^+$ leading to $[Rh(DPPE)]_2^{2+}$ was described for the first time [133]. In the dimer, each DPPE acts as a bridging ligand between the two rhodium centers; it is chelated to one metal through the phosphorus donors and it is coordinated to the second one through one of the phenyl substituents on the phosphorus. Other dimeric rhodium complexes, featuring a similar coordination pattern, which of course is available only when the ligand contains aryl substituents, have been reported, for both bidentate [161–167] and monodentate phosphines [96,168–172]. For the ligands BINAP, Synphos, and DIPAMP the structures of such dimeric species have been thoroughly characterized by means of NMR and X-ray crystallography [116,117,173]. The crystal structure of $[Rh(BINAP)]_2^{2+}$ is presented in Figure 15.

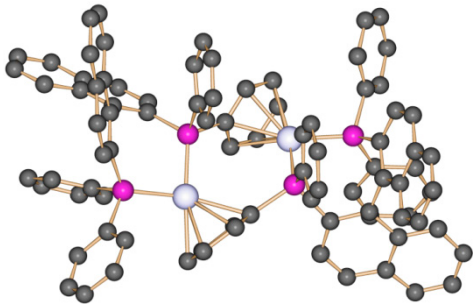

Figure 15. Molecular structure of $[Rh((R)\text{-Binap})]_2^{2+}$. Hydrogen atoms are omitted for clarity.

Such dimers have found application as catalyst precursors, for example in hydroacylation [163,174,175]. They are usually generated in situ in a nonpolar solvent, either DCM or dichloroethane, by hydrogenation of a cationic bis-diolefin rhodium complex, for example, $[Rh(COD)_2]OTf$, in the presence of a diphosphine like BINAP. ([2+2+2]cycloadditions: [176–184], hydrogen-mediated reductive C-C coupling: [185–187], enantioselective reductive cyclization: [188,189], intermolecular cyclotrimerization: [190–193]) It should be noted that the formation of these species and their role in catalysis is often overlooked.

These dimers are saturated 18 electron species which must dissociate into monomers in order to generate a catalytically active species. Such dissociation is hampered by their high stability—the stability constant of $[Rh(DIPAMP)]_2^{2+}$ for example is 52 L/mol [173]—a feature which might negatively affect the catalytic activity. An illustrative example is provided by the rhodium/BINAP promoted reductive cyclization of 1,6 diynes in DCM under a hydrogen atmosphere [194]. Kinetic investigations show that the reaction rate is independent of both the diyne and hydrogen concentration (zero partial order to each): it does not change when, at constant catalyst concentration, the catalyst/enzyme ratio is varied from 1:33 to 1:650 (Figure 16, left) and the hydrogen pressure increases from 1 up to 11 bars (Figure 16, right). More importantly, catalyst productivity increases at lower catalyst loadings [194].

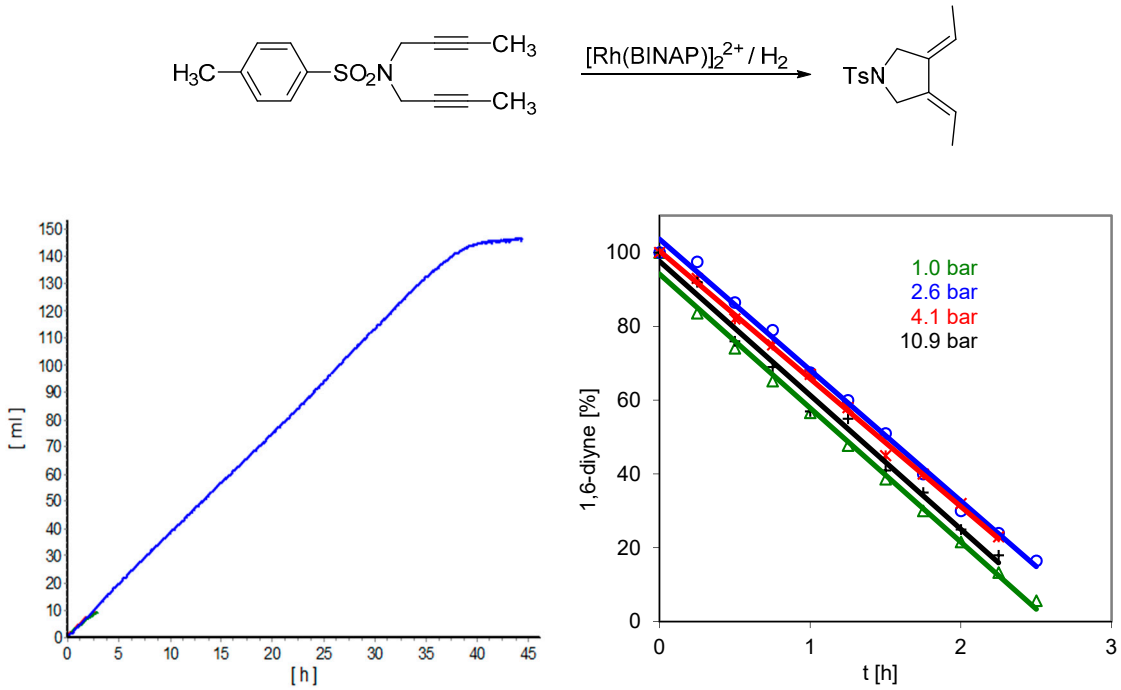

Figure 16. Rh/BINAP promoted cyclization of 1,6-diyne in DCM under a hydrogen atmosphere: hydrogen consumption (ml) as a function of time (h), left (0.01 mmol catalyst ($[Rh(BINAP)]_2^{2+}$), 0.33 or 3.30 mmol diyne, 25 °C in 10 mL DCM at normal hydrogen pressure). 1,6-diyne conversion in % as a function of time, at different hydrogen pressures, right (0.01 mmol catalyst ($[Rh(BINAP)]_2^{2+}$), 0.33 mmol diyne, 25 °C in 20 mL DCM at different hydrogen pressures).

These experimental findings can be easily accounted for if generation of the catalytically active species from the dimeric precursor $[Rh(BINAP)]_2^{2+}$ is the rate-determining step (Scheme 14). Because the steps which make up the catalytic cycle occur after the rate-determining step, disclosure of the actual reaction mechanism is difficult.

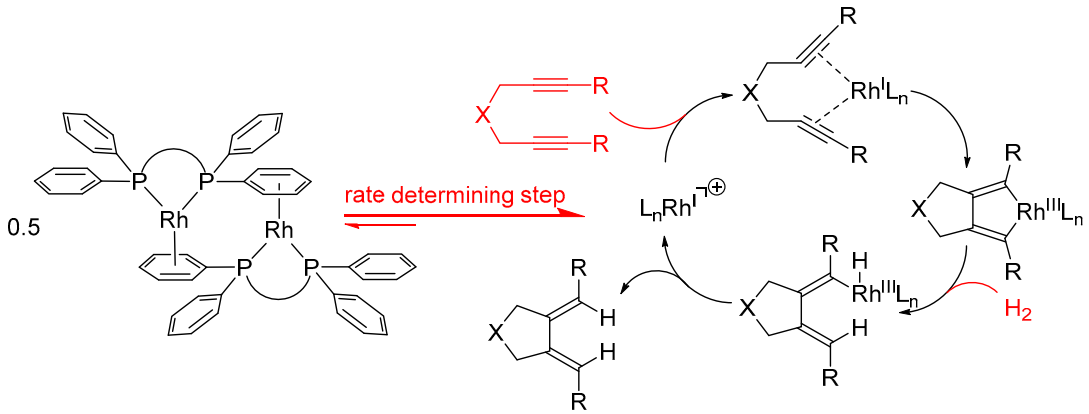

Scheme 14. Mechanism of rhodium/BINAP promoted reductive cyclization of 1,6-diyne in DCM under a hydrogen atmosphere. [195]

Based on this knowledge, the formation of such dimeric species could be prevented by carrying out the reaction in a coordinating solvent, thus preventing the formation of the arene bridged complex in favor of the solvent complex. As shown in Figure 17, by using THF or MeOH, activity could be improved by a factor of ca. 20.

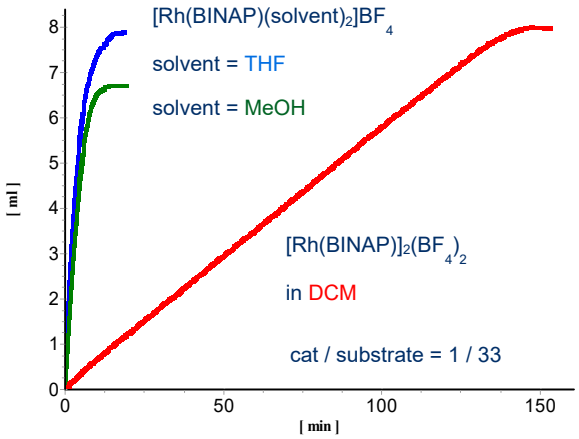

Figure 17. Hydrogen uptake (ml) as a function of time (min) in the reductive cyclization of 1,6 diyne as promoted by [Rh(BINAP)(THF)$_2$]BF$_4$ in THF, blue curve, [Rh(BINAP)(MeOH)$_2$]BF$_4$ in MeOH, green curve, and [Rh(BINAP)]$_2$(BF$_4$)$_2$ in DCM, red curve. In all cases reactions were run using 0.01 mmol catalyst ([Rh(BINAP)]$_2^{2+}$), 0.33 mmol diyne, at 25 °C in 10 mL solvent under normal hydrogen pressure.

Arene complexes can also play an important role in Rh-catalyzed cross-coupling reactions. Cross-coupling reactions are traditionally promoted by palladium catalysts, yet cationic diphosphine rhodium complexes have been shown to be also competent catalysts for this important transformation [196]. The oxidative addition of haloarenes to rhodium complexes supported by monophosphine [197–200], diphosphine [201], pincer [202–208] and multidentate nitrogen ligands [209,210] has been studied in depth and is assumed to be the first important elementary step in the catalytic cycle of the Suzuki–Miyaura coupling reaction between haloarenes and arylboronic acids. Transmetallation by the nucleophilic partner and subsequent reductive elimination to generate the new C–C bond complete the cycle. When the rhodium catalyst is generated in situ using ligands such as DIPAMP and DPPE, the yields of the biaryl product are strongly affected by the type of aryl halide: it is excellent in the case of iodobenzene (>97%), decreases with bromobenzene (>71%), and is poor with chlorobenzene (4–8%), a trend reflecting previous findings [196]. The stability of the η^6-arene complex [Rh(DIPAMP)(η^6-biphenyl)]BF$_4$ with the product biphenyl was determined at room temperature by UV-Vis spectroscopy and is 200 L mol^{-1}. In contrast, the stability constant of the η^6-arene complex [Rh(DIPAMP)(η^6-C$_6$H$_5$Cl)]BF$_4$, the formation of which precedes the oxidative addition of the substrate chlorobenzene to rhodium, is only 0.6 L mol^{-1} (Scheme 15). Therefore, in the case under investigation, the poor yield is not only due to the unfavorable activation of the strong C–Cl bond in the substrate, but also to product inhibition. Indeed the active catalyst is completely deactivated after only a few catalytic cycles [196].

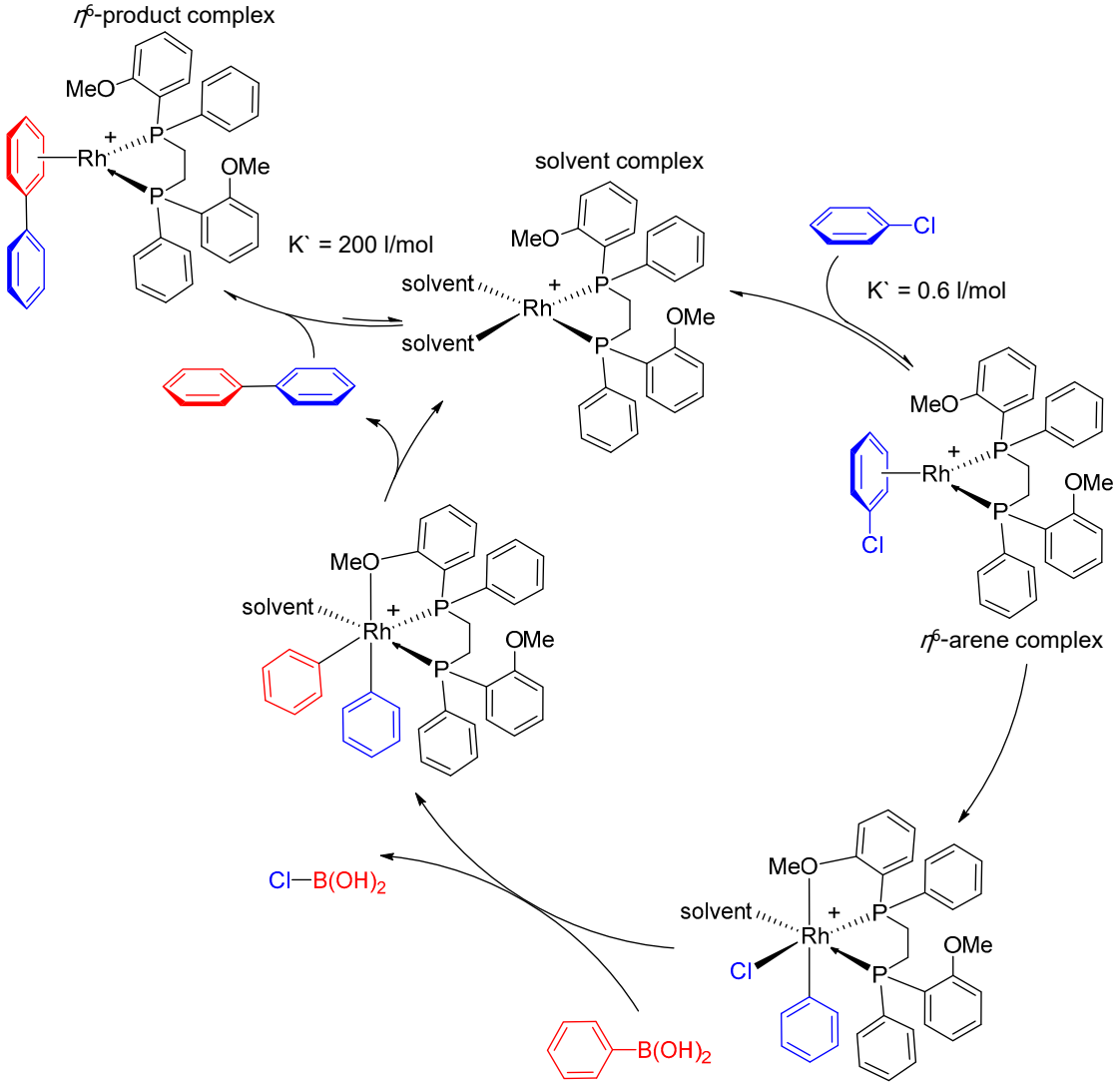

Scheme 15. Proposed catalytic cycle for the rhodium/DIPAMP promoted cross-coupling of chlorobenzene with phenylboronic acid.

4.3. Trinuclear Complexes

Addition of a base to the solvent complex $[Rh(diphosphine)(solvent)_2]^+$ leads to the formation of trinuclear rhodium complexes of the general formula $[Rh_3(diphosphine)_3(\mu_3\text{-}X)_2]^+$ ($X = OMe^-$, OH^- ...). The first example was reported with the ligand DPPE in MeOH [133]. Similar complexes with ligands like *t*-Bu-BisP*, Synphos, BINAP, Me-DuPhos, DIPAMP, and DPPP were published later [40,117,211,212]. In this complex type, an example of which is shown in Figure 18, the three rhodium atoms lie at the vertexes of a regular triangle, each coordinated to a bidentate diphosphine located perpendicular to the Rh_3 plane. Above and below the plane are the two μ_3-bridging anions.

Scheme 16 introduces the general reaction sequence, initially considered as irreversible [211], whereby the trinuclear complexes are formed starting from the solvent complex. In-depth investigations have shown that each step of such sequence is, in principle, reversible [213].

The base is necessary in order to generate the bridging anions either from the solvent (MeO^-) or from adventitious water present in solution (OH^-). ^{103}Rh NMR allows distinguishing among the different species that may be formed with the ligand Me–DuPhos: $[Rh_3(Me\text{-}DuPhos)_3(\mu_3\text{-}OMe)_2]BF_4$, $[Rh_3(Me\text{-}DuPhos)_3(\mu_3\text{-}OMe)(\mu_3\text{-}OH)]BF_4$ and $Rh_3(Me\text{-}DuPhos)_3(\mu_3\text{-}OH)_2]BF_4$ as illustrated in Figure 19.

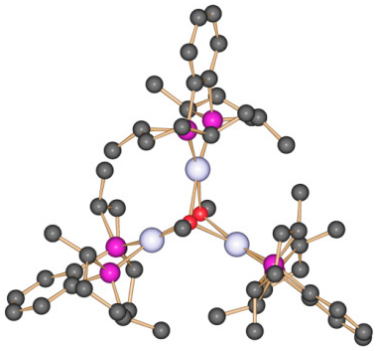

Figure 18. Molecular structure of the cation $[Rh_3(Me\text{-}DuPhos)_3(\mu_3\text{-}OMe)_2]^+$. Hydrogen atoms are omitted for clarity.

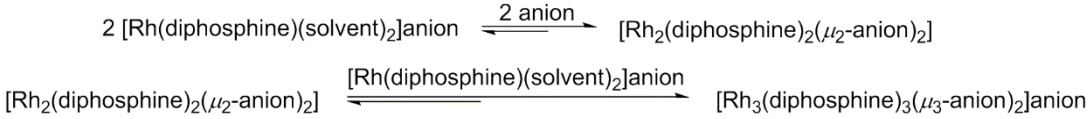

Scheme 16. General, reversible reaction sequence for the generation of μ_3-anion bridged trinuclear complexes.

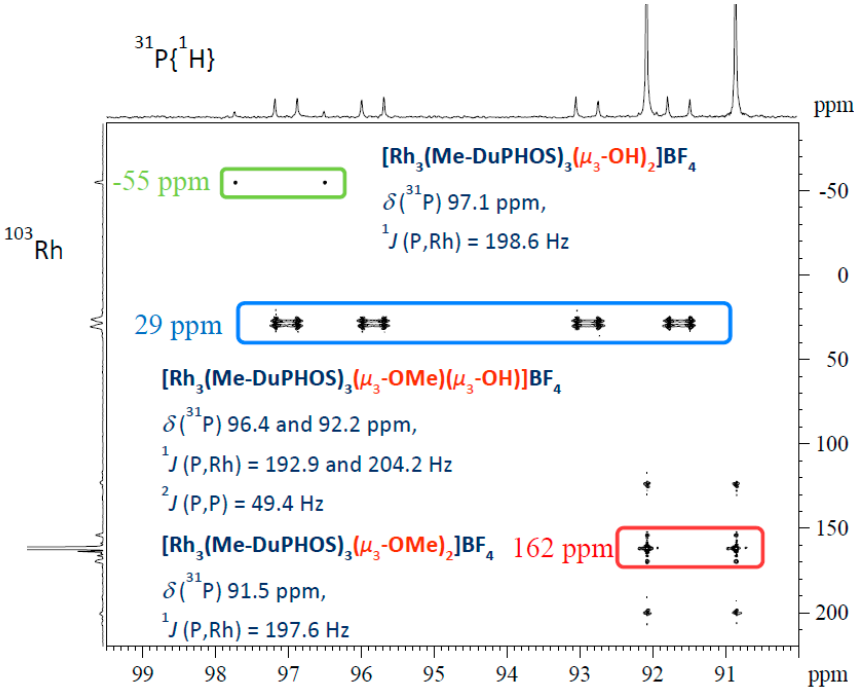

Figure 19. $^{31}P\{^1H\}$-^{103}Rh HMQC spectrum in MeOH-d_4 of the trinuclear species arising from treatment of $[Rh(Me\text{-}DuPhos)(MeOH)_2]BF_4$ with NEt_3/H_2O (1:1) [195].

In the course of Rh promoted catalytic hydrogenation, the formation of such species, which is manifested through a change in the color of the solution from orange to red-brown, leads to a reduction in catalytic activity [212]. Substrates which are sufficiently basic can also trigger the formation of such species, in the absence of any added base! The negative effect on activity though might be difficult to recognize. An example is provided by [2-(3-methoxy-phenyl)-cyclohex-1-enylmethyl]-dimethylamine [214]. When $[Rh(DIPAMP)(MeOH)_2]^+$ is added to a solution of this olefin at room temperature in a ratio 1:20, then NMR spectroscopy shows that up to 75% of the total rhodium content is present as $[Rh_3(DIPAMP)_3(\mu_3\text{-}OMe)_2]^+$ and, to a minor extent, as $[Rh_3(DIPAMP)_3(\mu_3\text{-}OMe)(OH)]^+$ (Figure 20) [40].

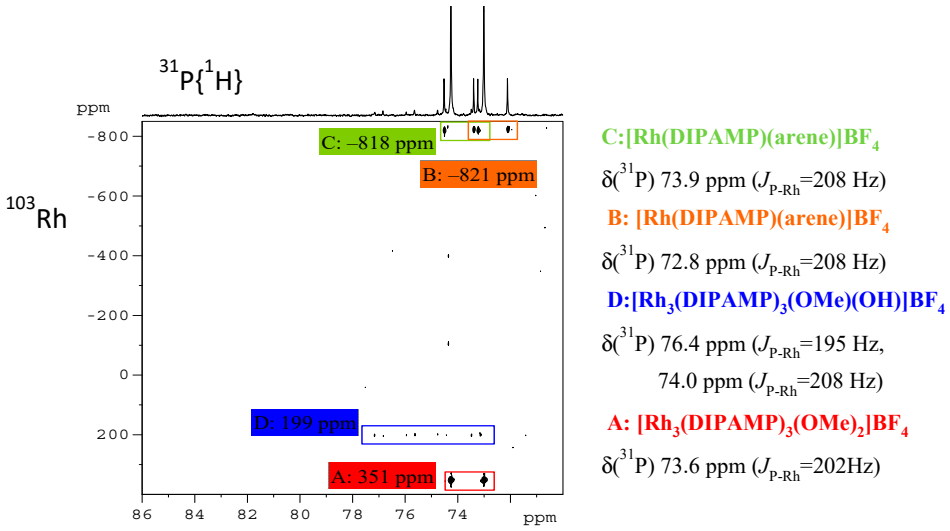

Figure 20. ^{31}P–^{103}Rh correlation spectrum of a mixture of the solvent complex [Rh(DIPAMP)(MeOH)$_2$]BF$_4$ (0.02 mmol) and 100 µL [2-(3-methoxyphenyl)-cyclohex-1-enylmethyl]-dimethylamine (0.4 mmol). The signals highlighted in red and blue correspond to the (μ_3-OMe)$_2$ and (μ_3-OMe)(μ_3-OH) bridged trinuclear complexes (75%), the signals highlighted in green and orange are due to diastereomeric arene complexes (25%). The substrate (purity of >99%) contains traces of water which lead to the formation of the mixed trinuclear complex [40].

Other examples, including the substrate (*E*)-1-(2-methyl-3-phenylallyl)piperidine, are described in reference [212].

Halides have also been recognized as possible sources of deactivation in reactions catalyzed by rhodium complexes. In the asymmetric hydrogenation of 2-methylenesuccinamic acid promoted by [Rh((*S*,*S*)-Et-DuPHOS)(COD)]BF$_4$ [215] activity could be increased by a factor of 26 when the substrate was thoroughly purified from chloride contaminants, leftovers from its synthesis [216]. The reduced activity in the presence of halides may be ascribed to the formation of very stable trinuclear rhodium complexes where halides act as μ_3-bridging anions [40]. The molecular structures of [Rh$_3$((*R*,*R*)*t*-Bu-BisP*)$_3$(μ_3-Cl)$_2$]$^+$ and [Rh$_3$((*R*,*R*)-Me-DuPhos)$_3$(μ_3-Br)$_2$]$^+$ are presented in Figure 21.

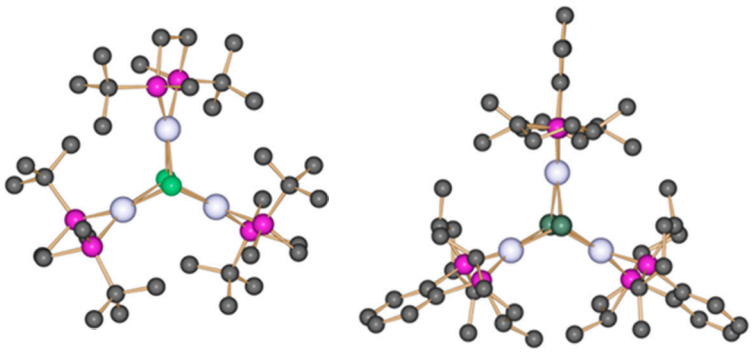

Figure 21. Molecular structures of the cations of [Rh$_3$((*R*,*R*)-*t*-Bu-BisP*)$_3$(μ_3-Cl)$_2$]$^+$, left, and [Rh$_3$((*S*,*S*)-Me-DuPhos)$_3$(μ_3-Br)$_2$]$^+$, right. Hydrogen atoms are omitted for clarity.

Such complexes are catalytically inactive; this was proven experimentally in the asymmetric hydrogenation of mac and dimethyl itaconate with the solvent complex [Rh(DIPAMP)(MeOH)$_2$]$^+$ in the presence of added sodium halides (Cl, Br, I) (Figure 22) [40].

Indeed, when [Rh(DIPAMP)(MeOH)$_2$]BF$_4$ and the prochiral olefin ((*Z*)-3-[1-(dimethylamino)-2-methylpent-2-en-3-yl]phenol) [217] are dissolved in MeOH-d_4 in a 1:10 ratio, the ^{31}P NMR spectrum of the resulting solution shows that almost 34% of the total signal intensity corresponds to the catalytically

inactive trinuclear μ_3-chloro-bridged complex $[Rh_3(DIPAMP)_3(\mu_3\text{-}Cl)_2]BF_4$, resulting from traces of chloride left in the substrate after its synthesis (Figure 23) [40]. Similar to the competitive inhibition in enzymatic catalysis (Scheme 10) halides compete with the substrate for the solvent complex: the amount of trinuclear complex and the extent of deactivation it causes depend on the relative concentrations of halides and the substrate and on the stability constants of the complexes they form with the metal. To prevent deactivation, special attention should therefore be paid to substrate purification, especially on the industrial scale where, due to economical reasons, very high substrate to catalyst ratios are used.

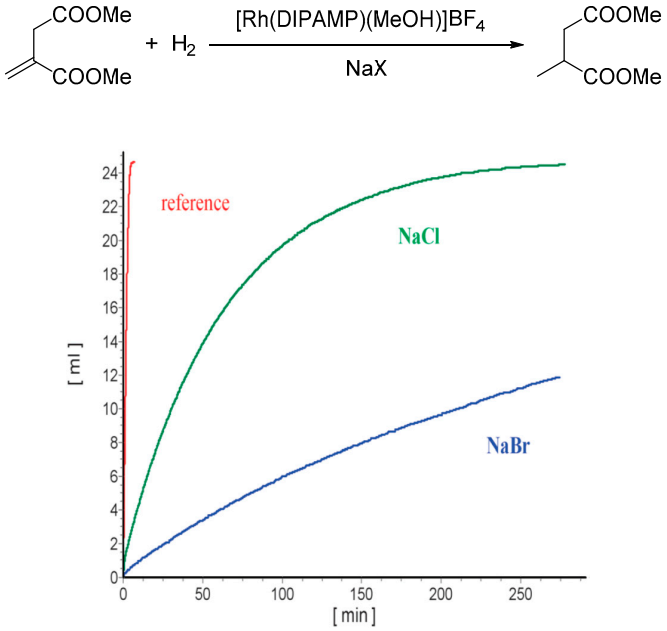

Figure 22. Hydrogen consumption (ml) for the hydrogenation of 1.0 mmol dimethyl itaconate with 0.01 mmol $[Rh(DIPAMP)(MeOH)_2]BF_4$ under addition of different sodium halides NaX: red: no additive (88% ee); green: 0.1 mmol NaCl, (82% ee); blue: 0.1 mmol NaBr, (80% ee); conditions: each 15 mL MeOH at 20 °C and 1 bar total pressure.

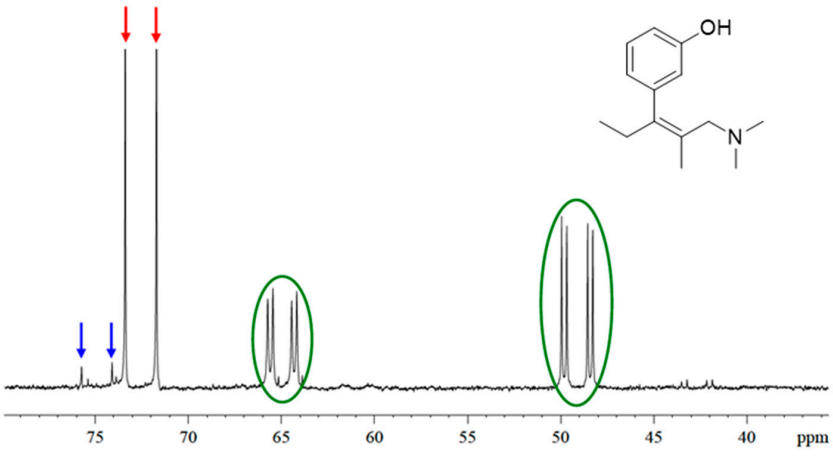

Figure 23. $^{31}P\{^1H\}$ NMR spectrum of a solution of $[Rh(DIPAMP)(MeOH\text{-}d_4)_2]BF_4$ and (3-[(2*R*,3*S*)-1-(dimethylamino)-2-methylpentan-3-yl]phenol (rhodium: substrate = 1:10). About 34% of the signal intensity (red arrows) is due to the doublet of the trinuclear complex $[Rh_3(DIPAMP)_3(\mu_3\text{-}Cl)_2]BF_4$. The signal set highlighted with blue arrows (2% of signal intensity) is due to the dinuclear complex $[Rh_2(DIPAMP)_2(\mu_2\text{-}Cl)_2]$). Highlighted in green is the substrate complex $[Rh(DIPAMP)(substrate)]BF_4$.

5. Catalyst Deactivation due to Irreversible Reactions of the Active Catalyst

Already in 1979 it was reported that the rate of itaconic acid hydrogenation with the rhodium–DIPAMP catalyst in methanol decreases with increasing substrate concentration [218]. Systematic investigations have shown that the substrate can react irreversibly with the catalyst to generate a Rh(III) alkyl complex. This represents a dead-end of the catalytic cycle because oxidative addition of molecular hydrogen is formally not possible on a Rh(III) complex. The inactive species has been thoroughly characterized and its molecular structure was unambiguously assigned by X-ray analysis [219,220]. Its rate of formation is influenced by substrate concentration, temperature, hydrogen pressure, and the presence of additives, either acidic or basic. The likely mechanism through which it is formed includes deprotonation of the β-carboxylic group of the coordinated substrate which leads to the formation of a rhodium–carboxylate bond, thus generating a neutral catalyst-substrate complex (Scheme 17). This step is obviously promoted by basic additives such as NEt_3. Next the OH of the α-carboxylic group oxidatively adds to rhodium generating a Rh(III) hydride species. Finally the double bond inserts into the Rh–H bond generating the Rh(III) alkyl complex.

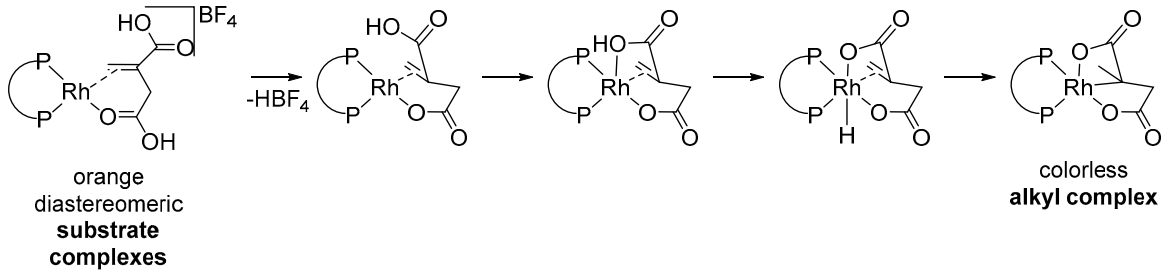

Scheme 17. Likely mechanism through which catalytically inactive Rh(III) alkyl complexes are formed during the hydrogenation of itaconic acid with cationic rhodium–diphosphine complexes.

This might be regarded as a general deactivation path which, regardless of the diphosphine ligand, could be open to other unsaturated substrates carrying carboxylic groups, as was shown for example for 2-acetamidoacrylic acid [221]. The catalytically inactive species resulting from the reaction of the latter with $[Rh(DPPE)(MeOH)_2]BF_4$ could be isolated and the presence of a Rh–C bond was confirmed by X-ray analysis: the Rh(III) alkyl complex, which is present in solution as a monomeric species as suggested by NMR investigations, crystallizes as a dimer with one carboxylate group acting as bridging ligand between the two rhodium centers. Interestingly this example demonstrates that one carboxylate group suffices to promote the formation of the inactive Rh(III) alkyl species (Figure 24).

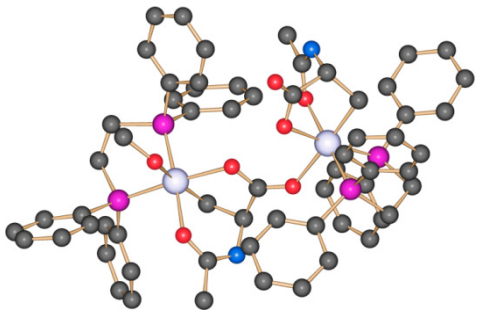

Figure 24. Solid state structure of the dimeric Rh(III)–alkyl complex arising from the reaction of 2-acetamidoacrylic acid with $[Rh(DPPE)(MeOH)_2]BF_4$, left. Hydrogen atoms are omitted for clarity.

Further investigations are needed to assess to what extent this deactivation path is open to other unsaturated substrates containing a carboxylic group. As to itaconic acid, it has been shown that the formation of inactive Rh(III) alkyl species represents a severe limitation [221] to the application of

cloud point extraction as a methodology to extract the catalyst active form from micellar solutions in order to recycle it [222].

Not only the substrate but also other reaction components can irreversibly react with the catalytically active species. This is the case for halogenated solvents as Rh(I) complexes can activate C–X bonds (X = halogen) and hence undergo oxidative addition [223]. DCM is a solvent frequently applied in catalysis but a perusal of the literature shows how this might not always be a sensible choice. Examples of DCM oxidative addition to dimeric rhodium complexes of the type [Rh_2(diphosphine)$_2$(μ_2-Cl)$_2$] are scarce, and for a long time only one example was known for the ligand DPPE [224], but more have been reported for neutral monomeric rhodium complexes such as Rh(I)-β-diketonate/diphosphine derivatives with the ligands DPPM, DPPE, and DPPP [225] and for [Rh(DMPE)$_2$Cl] [226]. Very electron-rich centers are required to promote breaking of the strong C–Cl bond. The activation of halobenzenes has been documented for cationic monomeric rhodium complexes with both di-[209,210] and monophosphines [197–200]. Several species can be formed following the oxidative addition of DCM to rhodium [227,228]: such species can be mononuclear and contain a terminal CH_2Cl group. They can be dinuclear and each rhodium center can have a terminal CH_2Cl group; they can be dinuclear and contain a bridging μ_2-CH_2 which results from the activation of both C–Cl bonds of CH_2Cl_2. The X-ray structures of two examples are reported in Figure 25 [229]

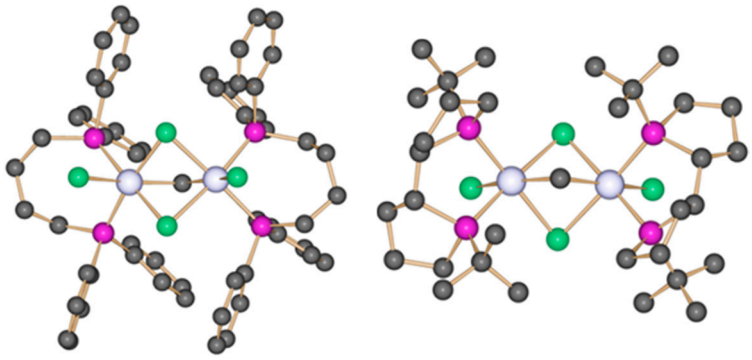

Figure 25. Molecular structure of [Rh_2(DPPB)$_2$(μ_2-Cl)$_2$(μ_2-CH_2)Cl_2], left, and [Rh_2((*1S,1S′,2R,2R′*)-TangPhos)$_2$(μ_2-Cl)$_2$(μ_2-CH_2)Cl_2], right. Hydrogen atoms are omitted for clarity.

The dinuclear species may also arise from further reaction of mononuclear rhodium complexes which have undergone DCM oxidative addition. The exact mechanism for the activation of DCM by neutral dimeric rhodium complexes stabilized by diphosphine ligands is not known but plausible pathways are shown in Scheme 18.

An issue, the consequences of which are often overlooked, is the establishment of the exact nature of the catalytically active species generated from the catalyst precursor. In the case of [Rh_2(diphosphine)$_2$(μ_2-Cl)$_2$], it is generally assumed that the dimeric precatalyst generates a highly reactive 14 electron monomeric species which initiates the catalytic cycle. This monomerization has been calculated for example for the ligand DPEPhos [64]. Simple metathesis experiments (Scheme 19) provided experimental evidence of the monomerization process [60,229].

On the other side in principle, a reversible equilibrium also exists between the classical cationic mononuclear Rh complexes [Rh(diphosphine)(solvent)$_2$]$^+$ and the dimeric neutral Rh complexes [Rh_2(diphosphine)$_2$(μ_2-Cl)$_2$], as described by the upper part of Scheme 16 [230]. With ammonia this reaction is irreversible (Scheme 20) [213]. This implies that, when discussing the mechanism of a catalytic cycle promoted by the dinuclear neutral species [Rh_2(diphosphine)$_2$(μ_2-Cl)$_2$], then the possibility of a mononuclear cationic species contributing to the observed activity should be taken into consideration.

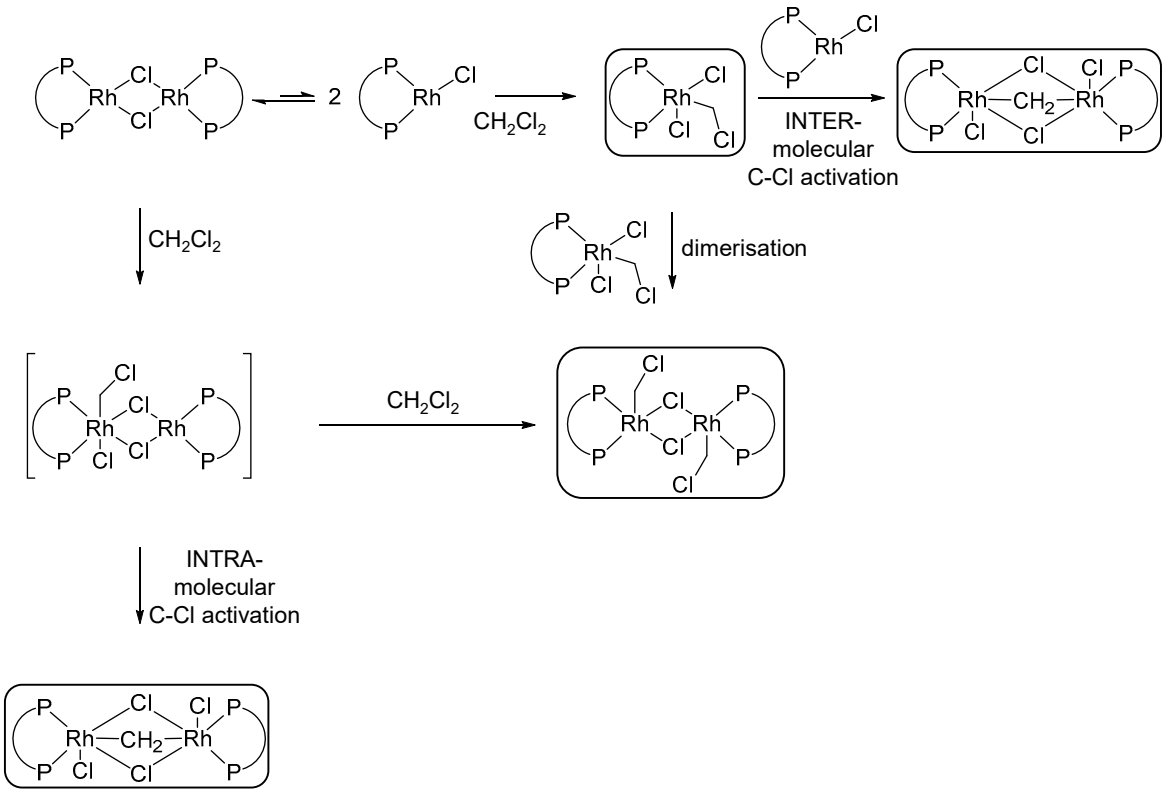

Scheme 18. Possible pathways for the oxidative addition of DCM to preformed neutral, dimeric Rh-complexes.

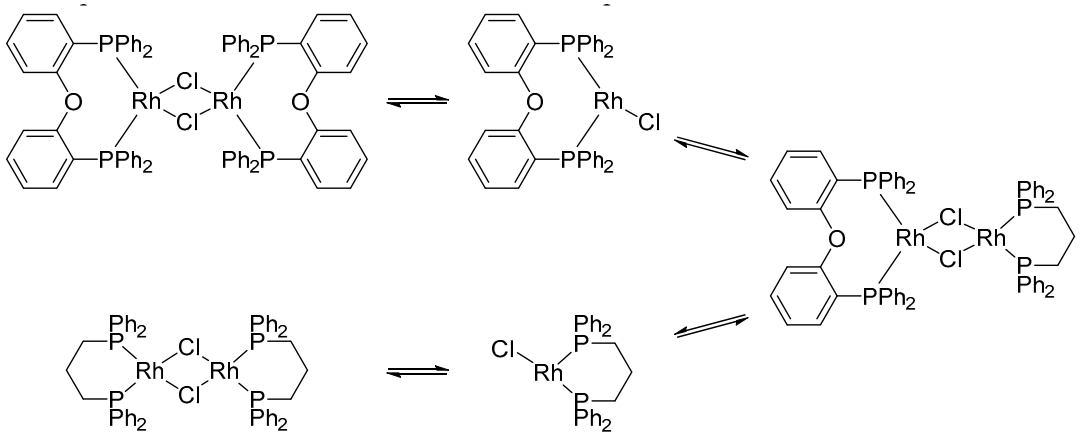

Scheme 19. Dimer–monomer equilibrium for complexes of the type $[Rh_2(diphosphine)_2(\mu_2\text{-}Cl)_2]$ for the ligands DPPP and DPEPhos. Experimental evidence based on ^{31}P NMR showing the formation of a dinuclear mixed species $[(DPPP)Rh((\mu_2\text{-}Cl)_2Rh(DPPE)]$ from the mononuclear fragments [(DPPP)RhCl] and [Rh(DPPE)Cl].

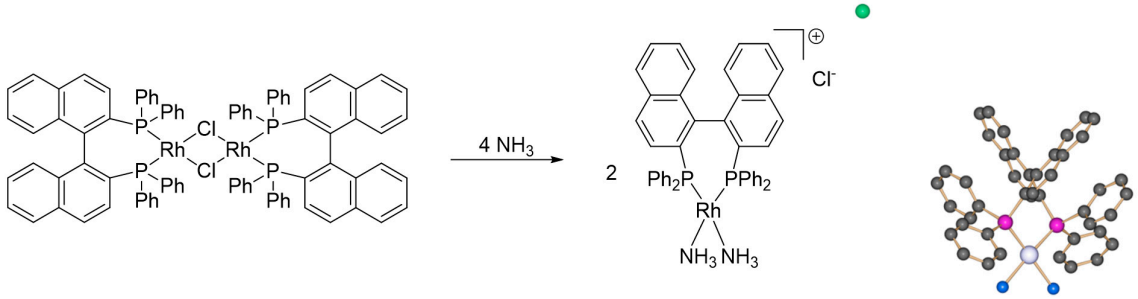

Scheme 20. Reaction scheme for the observed conversion of a dinuclear μ_2-chloro bridged complex into a monomeric cationic one, left, and the molecular structure of the resulting complex [Rh(BINAP)(NH_3)]Cl, right.

6. Conclusions

In the present work, the rich chemistry of rhodium/phosphine complexes, which are applied as homogeneous catalysts to promote a wide range of chemical transformations, has been used to showcase how the in situ generation of precatalysts, the conversion of precatalysts into the actually active species, as well as the reaction of the catalyst itself with other components in the reaction medium (substrates, solvents, additives) can lead to a number of deactivation phenomena. Such phenomena may go unnoticed or may be overlooked, thus preventing the full understanding of the catalytic process which is a prerequisite for its optimization.

As a summary of the discussion reported above, a few guidelines are presented here which may help the practitioner in the early stages of his/her investigation into a catalytic process promoted by rhodium–diphosphine catalysts.

The in situ preparation of a catalyst precursor from a suitable metal source and the desired ligand is very convenient in the screening of ligand libraries and reaction conditions. Yet fine-tuning of a catalytic process should include a detailed knowledge of the actual species generated during the in situ procedure. In the case of rhodium, the in situ generation of the catalyst precursor [Rh(diphosphine)(μ_2-X)]$_2$ (X = Cl−, OMe−, OH− ...) from [Rh(diolefin)(μ_2-X)]$_2$ and the corresponding diphosphine can in fact be far from selective and it is strongly dependent of the type of diphosphine, diolefin and reaction conditions. As a practical guide for the choice of proper reaction conditions, relevant information for the most common diphosphines can be found in reference [9a] and the relative supporting information.

The hydrogenation of prochiral olefins is promoted by catalyst precursors of the general formula [Rh(diphosphine)(diolefin)]$^+$ (dioelfin = COD, NBD). Generation of the active species [Rh(diphosphine)(solvent)$_2$]$^+$, in a proper solvent, requires hydrogenation of the diolefin. NBD-containing precursors are to be preferred as NBD is hydrogenated faster than COD. Prior to the addition of the substrate, the pre-hydrogenation time is then dictated by the used diphosphine. Data collected in Table A1 allow calculation of pre-hydrogenation time using the equation $t_{pre\text{-}hydrogenation} = 7 \times t_{1/2}$ with $t_{1/2} = \ln 2/k'$, seven half lives, in fact, correspond to 99.2% (practically complete) conversion of the diolefin in [Rh(diphosphine)(diolefin)]$^+$.

Knowledge of the correct pre-hydrogenation time is likewise important to prevent formation of polyhydride species, should hydrogenation of the catalyst precursor to generate the active species, in the absence of the substrate, last too long.

The choice of the solvent is also important in preventing deactivation phenomena: while a too strongly coordinating solvent may hamper substrate coordination, a moderately coordinating solvent such as MeOH can be easily displaced but at the same time prevent the aggregation of coordinatively unsaturated metal fragments to polynuclear inactive species. Aromatic solvents should be also avoided as they can sequester part of the active catalyst in the form of η^6-coordinated arene-Rh(I) complexes. Halogenated solvents like dichloromethane might not be a sensible choice either as rhodium can activate the rhodium–halide bond and generate rhodium (III)–halide species.

The use of purified substrates is also recommended as halides, which are common contaminants, may react with the rhodium catalyst generating polynuclear rhodium halide species.

Catalysis has been defined "a foundational pillar of green chemistry", and a sensible use of the catalyst to fully exploit its potential makes it even greener [231].

Funding: DFG (Deutsche Forschungsgemeinschaft) HE 2890/7-1 and HE 2890/7-2

Acknowledgments: We would like to sincerely thank PD Torsten Beweries and Detlef Selent for their helpful discussions and advice. In addition, we would like to thank PD Wolfgang Baumann for his support with analytical problems, especially those concerning NMR spectroscopy.

Conflicts of Interest: The authors declare no conflict of interest.

Appendix A

Table A1. Pseudo rate constants relative to diolefin hydrogenation for the hydrogenation of COD and NBD for different [Rh(diphosphine)(diolefin)]$^+$ complexes (25.0 °C; 1.0 bar total pressure). The values were obtained with MeOH as the solvent and with BF_4^- as the anion unless stated otherwise.

Diphosphine	Solvent	1st Order Hydrogenation Rate Constant (1/min)		Reference
		COD	NBD	
BINAP		$2.3 \cdot 10^{-1}$	26.8	[101]
	THF	$2.8 \cdot 10^{-1}$	20.5	[101]
	Propylene Carbonate	$1.4 \cdot 10^{-1}$	16.6	[101]
BPPM		$2.2 \cdot 10^{-1}$	1.2	[101]
CatASium®D(R)		ca. $1.7 \cdot 10^{-3}$	n.d.	[108]
CatASium®M(R)		$5.0 \cdot 10^{-2}$	25	[101]
	THF	$1.5 \cdot 10^{-1}$	12	[100]
	Propylene Carbonate	$8.5 \cdot 10^{-2}$	9.4	[100]
Chiraphos		$1.3 \cdot 10^{-3}$	3.0	[105]
Cyc-JaPhos		1.1	at least 700	[105]
DaniPhos		ca. 0.03	3.6	[100]
	THF	n.d.	4.8	[100]
DCPE		$7.5 \cdot 10^{-2}$	48.8	[105]
Difluorphos		$1.6 \cdot 10^{-1}$	28.6	[95]
DIOP		$2.3 \cdot 10^{-1}$	1.29	[104]
DIPAMP		ca. $2.9 \cdot 10^{-3}$	ca. 9	[173]
	EtOH	n.d.	13	[173]
	i-PrOH	n.d.	5.9	[173]
	THF	n.d.	5.0	[173]
	Trifluoroethanol	n.d.	3.9	[173]
	Propylene Carbonate	n.d.	4.8	[173]
DPOE		$2.5 \cdot 10^{-1}$	16.6	[105]
DPPB		$1.6 \cdot 10^{-1}$	1.25	[104]
DPPE		ca. $2.0 \cdot 10^{-3}$	17.3	[105]
DPPP		$2.4 \cdot 10^{-2}$	1.55	[105]
DTBM-SEGPhos		$6.3 \cdot 10^{-2}$	12.0	[95]
Duanphos		$6.8 \cdot 10^{-1}$	53.7	[95]
Et-Butiphane		$2.9 \cdot 10^{-2}$	n.d.	[91]
Et-DuPhos		$1.2 \cdot 10^{-1}$	52.2	[101,105]
Et-Ferrotane		$2.0 \cdot 10^{-1}$	19.3	[95]
H_8-BINAP		$8.5 \cdot 10^{-1}$	57.5	[95]
i-Pr-Butiphane		$1.0 \cdot 10^{-2}$	n.d.	[91]
JaPhos		7.15	230	[105]
Josiphos		$2.3 \cdot 10^{-2}$	ca. 34	[100]

Table A1. *Cont.*

Diphosphine	Solvent	1st Order Hydrogenation Rate Constant (1/min)		Reference
		COD	NBD	
Me-Butiphane		$1.0 \cdot 10^{-1}$	n.d.	[91]
Me-DuPhos		$1.1 \cdot 10^{-1}$	35.2	[101]
	THF	$1.6 \cdot 10^{-2}$	39	[101]
	Propylene Carbonate	$1.4 \cdot 10^{-2}$	18	[101]
Me-*α*-glup		$3.7 \cdot 10^{-1}$	13.4	[104]
Ph-*β*-glup-OH		$2.0 \cdot 10^{-1}$	9.5	[104]
Prophos		ca. $3.0 \cdot 10^{-3}$	9.2	[105]
Propraphosderivates				
R=2-pentyl		3.77	21.9	[104]
R=3-pentyl		4.09	21.4	[104]
R=cyclohexyl		5.44	20.2	[104]
R=cyclopentyl		2.94	18.4	[104]
R=methyl		$5.3 \cdot 10^{-1}$	8.2	[104]
SEGPhos		$4.7 \cdot 10^{-1}$	29.9	[95]
Synphos		$8.0 \cdot 10^{-1}$	67	[117]
Tangphos		$3.7 \cdot 10^{-1}$	194.4	[120]
t-Bu-BisP*		$2.1 \cdot 10^{-1}$	90	[120]
t-Bu-Ferrotane		$5.7 \cdot 10^{-1}$	ca. 50	[95]
3-Pen-SMS-Phos		n.d.	3.8	[23]

Table A2. Abbreviations including diphosphine ligands.

Abbreviations	
acac	acetylacetonateanion
COE	cyclooctene
COD	*cis*,*cis*-1,5-cyclooctadiene
DCM	dichloromethane
IUPAC	International Union of Pure and Applied Chemistry
mac	methyl-(*Z*)-α -acetamidocinnamate
NBD	bicyclo[2.2.1]hepta-2,5-diene
SHOP	Shell Higher Olefin Process
THF	tetrahydrofuran
Diphosphines	
BINAP	2,2′-bis(diphenylphosphino)-1,1′-binaphthyl
BPPM	2,3-bis(diphenylphosphino)-*N*-phenylmaleimide
CatASium® D(R)	*N*-Benzyl-(3*R*,4*R*)-bis(diphenylphosphino)pyrrolidine
CatASium® M(R)	3,4-Bis[(2*R*,5*R*)-2,5-dimethyl-1-phospholanyl]furan-2,5-dione
Chiraphos	2,3-bis(diphenylphosphino)butan
Cyc-JaPhos	1-(2-dicyclohexylphosphinophenyl)pyrol-2-dicyclohexylphosphine
DaniPhos	dicyclohexyl(1-(2-(diphenylphosphanyl)phenyl)ethyl)phosphane-(tricarbonyl)chrom
DCPB	1,4-bis(dicyclohexylphosphino)butane
DCPE	1,2-bis(dicyclohexylphosphino)ethane
Difluorphos	5,5′-bis(diphenylphosphino)-2,2,2′,2′-tetrafluoro-4,4′-bi-1,3-benzodioxole
DIOP	2,3-*O*-isopropylidene-2,3-dihydroxy-1,4-bis(diphenylphosphino)butane)
DIPAMP	1,2-bis[(2-methoxyphenyl)phenylphosphino]ethan
DM-SEGPhos	5,5′−bis[di(3,5-xylyl)phosphino]-4,4′-bi-1,3-benzodioxole
DPEPhos	bis[(2-diphenylphosphino)phenyl]ether
DPOE	1,2-bis(diphenylphosphinoxy)ethan
DPPB	1,4-bis(diphenylphosphino)butane
DPPE	1,2-bis(diphenylphosphino)ethan
DPPF	1,1′-bis(diphenylphosphino)ferrocene
DPPMP	2-[(diphenylphosphino)methyl]pyridine
DPPP	1,3-bis(diphenylphosphino)propane
DTBM-SEGPhos	5,5′-bis[di(3,5-di-*t*-butyl-4-methoxyphenyl)phosphino]-4,4′-bi-1,3-benzodioxole

Table A2. *Cont.*

Diphosphines	
Duanphos	(1,1′,2,2′)-2,2′-di-*t*-butyl-2,3,2′,3′-tetrahydro-1*H*,1′*H*(1,1′)biisophos-phindolyl
Et-ButiPhane	2,3-bis(2,5-diethylphospholanyl)benzo[b]thiophene
Et-DuPhos	1,2-bis-2,5-(diethylphospholano)benzene
Et-Ferrotane	1,1′-bis-(2,4-diethylphosphonato)ferrocene
H_8-BINAP	2,2′-bis(diphenylphospino)-5,5′,6,6′,7,7′,8,8′-octahydro-1,1′-binaphthyl
i-Pr-Butiphane	2,3-bis(2,5-diisopropylphospholanyl)benzo[b]thiophene
JaPhos	1-(2-dicyclohexylphosphino)butane
Josiphos	[2-(diphenylphosphino)ferrocenyl]-ethyldicyclohexylphosphine
Me-BPE	1,2-bis[(2,5)-2,5-dimethylphospholano]ethane
Me-Butiphane	2,3-bis(2,5-dimethylphospholanyl)benzo[b]thiophene
Me-DuPhos	1,2-bis-(2,5-dimethylphospholano)benzene
Me-*α*-glup	methyl-4,6-*O*-benzylidene-2,3-*0*-bis(diphenylphosphino)-*α*-*D*-glucopyranoside
MonoPhos	3,5-dioxa-4-phosphacyclohepta[2,1-*a*;3,4-*a*′]dinaphthalen-4-yl)-dimethylamine
Ph-*β*-glup-OH	Phenyl-2,3-*O*-bis(diphenylphosphino)-*β*-*D*-glucopyranoside
PPF-P(*t*-Bu)$_2$	1-[2-(diphenylphosphino)ferrocenyl]ethyl-di-*t*-butylphosphine
Prophos	1,2-bis(diphenylphosphino)propane
SEGPhos	5,5′-bis(diphenylphosphino)-4,4′-bi-1,3-benzodioxole
Synphos	[(5,6),(5′,6′)-bis(ethylenedioxy)biphenyl-2,2′-diyl]bis(diphenylphosphine)
Tangphos	1,1′-di-*t*-butyl-(2,2′)-diphospholane
t-Bu-BisP*	1,2-bis(*t*-butylmethylphosphanyl)ethane
t-Bu-Ferrotane	1,1′-Bis-(2,4-diethylphosphonato)ferrocene
3-Pen-SMS-Phos	1,2-bis[(*o*-3-pentyl-*O*-phenyl)(phenyl)phosphino]ethane

References and Notes

1. Berzelius, J.J. *Årsberättelse om Framstegen i Fysik och Kemi*; Royal Swedish Academy of Sciences, P.A. Norstedt & Söner: Stockholm, Sweden, 1835.
2. Berzelius, J.J. Quelques idees sur une nouvelle force agissant dans les combinaisons des corps organiques. *Ann. Chim.* **1836**, *61*, 146–151.
3. Ostwald, W. Über den Wärmewert der Bestandteile der Nahrungsmittel. *Z. Phys. Chem.* **1894**, *15*, 705–706.
4. Ostwald, W. Über Katalyse. *Ann. Nat.* **1910**, *9*, 1–25.
5. Steinborn, D. *Fundamentals of Organometallic Catalysis*; Wiley-VCH: Weinheim, Germany, 2012.
6. Wisniak, J. The History of Catalysis. From the Beginning to Nobel Prizes. *Educ. Chim.* **2010**, *21*, 60–69. [CrossRef]
7. Lindström, B.; Pettersson, L.J. A brief history of catalysis. *CATTECH* **2003**, *7*, 130–138. [CrossRef]
8. Laidler, K.J. The Development of Theories of Catalysis. *Arch. Hist. Exact Sci.* **1986**, *35*, 345–374. [CrossRef]
9. Laidler, K.J. A glossary of terms used in chemical kinetics, including reaction dynamics. *Pure Appl. Chem.* **1996**, *68*, 149–192. [CrossRef]
10. Kamer, P.C.J.; Vogt, D.; Thybaut, J. *Contemporary Catalysis: Science, Technology, and Applications*; Kamer, P.C.J., Vogt, D., Thybaut, J., Eds.; Royal Society of Chemistry: London, UK, 2017.
11. Hagen, J. *Industrial Catalysis: A Practical Approach*; Wiley-VCH Verlag GmbH & Co. KGaA: Weinheim, Germany, 2015.
12. Blaser, H.U. Looking Back on 35 Years of Industrial Catalysis. *CHIMIA Int. J. Chem.* **2015**, *69*, 393–406. [CrossRef]
13. Bartholomew, C.H.; Farrauto, R.J. *Fundamentals of Industrial Catalytic Processes*, 2nd ed.; John Wiley & Sons, Inc.: Hoboken, NJ, USA, 2005.
14. Cornils, B.; Herrmann, W.A.; Beller, M.; Paciello, R. (Eds.) *Applied Homogeneous Catalysis with Organometallic Compounds: A Comprehensive Handbook in Four Volumes*, 3rd ed.; Wiley-VCH Verlag GmbH & Co. KGaA: Weinheim, Germany, 2017.
15. Cornils, B.; Herrmann, W.A.; Zanthoff, H.; Wong, C.-H. (Eds.) *Catalysis from A to Z: A Concise Encyclopedia*, 4th ed.; John Wiley & Sons, Inc.: Hoboken, NJ, USA, 2013.
16. Slaugh, L.H.; Mullineaux, R.D. Novel Hydroformylation Catalysts. *J. Organomet. Chem.* **1968**, *13*, 469–477.

17. Osborn, J.A.; Jardine, F.H.; Young, J.F.; Wilkinson, G. The Preparation and Properties of Tris(triphenylphosphine)halogenorhodium(I) and Some Reactions thereof including Catalytic Homogeneous Hydrogenation of Olefins and Acetylenes and their Derivatives. *J. Chem. Soc. A* **1966**, 1711–1732. [CrossRef]
18. Scott, S.L. A Matter of Life(time) and Death. *ACS Catal.* **2018**, *8*, 8597–8599. [CrossRef]
19. Crabtree, R.H. Deactivation in Homogeneous Transition Metal Catalysis: Causes, Avoidance, and Cure. *Chem. Rev.* **2015**, *115*, 127–150. [CrossRef] [PubMed]
20. Argyle, M.D.; Bartholomew, C.H. Heterogeneous Catalyst Deactivation and Regeneration: A Review. *Catalysts* **2015**, *5*, 145–269. [CrossRef]
21. Van Leeuwen, P.W.N.M.; Chadwick, J.C. *Homogeneous Catalysts Activity-Stability-Deactivation*; Wiley-VCH: Weinheim, Germany, 2011.
22. Heller, D.; de Vries, A.H.M.; de Vries, J.G. Catalyst Inhibition and Deactivation in Homogeneous Hydrogenation. In *Handbook of Homogeneous Hydrogenation*; de Vries, H.G., Elsevier, C., Eds.; Wiley-VCH Verlag GmbH & Co. KGaA: Weinheim, Germany, 2007; Chapter 44; pp. 1483–1516.
23. Meissner, A.; Alberico, E.; Drexler, H.-J.; Baumann, W.; Heller, D. Rhodium diphosphine complexes: a case study for catalyst activation and deactivation. *Catal. Sci. Technol.* **2014**, *4*, 3409–3425. [CrossRef]
24. Yuan, S.-W.; Han, H.; Li, Y.-L.; Wu, X.; Bao, X.; Gu, Z.-Y.; Xia, J.-B. Intermolecular C−H Amidation of (Hetero)arenes to Produce Amides through Rhodium-Catalyzed Carbonylation of Nitrene Intermediates. *Angew. Chem. Int. Ed.* **2019**, *131*, 8979–8984.
25. Oonishi, Y.; Masusaki, S.; Sakamoto, S.; Sato, Y. Rhodium(I)-Catalyzed Enantioselective Cyclization of Enynes by Intramolecular Cleavage of the Rh−C Bond by a Tethered Hydroxy Group. *Angew. Chem. Int. Ed.* **2019**, *131*, 8687.
26. Zheng, J.; Breit, B. Regiodivergent Hydroaminoalkylation of Alkynes and Allenes by a Combined Rhodium and Photoredox Catalytic System. *Angew. Chem. Int. Ed.* **2019**, *131*, 3430–3435. [CrossRef]
27. Ohmura, T.; Sasaki, I.; Suginome, M. Catalytic Generation of Rhodium Silylenoid for Alkene–Alkyne–Silylene [2 + 2 + 1] Cycloaddition. *Org. Lett.* **2019**, *21*, 1649–1653. [CrossRef]
28. Yang, X.-H.; Davison, R.T.; Dong, V.M. Catalytic Hydrothiolation: Regio- and Enantioselective Coupling of Thiols and Dienes. *J. Am. Chem. Soc.* **2018**, *140*, 10443–10446. [CrossRef]
29. Wu, S.T.; Luo, S.Y.; Guo, W.J.; Wang, T.; Xie, Q.X.; Wang, J.H.; Liu, G.Y. Direct Conversion of Ethyl Ketone to Alkyl Ketone via Chelation-Assisted Rhodium(I)-Catalyzed Carbon Carbon Bond Cleavage: Ligands Play an Important Role in the Inhibition of beta-Hydrogen Elimination. *Organometallics* **2018**, *37*, 2335–2341. [CrossRef]
30. Choi, K.; Park, H.; Lee, C. Rhodium-Catalyzed Tandem Addition–Cyclization–Rearrangement of Alkynylhydrazones with Organoboronic Acids. *J. Am. Chem. Soc.* **2018**, *140*, 10407–10411. [CrossRef] [PubMed]
31. Zheng, W.F.; Xu, Q.J.; Kang, Q. Rhodium/Lewis Acid Catalyzed Regioselective Addition of 1,3-Dicarbonyl Compounds to Internal Alkynes. *Organometallics* **2017**, *36*, 2323–2330. [CrossRef]
32. Yu, Y.; Xu, M. Chiral phosphorus-olefin ligands for asymmetric catalysis. *Huaxue Xuebao* **2017**, *75*, 655–670. [CrossRef]
33. Wang, H.W.; Lu, Y.; Zhang, B.; He, J.; Xu, H.J.; Kang, Y.S.; Sun, W.Y.; Yu, J.Q. Ligand-Promoted Rhodium(III)-Catalyzed ortho-C-H Amination with Free Amines. *Angew. Chem. Int. Ed.* **2017**, *56*, 7449–7453. [CrossRef] [PubMed]
34. Saito, H.; Nogi, K.; Yorimitsu, H. Rh/Cu-cocatalyzed Ring-opening Diborylation of Dibenzothiophenes for Aromatic Metamorphosis via Diborylbiaryls. *Chem. Lett.* **2017**, *46*, 1131–1134. [CrossRef]
35. Furusawa, T.; Tanimoto, H.; Nishiyama, Y.; Morimoto, T.; Kakiuchi, K. Rhodium-catalyzed Carbonylative Annulation of 2-Bromobenzylic Alcohols with Internal Alkynes Using Furfural via beta-Aryl Elimination. *Chem. Lett.* **2017**, *46*, 926–929. [CrossRef]
36. Loh, C.C.J.; Schmid, M.; Peters, B.; Fang, X.; Lautens, M. Benzylic Functionalization of Anthrones via the Asymmetric Ring Opening of Oxabicycles Utilizing a Fourth-Generation Rhodium Catalytic System. *Angew. Chem. Int. Ed.* **2016**, *55*, 4600–4604. [CrossRef] [PubMed]
37. Lee, T.; Hartwig, J.F. Rhodium-Catalyzed Enantioselective Silylation of Cyclopropyl C-H Bonds. *Angew. Chem. Int. Ed.* **2016**, *55*, 8723–8727. [CrossRef]

38. Meissner, A.; Preetz, A.; Drexler, H.-J.; Baumann, W.; Spannenberg, A.; Koenig, A.; Heller, D. In Situ Synthesis of Neutral Dinuclear Rhodium Diphosphine Complexes [{Rh(diphosphine)(μ_2-X)}$_2$]: Systematic Investigations. *Chem. Plus. Chem.* **2015**, *80*, 169–180.
39. Meissner, A.; Koenig, A.; Drexler, H.-J.; Thede, R.; Baumann, W.; Heller, D. New Pentacoordinated Rhodium Species as Unexpected Products during the In Situ Generation of Dimeric Diphosphine-Rhodium Neutral Catalysts. *Chem. Eur. J.* **2014**, *20*, 14721–14728. [CrossRef] [PubMed]
40. Preetz, A.; Kohrt, C.; Meissner, A.; Wei, S.; Buschmann, H.; Heller, D. Halide bridged trinuclear rhodium complexes and their inhibiting influence on catalysis. *Catal. Sci. Technol.* **2013**, *3*, 462–468. [CrossRef]
41. Lumbroso, A.; Vautravers, N.R.; Breit, B. Rhodium-Catalyzed Selective anti-Markovnikov Addition of Carboxylic Acids to Alkynes. *Org. Lett.* **2010**, *12*, 5498–5501. [CrossRef] [PubMed]
42. Koschker, P.; Lumbroso, A.; Breit, B. Enantioselective Synthesis of Branched Allylic Esters via Rhodium-Catalyzed Coupling of Allenes with Carboxylic Acids. *J. Am. Chem. Soc.* **2011**, *133*, 20746–20749. [CrossRef] [PubMed]
43. Lumbroso, A.; Koschker, P.; Vautravers, N.R.; Breit, B. Redox-Neutral Atom-Economic Rhodium-Catalyzed Coupling of Terminal Alkynes with Carboxylic Acids Toward Branched Allylic Esters. *J. Am. Chem. Soc.* **2011**, *133*, 2386–2389. [CrossRef] [PubMed]
44. Pritzius, A.B.; Breit, B. Asymmetric Rhodium-Catalyzed Addition of Thiols to Allenes: Synthesis of Branched Allylic Thioethers and Sulfones. *Angew. Chem. Int. Ed.* **2015**, *54*, 3121–3125. [CrossRef] [PubMed]
45. Beck, T.M.; Breit, B. Regio- and Enantioselective Rhodium-Catalyzed Addition of 1,3-Diketones to Allenes: Construction of Asymmetric Tertiary and Quaternary All Carbon Centers. *Angew. Chem. Int. Ed.* **2017**, *56*, 1903–1907. [CrossRef]
46. Parveen, S.; Li, C.K.; Hassan, A.; Breit, B. Chemo-, Regio-, and Enantioselective Rhodium-Catalyzed Allylation of Pyridazinones with Terminal Allenes. *Org. Lett.* **2017**, *19*, 2326–2329. [CrossRef] [PubMed]
47. Berthold, D.; Breit, B. Chemo-, Regio-, and Enantioselective Rhodium-Catalyzed Allylation of Triazoles with Internal Alkynes and Terminal Allenes. *Org. Lett.* **2018**, *20*, 598–601. [CrossRef]
48. Wei, S.; Pedroni, J.; Meissner, A.; Lumbroso, A.; Drexler, H.-J.; Heller, D.; Breit, B. Development of an Improved Rhodium Catalyst for Z-Selective Anti-Markovnikov Addition of Carboxylic Acids to Terminal Alkynes. *Chem. Eur. J.* **2013**, *19*, 12067–12076. [CrossRef]
49. Keller, E.; Pierrard, J.-S. (Eds.) *All Pictures Showing X-ray Structures Were Prepared Using the program SCHAKAL*; SCHAKAL99; University of Freiburg: Breisgau, Germany, 1999.
50. Möller, S.; Drexler, H.-J.; Heller, D. Two Precatalysts for Application in Propargylic CH Activation. *Acta Cryst. C* **2019**, submitted.
51. Moon, S.; Nishii, Y.; Miura, M. Thioether-Directed Peri-Selective C–H Arylation under Rhodium Catalysis: Synthesis of Arene-Fused Thioxanthenes. *Org. Lett.* **2019**, *21*, 233–236. [CrossRef] [PubMed]
52. Satake, S.; Kurihara, T.; Nishikawa, K.; Mochizuki, T.; Hatano, M.; Ishihara, K.; Yoshino, T.; Matsunaga, S. Pentamethylcyclopentadienyl Rhodium(III)–Chiral Disulfonate Hybrid Catalysis for Enantioselective C–H Bond Functionalization. *Nat. Catal.* **2018**, *1*, 585–591. [CrossRef]
53. Ghosh, K.; Mihara, G.; Nishii, Y.; Miura, M. Nondirected C-H Alkenylation of Arenes with Alkenes under Rhodium Catalysis. *Chem. Lett.* **2019**, *48*, 148–151. [CrossRef]
54. Fischer, C.; Koenig, A.; Meissner, A.; Thede, R.; Selle, C.; Pribbenow, C.; Heller, D. Quantitative UV/Vis Spectroscopic Investigations of the In Situ Synthesis of Neutral μ_2-Chloro-Bridged Dinuclear (Diphosphine)rhodium Complexes. *Eur. J. Inorg. Chem.* **2014**, *34*, 5849–5855. [CrossRef]
55. Duan, C.-L.; Tan, Y.-X.; Zhang, J.-L.; Yang, S.; Dong, H.-Q.; Tian, P.; Lin, G.-Q. Highly Enantioselective Rhodium-Catalyzed Cross-Addition of Silylacetylenes to Cyclohexadienone-Tethered Internal Alkynes. *Org. Lett.* **2019**, *21*, 1690–1693. [CrossRef]
56. Hilpert, L.J.; Sieger, S.V.; Haydl, A.M.; Breit, B. Palladium- and Rhodium-Catalyzed Dynamic Kinetic Resolution of Racemic Internal Allenes Towards Chiral Pyrazoles. *Angew. Chem. Int. Ed.* **2019**, *131*, 3416–3419. [CrossRef]
57. Tanaka, K. *Rhodium Catalysis in Organic Synthesis: Methods and Reactions*; Wiley-VCerlag GmbH & Co. KGaA: Weinheim, Germany, 2018.
58. Fairlie, D.P.; Bosnich, B. Homogeneous Catalysis - Conversion of 4-Pentenals to Cyclopentanones by Efficient Rhodium-Catalyzed Hydroacylation. *Organometallics* **1988**, *7*, 936–945. [CrossRef]

59. Fischer, C.; Beweries, T.; Preetz, A.; Drexler, H.-J.; Baumann, W.; Peitz, S.; Rosenthal, U.; Heller, D. Kinetic and Mechanistic Investigations in Homogeneous Catalysis Using Operando UV/vis Spectroscopy. *Catal. Today* **2010**, *155*, 282–288. [CrossRef]
60. Mannu, A.; Drexler, H.-J.; Thede, R.; Ferro, M.; Baumann, W.; Rüger, J.; Heller, D. Oxidative Addition of CH_2Cl_2 to Neutral Dimeric Rhodium Diphosphine Complexes. *J. Organomet. Chem.* **2018**, *871*, 178–184. [CrossRef]
61. Möller, S.; Drexler, H.-J.; Kubis, C.; Alberico, E.; Heller, D. Investigations into the Mechanism of the In Situ Formation of Neutral Dinuclear Rhodium Complexes. *J. Organomet. Chem.* **2019**. submitted.
62. Time for 98 % conversion under the following reaction conditions: Ca. $1.0{\cdot}10^{-2}$ mmol [Rh(diolefin)(μ_2-Cl)]$_2$ and $2.0{\cdot}10^{-2}$ mmol ligand in 5 ml solvent.
63. Lumbroso, A.; Cooke, M.L.; Breit, B. Catalytic Asymmetric Synthesis of Allylic Alcohols and Derivatives and their Applications in Organic Synthesis. *Angew. Chem. Int. Ed.* **2013**, *52*, 1890–1932. [CrossRef] [PubMed]
64. Gellrich, U.; Meissner, A.; Steffani, A.; Kahny, M.; Drexler, H.J.; Heller, D.; Plattner, D.A.; Breit, B. Mechanistic Investigations of the Rhodium Catalyzed Propargylic CH Activation. *J. Am. Chem. Soc.* **2014**, *136*, 1097–1104. [CrossRef] [PubMed]
65. Li, C.; Breit, B. Rhodium-Catalyzed Chemo- and Regioselective Decarboxylative Addition of β-Ketoacids to Allenes: Efficient Construction of Tertiary and Quaternary Carbon Centers. *J. Am. Chem. Soc.* **2014**, *136*, 862–865. [CrossRef] [PubMed]
66. Koschker, P.; Kaehny, M.; Breit, B. Enantioselective Redox-Neutral Rh-Catalyzed Coupling of Terminal Alkynes with Carboxylic Acids Toward Branched Allylic Esters. *J. Am. Chem. Soc.* **2015**, *137*, 3131–3137. [CrossRef] [PubMed]
67. James, B.R.; Mahajan, D. Bis(ditertiaryphosphine) Complexes of Rhodium(I). Synthesis, Spectroscopy, and Activity for Catalytic Hydrogenation. *Can. J. Chem.* **1979**, *57*, 180–187. [CrossRef]
68. Castellanos-Paez, A.; Thayaparan, J.; Castillon, S.; Claver, C. Reactivity of Tetracarbonyl Dithiolate-Bridged Rhodium(I) Complexes with Diphosphines. *J. Organomet. Chem.* **1998**, *551*, 375–381. [CrossRef]
69. Slack, D.A.; Baird, M.C. Investigations of Olefin Hydrogenation Catalysts. The Major Species Present in Solutions Containing Rhodium(I) Complexes of Chelating Diphosphines. *J. Organomet. Chem.* **1977**, *142*, C69–C72. [CrossRef]
70. Crosman, A.; Hoelderich, W.F. Enantioselective Hydrogenation over Immobilized Rhodium Diphosphine Complexes on Aluminated SBA-15. *J. Catal.* **2005**, *232*, 43–50. [CrossRef]
71. Van Haaren, R.J.; Zuidema, E.; Fraanje, J.; Goubitz, K.; Kamer, P.C.J.; van Leeuwen, P.W.N.M.; van Strijdonck, G.P.F. Probing the Mechanism of Rhodium (I) Catalyzed Dehydrocoupling of di-n-hexylsilane. *C. R. Chim.* **2002**, *5*, 431–440. [CrossRef]
72. Wagner, H.H.; Hausmann, H.; Hoelderich, W.F. Immobilization of Rhodium Diphosphine Complexes on Mesoporous Al-MCM-41 Materials: Catalysts for Enantioselective Hydrogenation. *J. Catal.* **2001**, *203*, 150–156. [CrossRef]
73. Sinou, D.; Bakos, J. (S,S)-2,3-Bis[Di(m-Sodiumsulfonatophenyl)-Phosphino]Butane (Chiraphosts) and (S,S)-2,4-Bis[Di(m-Sodiumsulfonatophenyl)- Phosphino]Pentane (BDPPts). *Inorg. Synth.* **1998**, *32*, 36–40.
74. Baxley, G.T.; Weakley, T.J.R.; Miller, W.K.; Lyon, D.K.; Tyler, D.R. Synthesis and Catalytic Chemistry of Two New Water-soluble Chelating Phosphines. Comparison of Ionic and Nonionic Functionalities. *J. Mol. Catal. A Chem.* **1997**, *116*, 191–198. [CrossRef]
75. Bartik, T.; Bunn, B.B.; Bartik, B.; Hanson, B.E. Synthesis, Reactions, and Catalytic Chemistry of the Water-Soluble Chelating Phosphine 1,2-Bis[bis(m-sodiosulfonatophenyl)phosphino]ethane (DPPETS). Complexes with Nickel, Palladium, Platinum, and Rhodium. *Inorg. Chem.* **1994**, *33*, 164–169. [CrossRef]
76. Bakos, J.; Tóth, I.; Heil, B.; Szalontai, G.; Párkányi, L.; Fülöp, V. Catalytic and Structural Studies of Rh^I Complexes of (−)-(2S,4S)-2,4-bis(diphenylphosphino)pentane. Asymmetric Hydrogenation of Acetophenonebenzylimine and Acetophenone. *J. Organomet. Chem.* **1989**, *370*, 263–276. [CrossRef]
77. Meng, G.; Szostak, M. Rhodium-Catalyzed C–H Bond Functionalization with Amides by Double C–H/C–N Bond Activation. *Org. Lett.* **2016**, *18*, 796–799. [CrossRef] [PubMed]
78. Mizukami, A.; Ise, Y.; Kimachi, T.; Inamoto, K. Rhodium-Catalyzed Cyclization of 2-Ethynylanilines in the Presence of Isocyanates: Approach toward Indole-3-carboxamides. *Org. Lett.* **2016**, *18*, 748–751. [CrossRef] [PubMed]

79. Zhao, C.; Liu, L.-C.; Wang, J.; Jiang, C.; Zhang, Q.-W.; He, W. Rh(I)-Catalyzed Insertion of Allenes into C–C Bonds of Benzocyclobutenols. *Org. Lett.* **2016**, *18*, 328–331. [CrossRef]
80. Chen, D.; Zhang, X.; Qi, W.-Y.; Xu, B.; Xu, M.-H. Rhodium(I)-Catalyzed Asymmetric Carbene Insertion into B–H Bonds: Highly Enantioselective Access to Functionalized Organoboranes. *J. Am. Chem. Soc.* **2015**, *137*, 5268–5271. [CrossRef]
81. Lim, D.S.W.; Lew, T.T.S.; Zhang, Y. Direct Amidation of N-Boc- and N-Cbz-Protected Amines via Rhodium-Catalyzed Coupling of Arylboroxines and Carbamates. *Org. Lett.* **2015**, *17*, 6054–6057. [CrossRef]
82. Gopula, B.; Yang, S.-H.; Kuo, T.-S.; Hsieh, J.-C.; Wu, P.-Y.; Henschke, J.P.; Wu, H.-L. Direct Synthesis of Chiral 3-Arylsuccinimides by Rhodium-Catalyzed Enantioselective Conjugate Addition of Arylboronic Acids to Maleimides. *Chem. Eur. J.* **2015**, *21*, 11050–11055. [CrossRef]
83. Lee, S.; Lee, W.L.; Yun, J. Rhodium-Catalyzed Addition of Alkyltrifluoroborate Salts to Imines. *Adv. Synth. Catal.* **2015**, *357*, 2219–2222. [CrossRef]
84. Rao, H.; Yang, L.; Shuai, Q.; Li, C.-J. Rhodium-Catalyzed Aerobic Coupling between Aldehydes and Arenesulfinic Acid Salts: A Novel Synthesis of Aryl Ketones. *Adv. Synth. Catal.* **2011**, *353*, 1701–1706. [CrossRef]
85. Morimoto, T.; Yamasaki, K.; Hirano, A.; Tsutsumi, K.; Kagawa, N.; Kakiuchi, K.; Harada, Y.; Fukumoto, Y.; Chatani, N.; Nishioka, T. Rh(I)-Catalyzed CO Gas-Free Carbonylative Cyclization Reactions of Alkynes with 2-Bromophenylboronic Acids Using Formaldehyde. *Org. Lett.* **2009**, *11*, 1777–1780. [CrossRef] [PubMed]
86. Cornils, B.; Herrmann, W.A.; Schlögl, R.; Wong, C.-H. (Eds.) *Catalysis from A to Z*, 2nd ed.; Wiley-VCH: Weinheim, Germany, 2003.
87. Temkin, O.N. Mechanisms of Formation of Catalytically Active Metal Complexes. In *Homogeneous Catalysis with Metal Complexes: Kinetic Aspects and Mechanisms*, 1st ed.; Temkin, O.N., Ed.; John Wiley & Sons Ltd.: Chichester, UK, 2012; Chapter 5, pp. 453–544.
88. Evans, D.; Osborn, J.A.; Wilkinson, G. Hydroformylation of Alkenes by Use of Rhodium Complex Catalysts. *J. Chem. Soc. A* **1968**, 3133–3142. [CrossRef]
89. Brown, C.K.; Wilkinson, G. Homogeneous Hydroformylation of Alkenes with Hydridocarbonyltris-(triphenylphosphine)rhodium(i) as Catalyst. *J. Chem. Soc. A* **1970**, 2753–2764. [CrossRef]
90. Adams, G.M.; Ryan, D.E.; Beattie, N.A.; McKay, A.I.; Lloyd-Jones, G.C.; Weller, A.S. Dehydropolymerization of H3B·NMeH2 Using a [Rh(DPEphos)]+ Catalyst: The Promoting Effect of NMeH2. *ACS Catal.* **2019**, *9*, 3657–3666. [CrossRef] [PubMed]
91. Fischer, C.; Schulz, S.; Drexler, H.-J.; Selle, C.; Lotz, M.; Sawall, M.; Neymeyr, K.; Heller, D. The Influence of Substituents in Diphosphine Ligands on the Hydrogenation Activity and Selectivity of the Corresponding Rhodium Complexes as Exemplified by ButiPhane. *ChemCatChem* **2012**, *4*, 81–88. [CrossRef]
92. 0.01 mmol rhodium complex and 1.0 mmol prochiral olefin in 15.0 ml MeOH at 25.0 °C and 1 bar total pressure
93. Nagel, U.; Kinzel, E.; Andrade, J.; Prescher, G. Enantioselektive Katalyse, 4. Synthese N-substituierter (R,R)-3,4-Bis(diphenylphosphino)-pyrrolidine und Anwendung ihrer Rhodiumkomplexe zur Asymmetrischen Hydrierung von α-(Acylamino)acrylsäure-Derivaten. *Chem. Ber.* **1986**, *119*, 3326–3343. [CrossRef]
94. Nagel, U.; Krink, T. Catalytic Hydrogenation with Rhodium Complexes Containing dipamp-pyrphos Hybrid Ligands. *Angew. Chem. Int. Ed. Engl.* **1993**, *32*, 1052–1054. [CrossRef]
95. Thiel, I.; Horstmann, M.; Jungk, P.; Keller, S.; Fischer, F.; Drexler, H.-J.; Heller, D.; Hapke, M. Insight into the Activation of *In Situ*-Generated Chiral Rh(I)-Catalysts and their Application in Cyclotrimerizations. *Chem. Eur. J.* **2017**, *23*, 17048–17057. [CrossRef]
96. Alberico, E.; Baumann, W.; de Vries, J.G.; Drexler, H.-J.; Gladiali, S.; Heller, D.; Henderickx, H.J.W.; Lefort, L. Unravelling the Reaction Path of Rhodium–MonoPhos-Catalysed Olefin Hydrogenation. *Chem. Eur. J.* **2011**, *17*, 12683–12695. [CrossRef] [PubMed]
97. Van den Berg, M. Rhodium-Catalyzed Asymmetric Hydrogenation Using Phosphoramidite Ligands. Ph.D. Thesis, University of Groningen, Groningen, The Netherlands, 2006. Available online: http://hdl.handle.net/11370/c6d065b0-5bc1-4a2a-a452-fb237d5a4e6e (accessed on 5 June 2019).
98. Esteruelas, M.A.; Herrero, J.; Martin, M.; Oro, M.L.A.; Real, V.M. Mechanism of the Hydrogenation of 2,5-Norbornadiene Catalyzed by $[Rh(NBD)(PPh_3)_2]BF_4$ in Dichloromethane: a Kinetic and Spectroscopic Investigation. *J. Organomet. Chem.* **2000**, *599*, 178–184. [CrossRef]

99. Heller, D.; Kortus, K.; Selke, R. Kinetische Untersuchungen zur Ligandenhydrierung in Katalysatorvorstufen für die Asymmetrische Reduktion prochiraler Olefine. *Liebigs Ann.* **1995**, 575–581. [CrossRef]
100. Braun, W.; Salzer, A.; Drexler, H.-J.; Spannenberg, A.; Heller, D. Investigations into the Hydrogenation of Diolefins and Prochiral Olefins Employing the "Daniphos"-type Ligands. *Dalton Trans.* **2003**, 1606–1613. [CrossRef]
101. Preetz, A.; Drexler, H.-J.; Fischer, C.; Dai, Z.; Börner, A.; Baumann, W.; Spannenberg, A.; Thede, R.; Heller, D. Rhodium Complex Catalyzed Asymmetric Hydrogenation - Transfer of Pre-Catalysts Into Active Species. *Chem. Eur. J.* **2008**, *14*, 1445–1451. [CrossRef]
102. Selent, D.; Heller, D. *In-Situ Techniques for Homogeneous Catalysis, in Catalysis From Principle to Application*; Beller, M., Renken, A., van Santen, R., Eds.; Wiley-VCH: Weinheim, Germany, 2012; Chapter 23; pp. 465–492.
103. Drexler, H.-J.; Preetz, A.; Schmidt, T.; Heller, D. Kinetics of Homogeneous Hydrogennations: Measurement and Interpretation. In *Handbook of Homogeneous Hydrogenation*; de Vries, H.G., Elsevier, C., Eds.; Wiley-VCH: Weinheim, Germany, 2007; Chapter 10; pp. 257–293.
104. Heller, D.; Borns, S.; Baumann, W.; Selke, R. Kinetic Investigations of the Hydrogenation of Diolefin Ligands in Catalyst Precursors for the Asymmetric Reduction of Prochiral Olefins, II. *Chem. Ber.* **1996**, *129*, 85–89. [CrossRef]
105. Drexler, H.-J.; Baumann, W.; Spannenberg, A.; Fischer, C.; Heller, D. COD- versus NBD-Precatalysts. Dramatic Difference in the Asymmetric Hydrogenation of Prochiral Olefins with Five Membered Diphosphine Rh-Hydrogenation Catalysts. *J. Organomet. Chem.* **2001**, *621*, 89–102. [CrossRef]
106. Baseda Krüger, M.; Selle, C.; Heller, D.; Baumann, W. Determination of Gas Concentrations in Liquids by Nuclear Magnetic Resonance: Hydrogen in Organic Solvents. *J. Chem. Eng. Data* **2012**, *57*, 1737–1744. [CrossRef]
107. Krüger, M.B. Bestimmung von Gaskonzentrationen in Flüssigen Medien Mittels NMR-Spektroskopie: Eine Methode für Kinetische und in-situ Studien. Ph.D. Thesis, University of Rostock, Rostock, Germany, 2013.
108. Greiner, L.; Ternbach, M.B. Kinetic Study of Homogeneous Alkene Hydrogenation by Model Discrimination. *Adv. Synth. Catal.* **2004**, *346*, 1392–1396. [CrossRef]
109. Drexler, H.-J.; Zhang, S.; Sun, A.; Spannenberg, A.; Arrieta, A.; Preetz, A.; Heller, D. Cationic Rh-Bisphosphane-Diolefin Complexes as Precatalysts for Enantioselective Catalysis - What Informations Do Single Crystal Structures Contain Regarding Product Chirality? *Tetrahedron Asymmetry* **2004**, *15*, 2139–2150. [CrossRef]
110. Brown, J.M.; Chaloner, P.A. The Mechanism of Asymmetric Hydrogenation Catalysed by Rhodium (I) Dipamp Complexes. *Tetrahedron Lett.* **1978**, *19*, 1877–1880. [CrossRef]
111. Brown, J.M.; Chaloner, P.A. The Mechanism of Asymmetric Homogeneous Hydrogenation. Rhodium (I) Complexes of Dehydroamino Acids Containing Asymmetric Ligands Related to Bis(1,2-diphenylphosphino)ethane. *J. Am. Chem. Soc.* **1980**, *102*, 3040–3048. [CrossRef]
112. De Vries, J.G.; Lefort, L. High-Throughput Experimentation and Ligand Libraries. In *Handbook of Homogeneous Hydrogenation*; de Vries, H.G., Elsevier, C., Eds.; Wiley-VCH: Weinheim, Germany, 2007; Chapter 36, pp. 1245–1278.
113. Preetz, A.; Drexler, H.-J.; Schulz, S.; Heller, D. BINAP: Rhodium-Diolefin Complexes in Asymmetric Hydrogenation. *Tetrahedron Asymm.* **2010**, *21*, 1226–1231. [CrossRef]
114. Cobley, C.J.; Lennon, I.C.; McCague, R.; Ramsden, J.A.; Zanotti-Gerosa, A. On the Economic Application of DuPHOS Rhodium(I) Catalysts: A Comparison of COD versus NBD Precatalysts. *Tetrahedron Lett.* **2001**, *42*, 7481–7483. [CrossRef]
115. Moxham, G.L.; Randell-Sly, H.E.; Brayshaw, S.K.; Woodward, R.L.; Weller, A.S.; Willis, M.C. A Second-Generation Catalyst for Intermolecular Hydroacylation of Alkenes and Alkynes Using β-S-Substituted Aldehydes: The Role of a Hemilabile P-O-P Ligand. *Angew. Chem. Int. Ed.* **2006**, *45*, 7618–7622. [CrossRef] [PubMed]
116. Preetz, A.; Fischer, C.; Kohrt, C.; Drexler, H.-J.; Baumann, W.; Heller, D. Cationic Rhodium-BINAP Complexes: Full Characterization of Solvate- and Arene Bridged Dimeric Species. *Organometallics* **2011**, *30*, 5155–5159. [CrossRef]
117. Meißner, A.; Drexler, H.-J.; Keller, S.; Selle, C.; Ratovelomanana-Vidal, V.; Heller, D. Synthesis and Characterisation of Cationic Synphos-Rhodium Complexes. *Eur. J. Inorg. Chem.* **2014**, 4836–4842. [CrossRef]

118. Webster, R.; Bçing, C.; Lautens, M. Reagent-Controlled Regiodivergent Resolution of Unsymmetrical Oxabicyclic Alkenes Using a Cationic Rhodium Catalyst. *J. Am. Chem. Soc.* **2009**, *131*, 444–445. [CrossRef]
119. Preetz, A.; Kohrt, C.; Drexler, H.-J.; Torrens, A.; Buschmann, H.; Lopez, M.G.; Heller, D. Asymmetric Ring Opening of Oxabicyclic Alkenes With *Cationic* Rhodium Complexes. *Adv. Synth. Catal.* **2010**, *352*, 2073–2080. [CrossRef]
120. Fischer, C.; Kohrt, C.; Drexler, H.-J.; Baumann, W.; Heller, D. Trinuclear Hydride Complexes of Rhodium. *Dalton Trans.* **2011**, *40*, 4162–4166. [CrossRef]
121. Kohrt, C.; Hansen, S.; Drexler, H.-J.; Rosenthal, U.; Schulz, A.; Heller, D. Molecular Vibration Spectroscopy Studies on Novel Trinuclear Rhodium-7-Hydride Complexes of the General Type {[Rh(PP*)X]$_3$(μ_2-X)$_3$(μ_3-X)}(BF$_4$)$_2$ (X = H, D). *Inorg. Chem.* **2012**, *51*, 7377–7383. [CrossRef] [PubMed]
122. Kohrt, C.; Baumann, W.; Spannenberg, A.; Drexler, H.-J.; Gridnev, I.; Heller, D. Formation of Trinuclear Rhodium-Hydride Complexes {[Rh(PP*)H]$_3$(μ_2-H)$_3$(μ_3-H)}(Anion)$_2$ - During Asymmetric Hydrogenation? *Chem. Eur. J.* **2013**, *19*, 7443–7451. [CrossRef] [PubMed]
123. Kohrt, C. Mehrkernige Hydridkomplexe des Rhodiums mit Bisphosphanliganden: Charakterisierung, Bildung und Anwendung. Ph.D. Thesis, University of Rostock, Rostock, Germany, 2013.
124. Gridnev, I.D.; Imamoto, T. Mechanism of Enantioselection in Rh-Catalyzed Asymmetric Hydrogenation. The origin of Utmost Catalytic performance. *Chem. Comm.* **2009**, 7447–7464. [CrossRef] [PubMed]
125. Indeed a mechanism for the formation of the trinuclear rhodium (III) polyhydride species {[Rh(diphosphine)H]$_3$(μ_2-H)$_3$(μ_3-H)}$^{2+}$ from the rhodium(I) solvate dihydride [Rh(III)(diphosphine)(H)$_2$(solvent)$_2$]$^+$ has been put forward, based on experimental evidence, which includes the intermediacy of a dinuclear rhodium (III) polyhydride species of general formula {[Rh(diphosphine)H]$_2$(μ_2-H)$_3$}[X]. The equilibria, the species present in solution and their relative concentrations, depends on the properties of the diphosphine ligand, the temperature and the solvent.
126. The hydrogenation of diolefins in complexes with diphosphines which do not contain aryl groups in nonpolar solvents such as DCM is even more complicated: With the ligand *t*-BuBisP* ^{1}H-^{103}Rh-HMQC-NMR spectra show the formation of three polyhydrido species. One of them has been assigned the structure {[Rh(*t*-Bu-BisP*)H]$_3$(μ_2-H)$_3$(μ_3-Cl)}$_2^+$, while that of the other two remain unclear.
127. Cornish-Bowden, A. *Fundamentals of Enzyme Kinetics*, 4th ed.; Wiley-VCH Verlag & Co. KgaA: Weinheim, Germany, 2012.
128. Kollár, L.; Törös, S.; Heil, B.; Markó, L. Phosphinerhodium Complexes as Homogeneous Catalysts: XI. Decarbonylation of Primary Alcohols Used as Solvents Under Conditions of Olefin Hydrogenation; a Side Reaction Leading to Catalyst Deactivation. *J. Organomet. Chem.* **1980**, *192*, 253–256.
129. Benn, R.; Rufińska, A. High-Resolution Metal-NMR Spectroscopy of Organometallic Compounds. *Angew. Chem. Int. Ed. Engl.* **1986**, *25*, 861–881. [CrossRef]
130. Von Philipsborn, W. Probing Organometallic Structure and Reactivity by Transition Metal NMR Spectroscopy. *Chem. Soc. Rev.* **1999**, *28*, 95–105. [CrossRef]
131. Ernsting, J.M.; Elsevier, C.J.; de Lange, W.G.J.; Timmer, K. Inverse Two-Dimensional ^{31}P, ^{103}Rh{^{1}H} NMR of Cationic Rhodium (1) Complexes Containing Chelating Diphosphines. *Magn. Reson. Chem.* **1991**, *29*, S118–S124. [CrossRef]
132. Leitner, W.; Bühl, M.; Fornika, R.; Six, C.; Baumann, W.; Dinjus, E.; Kessler, M.; Krüger, C.; Rufińska, A. ^{103}Rh Chemical Shifts in Complexes Bearing Chelating Bidentate Phosphine Ligands. *Organometallics* **1999**, *18*, 1196–1206. [CrossRef]
133. Halpern, J.; Riley, D.P.; Chan, A.S.C.; Pluth, J.J. Novel Coordination Chemistry and Catalytic Properties of Cationic 1,2-Bisjdiphenylphosphino)ethanerhodium(I) Complexes. *J. Am. Chem. Soc.* **1977**, *99*, 8055–8057. [CrossRef]
134. Halpern, J.; Chan, A.S.C.; Riley, D.P.; Pluth, J.J. Some Aspects of the Coordination Chemistry and Catalytic Properties of Cationic Rhodium-Phosphine Complexes. *Adv. Chem. Ser.* **1979**, *173*, 16–25.
135. Landis, C.R.; Halpern, J. Homogeneous Catalysis of Arene Hydrogenation by Cationic Rhodium Arene Complexes. *Organometallics* **1983**, *2*, 840–842. [CrossRef]
136. Fischer, C.; Thede, R.; Drexler, H.-J.; König, A.; Baumann, W.; Heller, D. Investigations into the Formation and Stability of Cationic Rhodium Diphosphane η6-Arene Complexes. *Chem. Eur. J.* **2012**, *18*, 11920–11928. [CrossRef] [PubMed]

137. Polster, J.; Lachmann, H. *Spectrometric Titrations: Analysis of Chemical Equilibria*; Wiley-VCH: Weinheim, Germany, 1989.
138. Benesi, H.A.; Hildebrand, J.H. A Spectrophotometric Investigation of the Interaction of Iodine with Aromatic Hydrocarbons. *J. Am. Chem. Soc.* **1949**, *71*, 2703–2707. [CrossRef]
139. Scott, R.L. Some Comments on the Benesi-Hildebrand Equation. *Rec. Trav. Chim.* **1956**, *75*, 787–789. [CrossRef]
140. Scatchard, G. The Attractions of Proteins for Small Molecules and Ions. *Ann. N. Y. Acad. Sci.* **1949**, *51*, 660–672. [CrossRef]
141. Gampp, H.; Maeder, M.; Meyer, C.J.; Zuberbühler, A.D. Calculation of Equilibrium Constants from Multiwavelength Spectroscopic Data—I: Mathematical Considerations. *Talanta* **1985**, *32*, 95–101. [CrossRef]
142. Gampp, H.; Maeder, M.; Meyer, C.J.; Zuberbühler, A.D. Calculation of Equilibrium Constants from Multiwavelength Spectroscopic data—II132, 95.: Specfit: Two User-Friendly Programs in Basic and Standard Fortran 77. *Talanta* **1985**, *32*, 257–264. [CrossRef]
143. Gampp, H.; Maeder, M.; Meyer, C.J.; Zuberbühler, A.D. Calculation of Equilibrium Constants From Multiwavelength Spectroscopic Data—III: Model-Free Analysis of Spectrophotometric and ESR Titrations. *Talanta* **1985**, *32*, 1133–1139. [CrossRef]
144. Gampp, H.; Maeder, M.; Meyer, C.J.; Zuberbühler, A.D. Calculation of Equilibrium Constants from Multiwavelength Spectroscopic Data—IV: Model-Free Least-Squares Refinement by Use of Evolving Factor Analysis. *Talanta* **1986**, *33*, 943–951. [CrossRef]
145. ReactLAB^{TM} Equilibria. Available online: http://jplusconsulting.com/products/reactlab-equilibria/ (accessed on 5 June 2019).
146. Fischer, C. UV-vis-Spektroskopie in der homogenen Katalyse – Komplexchemische Untersuchungen an Rhodium-Katalysatoren. Ph.D. Thesis, University of Rostock, Rostock, Germany, 2010.
147. Gridnev, I.D.; Higashi, N.; Asakura, K.; Imamoto, T. Mechanism of Asymmetric Hydrogenation Catalyzed by a Rhodium Complex of (S,S)-1,2-Bis(tert-butylmethylphosphino)ethane. Dihydride Mechanism of Asymmetric Hydrogenation. *J. Am. Chem. Soc.* **2000**, *122*, 7183–7194. [CrossRef]
148. Gridnev, I.D.; Yasutake, M.; Higashi, N.; Imamoto, T. Asymmetric Hydrogenation of Enamides with Rh-BisP* and Rh-MiniPHOS Catalysts. Scope, Limitations, and Mechanism. *J. Am. Chem. Soc.* **2001**, *123*, 5268–5276. [CrossRef] [PubMed]
149. Heller, D.; Drexler, H.-J.; Spannenberg, A.; Heller, B.; You, J.; Baumann, W. The Inhibiting Influence of Aromatic Solvents on the Activity of Asymmetric Hydrogenations. *Angew. Chem. Int. Ed.* **2002**, *41*, 777–780. [CrossRef]
150. Sablong, R.; van der Vlugt, J.I.; Thormann, R.; Mecking, S.; Vogt, D. Disperse Amphiphilic Submicron Particles as Non-Covalent Supports for Cationic Homogeneous Catalysts. *Adv. Synth. Catal.* **2005**, *347*, 633–636. [CrossRef]
151. Balué, J.; Bayón, J.C. Hydroformylation of Styrene Catalyzed by a Rhodium Thiolate Binuclear Catalyst Supported on a Cationic Exchange Resin. *J. Mol. Catal. A* **1999**, *137*, 193–203. [CrossRef]
152. Šebesta, R. (Ed.) *Enantioselective Homogeneous Supported Catalysis*; RSC: Cambridge, UK, 2012.
153. Pugin, B.; Blaser, H.-U. The Immobilization of Rhodium-4-(diphenylphosphino)-2-(diphenylphosphinomethyl)-pyrrolidine (Rh-PPM) Complexes: A Systematic Study. *Adv. Synth. Catal.* **2006**, *348*, 1743–1751. [CrossRef]
154. Leadbeater, N.E.; Marco, M. Preparation of Polymer-Supported Ligands and Metal Complexes for Use in Catalysis. *Chem. Rev.* **2002**, *102*, 3217–3274. [CrossRef] [PubMed]
155. Chapuis, C.; Barthe, M.; de Saint Laumer, J.-Y. Synthesis of Citronellal by RhI-Catalysed Asymmetric Isomerization of N,N-Diethyl-Substituted Geranyl- and Nerylamines or Geraniol and Nerol in the Presence of Chiral Diphosphino Ligands, under Homogeneous and Supported Conditions. *Helv. Chim. Acta* **2001**, *84*, 230–242. [CrossRef]
156. Bayston, D.J.; Fraser, J.L.; Ashton, M.R.; Baxter, A.D.; Polywka, M.E.C.; Moses, E. Preparation and Use of a Polymer Supported BINAP Hydrogenation Catalyst. *J. Org. Chem.* **1998**, *63*, 3137–3140. [CrossRef]
157. Renaud, E.; Baird, M.C. Effects of Catalyst Site Accessibility on Catalysis by Rhodium(I) Complexes of Amphiphilic Ligands $[Ph_2P(CH_2)nPMe_3]^+$(n = 2, 3, 6 or 10) tethered to a cation-exchange resin. *J. Chem. Soc. Dalton Trans.* **1992**, 2905–2906. [CrossRef]

158. Kalck, P.; de Oliveira, E.L.; Queau, R.; Peyrille, B.; Molinier, J. Dinuclear Rhodium Complexes Immobilized on Functionalized Diphenylphosphino-(Styrene-Divinylbenzene) Resins Giving High Selectivities for Linear Aldehydes in Hydroformylation reactions. *J. Organomet. Chem.* **1992**, *433*, C4–C8. [CrossRef]
159. Fischer, C.; Thede, R.; Baumann, W.; Drexler, H.-J.; König, A.; Heller, D. Investigations into Metal Leaching from Polystyrene-Supported Rhodium Catalysts. *ChemCatChem* **2016**, *8*, 352–356. [CrossRef]
160. Schwarze, M.; Milano-Brusco, J.-S.; Strempel, V.; Hamerla, T.; Wille, S.; Fischer, C.; Baumann, W.; Arlt, W.; Schomäcker, R. Rhodium Catalyzed Hydrogenation Reactions in Aqueous Micellar Systems as Green Solvents. *RSC Adv.* **2011**, *1*, 474–483.
161. Mikami, K.; Kataoka, S.; Yusa, Y.; Aikawa, K. Racemic but Tropos (Chirally Flexible) BIPHEP Ligands for Rh(I)-Complexes: Highly Enantioselective Ene-Type Cyclization of 1,6-Enynes. *Org. Lett.* **2004**, *6*, 3699–3701. [CrossRef] [PubMed]
162. Mikami, K.; Yusa, Y.; Hatano, M.; Wakabayashi, K.; Aikawa, K. Highly Enantioselective Spiro Cyclization of 1,6-Enynes Catalyzed by Cationic Skewphos Rhodium(I) Complex. *Chem. Commun.* **2004**, 98–99. [CrossRef] [PubMed]
163. Barnhart, R.W.; Wang, X.; Noheda, P.; Bergens, S.H.; Whelan, J.; Bosnich, B. Asymmetric Catalysis. Asymmetric Catalytic Intramolocular Hydrosilation and Hydroacylation. *Tetrahedron* **1994**, *50*, 4335–4346. [CrossRef]
164. Allen, D.G.; Wild, S.B.; Wood, D.L. Catalytic Asymmetric Hydrogenation of Prochiral Enamides by Rhodium(I) Complexes Containing the Enantiomers of (R*,R*)-(.+-.)-1,2-Phenylenebis(methylphenyl-phosphine) and its Arsenic Isosteres. *Organometallics* **1986**, *5*, 1009–1015. [CrossRef]
165. Miyashita, A.; Takaya, H.; Souchi, T.; Noyori, R. 2, 2′-Bis(diphenylphosphino)-1, 1′-binaphthyl(binap): A New Atropisomeric Bis(triaryl)phosphine. Synthesis and its Use in the Rh(l)-Catalyzed Asymmetric Hydrogenation of α-(Acylamino)acrylic Acids. *Tetrahedron* **1984**, *40*, 1245–1253. [CrossRef]
166. Riley, D.P.J. Solution Studies of the Asymmetric Hydrogenation Catalyst System Derived from The [Rhodium (1,2-Bis(diphenylphosphino)-1-cyclohexylethane)] Moiety. *Organomet. Chem.* **1982**, *234*, 85–97. [CrossRef]
167. Miyashita, A.; Yasuda, A.; Takaya, H.; Toriumi, K.; Ito, T.; Souchi, T.; Noyori, R. Synthesis of 2,2′-Bis(diphenylphosphino)-1,1′-binaphthyl (BINAP), an Atropisomeric Chiral Bis(triaryl)phosphine, and its Use in the Rhodium(I)-Catalyzed Asymmetric Hydrogenation of Alpha-(acylamino)acrylic Acids. *J. Am. Chem. Soc.* **1980**, *102*, 7932–7934. [CrossRef]
168. Gridnev, I.D.; Alberico, E.; Gladiali, S. Captured at Last: a Catalyst–Substrate Adduct and a Rh-Dihydride Solvate in the Asymmetric Hydrogenation by a Rh-Monophosphine Catalyst. *Chem. Commun.* **2012**, *48*, 2186–2188. [CrossRef]
169. Gridnev, I.D.; Fan, C.; Pringle, P.G. New Insights Into the Mechanism of Asymmetric Hydrogenation Catalysed by Monophosphonite–Rhodium Complexes. *Chem. Commun.* **2007**, 1319–1321. [CrossRef] [PubMed]
170. Rifat, A.; Patmore, N.J.; Mahon, M.F.; Weller, A.S. Rhodium Phosphines Partnered with the Carborane Monoanions $[CB_{11}H_6Y_6]^-$ (Y = H, Br). Synthesis and Evaluation as Alkene Hydrogenation Catalysts. *Organometallics* **2002**, *21*, 2856–2865. [CrossRef]
171. Marcazzan, P.; Ezhova, M.B.; Patrick, B.O.; James, B.R. Synthesis and Structure of Dimeric Rh-Bis(tertiary phosphine) Complexes, Exceptionally Useful Synthetic Precursors. *C. R. Chim.* **2002**, *5*, 373–378. [CrossRef]
172. Singewald, E.T.; Mirkin, C.A.; Stern, C.L. A Redox-Switchable Hemilabile Ligand: Electrochemical Control of the Coordination Environment of a RhI Complex. *Angew. Chem. Int. Ed.* **1995**, *35*, 1624–1627. [CrossRef]
173. Preetz, A.; Baumann, W.; Fischer, C.; Drexler, H.-J.; Schmidt, T.; Thede, R.; Heller, D. Asymmetric Hydrogenation. Dimerization of Solvate Complexes: Synthesis and Characterization of Dimeric $[Rh(DIPAMP)]_2^{2+}$, a Valuable Catalyst Precursor. *Organometallics* **2009**, *28*, 3673–3677. [CrossRef]
174. Fairlie, D.P.; Bosnich, B. Homogeneous Catalysis. Mechanism of Catalytic Hydroacylation: the Conversion of 4-Pentenals to Cyclopentanones. *Organometallics* **1988**, *7*, 946–954. [CrossRef]
175. Barnhart, R.W.; Xianqi, W.; Noheda, P.; Bergens, S.H.; Whelan, J.; Bosnich, B. Asymmetric Catalysis. Asymmetric Catalytic Intramolecular Hydroacylation of 4-Pentenals Using Chiral RhodiumDiphosphine Catalysts. *J. Am. Chem. Soc.* **1994**, *116*, 1821–1830. [CrossRef]
176. Masutomi, K.; Sugiyama, H.; Uekusa, H.; Shibata, Y.; Tanaka, K. Asymmetric Synthesis of Protected Cyclohexenylamines and Cyclohexenols by Rhodium-Catalyzed [2+2+2] Cycloaddition. *Angew. Chem. Int. Ed.* **2016**, *55*, 15373–15376. [CrossRef]

177. Aida, Y.; Sugiyama, H.; Uekusa, H.; Shibata, Y.; Tanaka, K. Rhodium-Catalyzed Asymmetric [2 + 2 + 2] Cycloaddition of α,ω-Diynes with Unsymmetrical 1,2-Disubstituted Alkenes. *Org. Lett.* **2016**, *18*, 2672–2675. [CrossRef]
178. Yoshizaki, S.; Nakamura, Y.; Masutomi, K.; Yoshida, T.; Noguchi, K.; Shibata, Y.; Tanaka, K. Rhodium-Catalyzed Asymmetric [2 + 2 + 2] Cycloaddition of 1,6-Enynes with Cyclopropylideneacetamides. *Org. Lett.* **2016**, *18*, 388–391. [CrossRef]
179. Shintani, R.; Takano, R.; Nozaki, K. Rhodium-Catalyzed Asymmetric Synthesis of Silicon-Stereogenic Silicon-Bridged Arylpyridinones. *Chem. Sci.* **2016**, *7*, 1205–1211. [CrossRef] [PubMed]
180. Torres, A.; Roglans, A.; Pla-Quintana, A. An Enantioselective Cascade Cyclopropanation Reaction Catalyzed by Rhodium(I): Asymmetric Synthesis of Vinylcyclopropanes. *Adv. Synth. Catal.* **2016**, *358*, 3512–3516. [CrossRef]
181. Fernandez, M.; Parera, M.; Parella, T.; Lledj, A.; le Bras, J.; Muzart, J.; Pla-Quintana, A.; Roglans, A. Rhodium-Catalyzed [2+2+2] Cycloadditions of Diynes with Morita–Baylis–Hillman Adducts: A Stereoselective Entry to Densely Functionalized Cyclohexadiene Scaffolds. *Adv. Synth. Catal.* **2016**, *358*, 1848–1853. [CrossRef]
182. Amatore, M.; Leboeuf, D.; Malacria, M.; Gandon, V.; Aubert, C. Highly Enantioselective Rhodium-Catalyzed [2+2+2] Cycloaddition of Diynes to Sulfonimines. *J. Am. Chem. Soc.* **2013**, *135*, 4576–4579. [CrossRef] [PubMed]
183. Araki, T.; Noguchi, K.; Tanaka, K. Enantioselective Synthesis of Planar-Chiral Carba-Paracyclophanes: Rhodium-Catalyzed [2+2+2] Cycloaddition of Cyclic Diynes with Terminal Monoynes. *Angew. Chem. Int. Ed.* **2013**, *52*, 5617–5621. [CrossRef] [PubMed]
184. Augé, M.; Barbazanges, M.; Tran, A.T.; Simonneau, A.; Elley, P.; Amouri, H.; Aubert, C.; Fensterbank, L.; Gandon, V.; Malacria, M.; et al. Atroposelective [2+2+2] Cycloadditions Catalyzed by a Rhodium(I)–Chiral Phosphate System. *Chem. Commun.* **2013**, *49*, 7833–7835. [CrossRef]
185. Lu, Y.; Woo, S.K.; Krische, M.J. Total Synthesis of Bryostatin 7 via C–C Bond-Forming Hydrogenation. *J. Am. Chem. Soc.* **2011**, *133*, 13876–13879. [CrossRef]
186. Kong, J.R.; Krische, M.J. Catalytic Carbonyl Z-Dienylation via Multicomponent Reductive Coupling of Acetylene to Aldehydes and α-Ketoesters Mediated by Hydrogen: Carbonyl Insertion into Cationic Rhodacyclopentadienes. *J. Am. Chem. Soc.* **2006**, *128*, 16040–16041. [CrossRef]
187. Kong, J.-R.; Cho, C.-W.; Krische, M.J. Hydrogen-Mediated Reductive Coupling of Conjugated Alkynes with Ethyl (N-Sulfinyl)iminoacetates: Synthesis of Unnatural α-Amino Acids via Rhodium-Catalyzed C−C Bond Forming Hydrogenation. *J. Am. Chem. Soc.* **2005**, *127*, 11269–11276. [CrossRef]
188. Rhee, J.U.; Krische, M.J. Highly Enantioselective Reductive Cyclization of Acetylenic Aldehydes via Rhodium Catalyzed Asymmetric Hydrogenation. *J. Am. Chem. Soc.* **2006**, *128*, 10674–10675. [CrossRef]
189. Jang, H.-Y.; Hughes, F.W.; Gong, H.; Zhang, J.; Brodbelt, J.S.; Krische, M.J. Enantioselective Reductive Cyclization of 1,6-Enynes via Rhodium-Catalyzed Asymmetric Hydrogenation: C−C Bond Formation Precedes Hydrogen Activation. *J. Am. Chem. Soc.* **2005**, *127*, 6174–6175. [CrossRef] [PubMed]
190. Masutomi, K.; Sakiyama, N.; Noguchi, K.; Tanaka, K. Rhodium-Catalyzed Regio-, Diastereo-, and Enantioselective [2+2+2] Cycloaddition of 1,6-Enynes with Acrylamides. *Angew. Chem. Int. Ed.* **2012**, *51*, 13031–13035. [CrossRef] [PubMed]
191. Sakiyama, N.; Noguchi, K.; Tanaka, K. Rhodium-Catalyzed Intramolecular Cyclization of Naphthol- or Phenol-Linked 1,6-Enynes Through the Cleavage and Formation of sp^2 C-O Bonds. *Angew. Chem. Int. Ed.* **2012**, *51*, 5976–5980. [CrossRef] [PubMed]
192. Ishida, M.; Shibata, Y.; Noguchi, K.; Tanaka, K. Rhodium-Catalyzed Asymmetric [2+2+2] Cyclization of 1,6-Enynes and Aldehydes. *Chem. Eur. J.* **2011**, *17*, 12578–12581. [CrossRef] [PubMed]
193. Miyauchi, Y.; Kobayashi, M.; Tanaka, K. Rhodium-Catalyzed Intermolecular [2+2+2] Cross-Trimerization of Aryl Ethynyl Ethers and Carbonyl Compounds To Produce Dienyl Esters. *Angew. Chem. Int. Ed.* **2011**, *50*, 10922–10926. [CrossRef] [PubMed]
194. Jang, H.-Y.; Krische, M.J. Rhodium-Catalyzed Reductive Cyclization of 1,6-Diynes and 1,6-Enynes Mediated by Hydrogen: Catalytic C−C Bond Formation via Capture of Hydrogenation Intermediates. *J. Am. Chem. Soc.* **2004**, *126*, 7875–7880. [CrossRef] [PubMed]
195. Preetz, A. Rhodium-Präkatalysatoren in der asymmetrischen Katalyse. Ph.D. Thesis, University of Rostock, Rostock, Germany, 2008.

196. König, A.; Fischer, C.; Alberico, E.; Selle, C.; Drexler, H.-J.; Baumann, W.; Heller, D. Oxidative Addition of Aryl Halides to Cationic Bis(phosphane)rhodium Complexes: Application in C–C Bond Formation. *Eur. J. Inorg. Chem.* **2017**, 2040–2047. [CrossRef]
197. Jiao, Y.; Brennessel, W.W.; Jones, W.D. Oxidative Addition of Chlorohydrocarbons to a Rhodium Tris(pyrazolyl)borate Complex. *Organometallics* **2015**, *34*, 1552–1566. [CrossRef]
198. Townsend, N.S.; Chaplin, A.B.; Naser, M.A.; Thompson, A.L.; Rees, N.H.; Macgregor, S.A.; Weller, A.S. Reactivity of the Latent 12-Electron Fragment $[Rh(P{i}Bu_3)_2]^+$ with Aryl Bromides: Aryl-Br and Phosphine Ligand C-H Activation. *Chem. Eur. J.* **2010**, *16*, 8376–8389. [CrossRef]
199. Chen, S.; Li, Y.; Zhao, J.; Li, X. Chelation-Assisted Carbon-Halogen Bond Activation by a Rhodium(I) Complex. *Inorg. Chem.* **2009**, *48*, 1198–1206. [CrossRef]
200. Douglas, T.M.; Chaplin, A.B.; Weller, A.S. Dihydrogen Loss from a 14-Electron Rhodium(III) Bis-Phosphine Dihydride To Give a Rhodium(I) Complex That Undergoes Oxidative Addition with Aryl Chlorides. *Organometallics* **2008**, *27*, 2918–2921. [CrossRef]
201. Pike, S.D.; Weller, A.S. C–Cl activation of the weakly coordinating anion $[B(3,5\text{-}Cl_2C_6H_3)_4]^-$ at a Rh(I) centre in solution and the solid-state. *Dalton Trans.* **2013**, *42*, 12832–12835. [CrossRef] [PubMed]
202. Curto, S.G.; Esteruelas, M.A.; Olivan, M.; Onate, E.; Velez, A. Selective C–Cl Bond Oxidative Addition of Chloroarenes to a POP–Rhodium Complex. *Organometallics* **2017**, *36*, 114–128. [CrossRef]
203. Puri, M.; Gatard, S.; Smith, D.A.; Ozerov, O.V. Competition Studies of Oxidative Addition of Aryl Halides to the (PNP)Rh Fragment. *Organometallics* **2011**, *30*, 2472–2482. [CrossRef]
204. Gatard, S.; Guo, C.; Foxman, B.M.; Ozerov, O.V. Thioether, Dinitrogen, and Olefin Complexes of (PNP)Rh: Kinetics and Thermodynamics of Exchange and Oxidative Addition Reactions. *Organometallics* **2007**, *26*, 6066–6075. [CrossRef]
205. Gatard, S.; Celenligil-Cetin, R.; Guo, C.; Foxman, B.M.; Ozerov, O.V. Carbon−Halide Oxidative Addition and Carbon−Carbon Reductive Elimination at a (PNP)Rh Center. *J. Am. Chem. Soc.* **2006**, *128*, 2808–2809. [CrossRef]
206. Timpa, S.D.; Pell, C.J.; Zhou, J.; Ozerov, O.V. Fate of Aryl/Amido Complexes of Rhodium(III) Supported by a POCOP Pincer Ligand: C–N Reductive Elimination, β-Hydrogen Elimination, and Relevance to Catalysis. *Organometallics* **2014**, *33*, 5254–5262. [CrossRef]
207. Timpa, S.D.; Fafard, C.M.; Herberta, D.E.; Ozerov, O.V. Catalysis of Kumada–Tamao–Corriu Coupling by a (POCOP)Rh Pincer Complex. *Dalton Trans.* **2011**, *40*, 5426–5429. [CrossRef]
208. Ito, J.-I.; Miyakawa, T.; Nishiyama, H. Amine-Assisted C−Cl Bond Activation of Aryl Chlorides by a (Phebox)Rh-Chloro Complex. *Organometallics* **2008**, *27*, 3312–3315. [CrossRef]
209. Qian, Y.Y.; Lee, M.H.; Yang, W.; Chan, K.S. Aryl Carbon–Chlorine (Ar–Cl) and Aryl Carbon–Fluorine (Ar–F) Bond Cleavages by Rhodium Porphyrins. *J. Organomet. Chem.* **2015**, *791*, 82–89. [CrossRef]
210. Willems, S.T.H.; Budzelaar, P.H.M.; Moonen, N.N.P.; de Gelder, R.; Smits, J.M.M.; Gal, A.W. Coordination and Oxidative Addition at a Low-Coordinate Rhodium(I) β-Diiminate Centre. *Chem. Eur. J.* **2002**, *8*, 1310–1320. [CrossRef]
211. Yamagata, T.; Tani, K.; Tatsuno, Y.; Saito, T. A New Rhodium Trinuclear Complex Containing Highly Protected Hydroxo Groups, $[\{Rh(binap)\}_3(\mu_3\text{-}OH)2]ClO_4$, Responsible for Deactivation of the 1,3-Hydrogen Migration Catalyst of Allylamine [Binap = 2,2′-Bis(diphenylphosphino)-1,1′-binaphthyl]. *J. Chem. Soc. Chem. Commun.* **1988**, 466–468. [CrossRef]
212. Preetz, A.; Baumann, W.; Drexler, H.-J.; Fischer, C.; Sun, J.; Spannenberg, A.; Zimmer, O.; Hell, W.; Heller, D. Trinuclear Rhodium Complexes and Their Relevance for Asymmetric Hydrogenation. *Chem. Asian. J.* **2008**, *3*, 1979–1982. [CrossRef] [PubMed]
213. Horstmann, M.; Drexler, H.-J.; Baumann, W.; Heller, D. Ammine and Amido Complexes of Rhodium: Synthesis, Application and Contributions to Analytics. Unpublished work. 2019.
214. [2-(3-Methoxy-phenyl)-cyclohex-1-enylmethyl]-dimethylamine, which can be transformed by a stereoselective hydrogenation to Tramadol, an important analgesic drug used world-wide, is a member of a class of 1,2-disubstituded cyclohexene derivatives which are important intermediates in the synthesis of pharmaceutically active compounds acting on the central nervous system.
215. The hydrogenation product is a key intermediate in the synthesis of 4-amino-2-(*R*)-methylbutan-1-ol en route towards the receptor antagonist TAK-637.

216. Cobley, C.J.; Lennon, I.C.; Praquin, C.; Zanotti-Gerosa, A. Highly Efficient Asymmetric Hydrogenation of 2-Methylenesuccinamic Acid Using a Rh-DuPHOS Catalyst. *Org. Process Res. Dev.* **2003**, *7*, 407–411. [CrossRef]
217. The prochiral olefin (*Z*)-3-[1-(dimethylamino)-2-methylpent-2-en-3-yl]phenol is an important precursor of the new analgesic drug Tapentadol which is as an open-chain analogue of Tramadol. The (*R*,*R*) stereoisomer of Tapentadol is a novel, centrally acting analgesic with a dual mode of action: M-opioid receptor (MOR) agonism and norepinephrine reuptake inhibition.
218. Christopfel, W.C.; Vineyard, B.D. Catalytic Asymmetric Hydrogenation With a Rhodium(I) Chiral Bisphosphine System. A Study of Itaconic Acid and Some of its Derivatives and Homologs. *J. Am. Chem. Soc.* **1979**, *101*, 4406–4408. [CrossRef]
219. Schmidt, T.; Drexler, H.-J.; Sun, J.; Dai, Z.; Baumann, W.; Preetz, A.; Heller, D. Unusual Deactivation in the Asymmetric Hydrogenation of Itaconic Acid. *Adv. Synth. Catal.* **2009**, *351*, 750–754. [CrossRef]
220. Schmidt, T.; Baumann, W.; Drexler, H.-J.; Heller, D. Unusual Deactivation in the Asymmetric Hydrogenation of Itaconic Acid. *J. Organomet. Chem.* **2011**, *696*, 1760–1767. [CrossRef]
221. Schmidt, M.; Schreiber, S.; Franz, L.; Langhoff, H.; Farhang, A.; Horstmann, M.; Drexler, H.-J.; Heller, D.; Schwarze, M. Hydrogenation of Itaconic Acid in Micellar Solutions: Catalyst Recycling with Cloud Point Extraction? *Ind. Eng. Chem. Res.* **2019**, *58*, 2445–2453. [CrossRef]
222. Other possibilities are extraction with organic solvents, micellar-enhanced ultrafiltration (MEUF) and phase separation.
223. Friedrich, H.B.; Moss, J.R. Halogenoalkyl Complexes of Transition Metals. *Adv. Organomet. Chem.* **1991**, *33*, 235–290.
224. Ball, G.E.; Cullen, W.R.; Fryzuk, M.D.; James, B.R.; Rettig, S.J. Oxidative Addition of Dichloromethane to $[(dppe)Rh]_2(\mu\text{-}Cl)_2$ (dppe = $Ph_2PCH_2CH_2PPh_2$). X-ray structure of $[(dppe)RhCl]_2(\mu\text{-}Cl)_2(\mu\text{-}CH_2)$. *Organometallics* **1991**, *10*, 3767–3769. [CrossRef]
225. Fennis, P.J.; Budzelaar, P.H.M.; Frijns, J.H.G. Dichloromethane Addition to Rhodium-β-Diketonate Complexes of Diphosphines and Pyridyl-Substituted Diphosphines. *J. Organomet. Chem.* **1990**, *393*, 287–298. [CrossRef]
226. Marder, T.B.; Fultz, W.C.; Calabrese, J.C.; Harlow, R.L.; Milstein, D. Activation of Dichloromethane by Basic Rhodium(I) and Iridium(I) Phosphine Complexes. Synthesis and Structures of *fac*-$[Rh(PMe_3)_3Cl_2(CH_2PMe_3)]Cl{\cdot}CH_2Cl_2$ and *trans*-$[Rh(Me_2PCH_2CH_2PMe_2)_2Cl(CH_2Cl)]Cl$. *J. Chem. Soc. Chem. Commun.* **1987**, 1543–1545. [CrossRef]
227. Blank, B.; Glatz, G.; Kempe, R. Single and Double C-Cl-Activation of Methylene Chloride by P,N-ligand Coordinated Rhodium Complexes. *Chem. Asian J.* **2009**, *4*, 321–327. [CrossRef] [PubMed]
228. Ciriano, M.A.; Tena, M.A.; Oro, A. Reactions of Chloroform and *gem*-Dichlorocarbons with Binuclear Rhodium Complexes Leading to Functionalized Methylene-Bridged Compounds. *J. Chem. Soc. Dalton Trans.* **1992**, 2123–2124. [CrossRef]
229. Mannu, A.; Ferro, M.; Möller, S.; Heller, D. Monomerisation of $[Rh_2(1,3\text{-Bis-(Diphenylphosphino)-Propane})_2(\mu_2\text{-}Cl)_2]$ Detected by Pulsed Gradient Spin Echo Spectroscopy and ^{31}P Nmr Monitoring of Metathesis Experiments. *J. Chem. Res.* **2018**, *42*, 402–404. [CrossRef]
230. This reaction has been known for a long time and is used in the synthesis of mononuclear cationic complexes from neutral μ2-chloro brigded precursors by chloride abstraction with a silver salt.
231. Anastas, P.T.; Kirchhoff, M.M.; Williamson, T.C. Catalysis as a Foundational Pillar of Green Chemistry. *Appl. Catal. A Gen.* **2001**, *221*, 3–13. [CrossRef]